FINAL YEAR PROJECT

SCHOOL OF ELECTRICAL, ELECTRONIC AND COMPUTER ENGINEERING

UNIVERSITY OF WESTERN AUSTRALIA

FRIDAY 23RD OCTOBER 2009

PROJECT SUPERVISOR: PROFESSOR THOMAS BRÄUNL

2009 REV MANAGEMENT

AND

ON-BOARD EMBEDDED SYSTEMS

DANIEL KINGDOM – 10528767

This dissertation is submitted in partial fulfilment of the requirement of the award of Bachelor of Engineering.

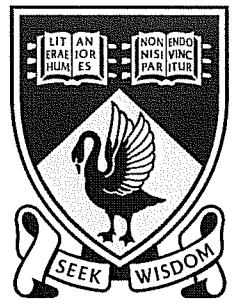

THE UNIVERSITY OF WESTERN AUSTRALIA

ABSTRACT

The Renewable Energy Vehicle project consists of 3 electric vehicle conversions including a 2008 Hyundai Getz, 2002 Lotus Elsie and a 2001 Formula-SAE Motorsport. In addition to electric vehicle conversion projects, a BMW X5 is being converted for drive by wire, with the ultimate goal of Autonomous driving and driver assistance technologies. The 2009 Semester 2 REV team is made up of 44 Students completing a 3rd Design project, Final year project, and Post-graduate work or are participating as a volunteer. The students come from a variety of disciplines including, Electrical & Electronic Engineering, Computer Engineering, Computer Science, Mechatronics and Mechanical Engineering. The author holds the position of Student Manager, and is responsible for administrative and managerial tasks in addition to contributing technically to project.

This document focuses on the technical aspect of the work of presenter, and includes a number of new systems and sub-systems that add new functionality or re-produce functionality that was present before the vehicles conversion. Such systems include: The Hardware Black Box Recorder that collects and stores vehicle information, also supporting an embedded USB Host and 2GB of flash memory; AC and DC power measurement systems capturing the actual power consumption of the vehicle and calculating remaining battery capacity; Battery management functionality to protect the Lithium-Iron-Phosphate (LiFePO4) cells in the vehicles traction battery pack; Galvanic isolation systems to protect digital devices including the EyeBot Controller and finally emulating OEM sensors that existed in the original vehicle including fuel gauge, and tachometer.

ACKNOWLEDGEMENTS

The author would like to acknowledge the work of the following people, whom have help to make the REV project an ongoing success. Firstly the author would like to show his appreciation to the REV supervisors Professor Thomas Bräunl and Dr Kamy Cheng. Who without the author would not have had the opportunity to work on such a unique and fulfilling thesis, and provided many hours of support and advice over the 2009 year.

Secondly the author would like to thank the members of the 2009 REV team, for their hard work and dedication throughout the year.

Adam Doster
Amar Shah
Andrew Morrigan
Anne Flinchbaugh
Bobby Powers
Bryan Teague
Calin Borceanu
Cameron Watts
Chris Hellsten
Christian Tietzel
Colin Dickie
Daksh Varma
Daniel Harris
David Caleb Tang
Frans Ho
Franz Viertler
Grace Ong
Ian Hooper
Ivo Vekemans
Jack Nay
James Laing
Jason Fairclough
Jennifer Berry
John Pearce
Jon Mullan
Jonathan Eng
Jonathan Wan
Jurek Malarecki
Karri Harper-Meredith
Marius Ivanescu
Martin Duff
Nicholas Randell
Peter Corke
Tim Wallace
Tiong Kun Ooi
Tom Banasiak
Wesley Wang
William Crock
William Price
Xin Cen
Zhi Guo

Appreciation also extends to Steven Whitely for returning to UWA after graduating to provide assistance to a fresh team and assist us in getting up to speed.

The author would also like to thank the UWA workshop staff for their assistance and advice throughout the year:

Donald Allen
Jonathan Brant
George Voyt
Kenneth Fogden
John Schurmann

The team at EV Works for their assistance and advice:

Rob Mason
Rod Dilkes

For technical advice about the BMS modules:

Ivan Neubronner

The Australian Electric Vehicle Association, Perth Branch, for their support throughout the project.

For assistance with editing: Jess Braun, Helen Kingdom

My girlfriend Rebecka Turner and my parents for their support and re-assurance over the many months of 60-70 hour weeks at university.

TABLE OF CONTENTS

LIST OF FIGURES

LIST OF TABLES

List Of Equations

NOMENCLATURE

3G – 3rd generation telecommunications hardware standards

100BaseT – 100Mbps Ethernet over twisted pair cable

ADC – Analogue to Digital Converter

ASCII – American Standard Code for Information Interchange (Character Map)

AT – Specific command set for communication over modem devices

Bbl – A barrel usually of oil, equivalent to 42 US gallons.

BMS – Battery Management System

C – Rated capacity of a battery cell

CAN – Controller Area Network

DCE – Data Communication Equipment

DTE – Data Terminal Equipment

EEPROM – Electrically Erasable Programmable Read Only Memory

EMI – Electro-Magnetic Interference

EyeBot M6 – A self contained Linux based controller developed at UWA.

FAT – File Allocation Tables, A file system commonly associated with DOS

FPGA – Field Programmable Gate Array

GPS – Global Positioning System

Hexadecimal – A base 16 numbering system using the characters 0-F

HSDPA – High Speed Downlink Packet Access

HSPA – High Speed Packet Access

HV – Hazardous Voltage

I^2C – A two wire bidirectional serial bus.

IO – Input / Output

Little Endian – Byte/bit ordering where the most significant Byte/bit is sent first

LSB/LSb – Least Significant Byte / bit

MMB\D – Millions of Barrels per day (referring to crude oil production)

MSB/MSb – Most Significant Byte / bit

Null-modem Cable/Adapter – A cable made to connect a DCE to DCE or DTE to DTE via crossing over the pairs. Eg Receive and transmit would be crossed in the cable such that the transmit at one end is connected to the receive at the other.

OECD – Organisation for Economic Co-operation and Development

OPEC – Organisation of Petroleum Export Countries

PC – Personal Computer

PCB – Printed Circuit Board

Plug-in hybrids – Hybrid electric vehicles (i.e. petrol\electric) that has a battery that can be plugged into a charging station.

PTC – Positive Thermal Co-efficient device – a device whoos resistance increases with temperature.

RMS – Root Mean Square

Rollover Cable – an EIA-561 Cable where the pair crossed over.

RTCC – Real Time Clock Calendar

SELV – Separate Extra Low Voltage – Voltage below 50V DC with a separate ground / Earth

SMBus – System Bus – similar to I^2C except operates on 3.3V

SPI – Serial Peripheral Interconnect – A three wire bi-direction serial bus

Traction Pack – Battery Pack of an electric car

TVS - Transient Voltage Suppression device

UART – Universal Asynchronous Receiver/Transmitter

USB – Universal Serial Bus

UTC – Universal Time Co-ordinated

1. INTRODUCTION

The Renewable Energy Vehicle (REV) project was initiated under the supervision of Dr Kamy Cheng and Dr Lawrence Borle in July 2004[1]. The initial goal was to develop an electric vehicle fuelled with a hydrogen fuel cell stack, and supplemented by a $LiFePO_4$ battery system. However since this time the practicality and perhaps more importantly the sustainability of the hydrogen economy have been questioned[2].

While hydrogen is the most abundant element on the planet, it does not exist in its elemental form in nature, and thus must be synthesised. A number of sources for synthesising hydrogen are known, including the electrolysis of water, steam reforming from methane and biomass, and coal. Currently one of the most efficient methods of producing hydrogen is through industrial natural gas reformers achieving an energetic HHV (maximum heating value) efficiency of 90%[2]. However since it is sourced from a non-renewable energy source it can be considered non-sustainable. Electrolysis from water is a renewable method of producing hydrogen, however it has considerable requirements for clean water and energy input, only 25% of the energy used to produce hydrogen this way can be recovered back into electrical energy using fuel cells[2]. The following case study is a good indication on the quantity of resources to support a hydrogen economy.

"About 550 jumbo jets leave Frankfurt Airport every day, each loaded with 130 tons of kerosene. If replaced on a 1 : 1 energy base by 50 tons of liquid hydrogen, the daily needs would be 2500 tons or 36 000 m^3 of the cryogenic liquid, enough to fill 18 Olympic-size swimming pools. Every day 22 500 tons of water would have to be electrolysed. The continuous output of eight 1-GW power plants would be required for electrolysis, liquefaction, and transport of hydrogen. If all 550 planes leaving the airport were converted to hydrogen, the entire water consumption of Frankfurt (650 000 inhabitants) and the output of 25 full-size power plants would be needed to meet the hydrogen demand of air planes leaving just one airport in Germany"[2].

The transportation requirements for liquefied hydrogen via pipeline, road or rail also cannot compete with the efficiency of an electric grid network[2]. With the

future existence of a hydrogen economy continuing to look less feasible the projects aim was adjusted to that of an 'electron' economy and the production of battery electric vehicles, under the supervision of Professor Thomas Bräunl, and Dr Kamy Cheng in beginning of 2008.

The electrochemical energy storage system (i.e. a battery) is one of the most significant components of a battery electric vehicle. Desired features of an electric vehicle battery system include high specific energy, high specific power, high charge acceptance rate (fast charging), long cycle life, long calendar life, low self-discharge rate, low cost, and recyclability[3]. EV (electric vehicles) initially operated on lead-acid batteries; however modern vehicles are fitted with Ni-MH and Li-ion batteries which offer better specific energy/power and a dramatic weight reduction.

Li-ion batteries were chosen for the REV projects, more specifically $LiFePO_4$ these batteries exceed in most of the above requirements par from cost. An obvious winner is the energy density at 90Wh/kg (TS-LFP90AHA [4]) compared to NiMH (typically 50-60 Wh/kg[5]) and NiCd (40 to 50 Wh/kg[5]). $LiFePO_4$ also has a low self-discharge current less than 3% per month[4], and a large cycle life greater than 3000 times for 70% DOD (Depth of Discharge) and greater than 2000 cycles for 80% DOD[4]. It is hoped that as demand improves for these batteries that mass-production will reduce the cost of the $LiFePO_4$ cells.

The author's primary role for 2009 was to manage the REV team and overlook the four independent projects. 2009 was an exciting year for the REV project as the project branched out after the success of the 2008 Rev Eco (Hyundai Getz). Although the Getz was in a running condition, it still received many upgrades including a new ventilation system for the rear cage, TBS connectivity (via the TBS Gateway), reliability and safety enhancements, as well as many others. With the signing on of our new sponsor Gull the Getz also was fitted with new decals and a new colour scheme (see Figure 1).

FIGURE 1 - THE REV ECHO - HYUNDAI GETZ

One of the new exciting additions for 2009 is the REV Racer which is an electric conversion of a 2002 Lotus Elise. This project is aimed at debunking perhaps one of the most common myths about electric cars, that "Electric Cars are slow". After the removal of the internal combustion engine it was replaced with a UQM Power Phase 75 Brushless DC motor and matching DD45-400L Inverter/ Motor Controller. This motor produces a maximum of 75kW with a constant torque output of 220 Nm Peak from 0 to 4500 rpm and a maximum speed of 8000 rev/min[6]. The UQM motor is coupled to the stock transmission (see Figure 3) with a custom mounting plate developed by the mechanical team.

FIGURE 2 - REV RACER - 2002 LOTUS ELISE

The vehicle is fitted with three separate traction packs fitted in the fuel tank area, above the motor/gearbox, and underneath the boot area. A total of 99, 60Ah $LiFePO_4$ cells from Thunder Sky are installed in the three packs, producing a nominal voltage of 316.8V DC, the UQM inverter is capable of produce peak power with an input voltage of 250-425V DC[6]. The vehicle is also fitted with a

car PC (dual core atom CPU), and a new REV design Black Box / BMS Master Controller.

FIGURE 3 - UQM POWER PHASE 75 WITH GEARBOX

2009 also saw the addition of the REV SAE, this is a battery electric conversion of the 2001 UWA motorsports SAE vehicle (see Figure 4). The original goal of this project was to develop a wheel hub based, light weight racer. The design direction change after the implementation of wheel hub motors raised design issues about unsprung mass and complications installing a motor assembly into the existing suspension and hub uprights. The vehicle has instead been designed around using independent inboard brushless DC motors for the two rear wheels. An electronic diff control circuitry was developed to adjust individual motor speeds based upon current driving activities.

FIGURE 4 - REV SAE - 2001 MOTORSPORTS SAE CHASSIS

The REV Drive-by-wire project was continued into 2009, the host vehicle is a donated BMW X5 SUV (see Figure 5). This project is centred on the addition of systems to facilitate autonomous control of the steering, brakes and accelerator. Analogue RC styled servo motors were installed, for each of the required functions. The control signal is generated by the installed Eyebot M6 controller. The long term goal of this project is to develop driver assistance technology, such as lane detection and crash avoidance technologies using the image processing capabilities of the Eyebot Controller.

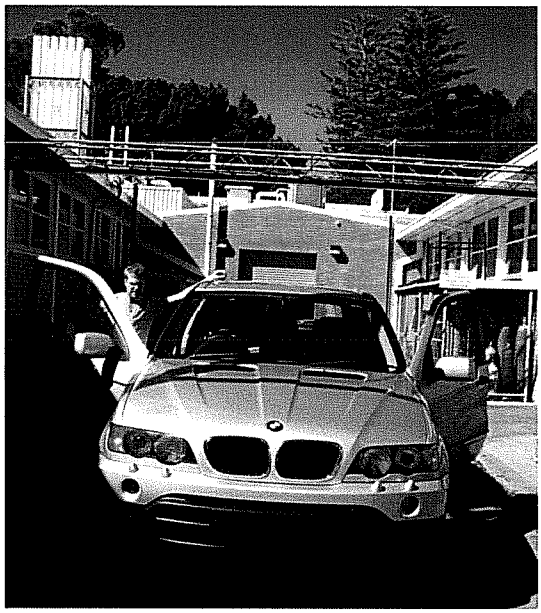

FIGURE 5 - REV DRIVE-BY-WIRE, BMW X5

Team management consisted in part of the following duties team logistics, acquisition of materials \ parts, chairing the bi-weekly meetings (see Figure 6), coordinating events with sponsors, assisting with the various public expositions throughout the year, and running presentations for university visitors. Project steering was also a very frequent task and involved assisting other team members to make both technical and functional decisions, assisting the projecta develop to meet the required project goals. By the very nature of the personal communication required and number of students involved in the REV project this proved to be a very time consuming activity. The author also contributed technically to the REV project, this document will focus on the technical activities undertaken rather than the management functions.

FIGURE 6 - TEAM MEETINGS

The author contributed technical designs to both the REV Racer and REV Eco. Prior to the author's appointment a new Battery Management System (BMS) module was selected to be installed in the REV Racer. This system was a custom design by Ivan Neubronner and thus required a new master controller, which was then merged into a larger project (the Hardware Black Box). The addition of a Hardware Black Box system would allow for the collection of important vehicle metrics, allowing for future research and vehicle tuning to be supported by quantitative data from the vehicle. The Black Box system was designed to be modular in nature, and must be flexible so the design can be used in multiple vehicles.

The design should be able to record for extended periods of time, and must be protected from the large DC potentials that can exist from different systems in the car. The design must also allow the user to easily retrieve collected data, through some form of digital media and easily perform basic maintenance (i.e. clear data logger memory). The Black Box must also consume minimal power, so data-logging can occur around the clock unlike the current software black box systems.

Simpler designs were also created for the Getz, to remedy particular issues as they arose. This included the 3G Power Management Module, to overcome a hardware limitation of the 3G router installed in the vehicle; and the TBS Gateway, that was developed to allow the Eyebot to collect traction pack metrics in addition to the direct drive of gauges on the vehicles instrument cluster and increasing the pool of available digital IO.

1. Literature Review

2.1 Battery Electric Vehicles As A Sustainable Mode of Transport

Electric road vehicles are not a new innovation, "the truth is that in the early 1900's the electric car was a common site on the American roads"[7]. Electric cars were popular with women and doctors as a reliable and easy to start vehicle, as an interesting side note the term cranky supposedly comes from the difficulty in crank starting gasoline cars of the time. The first electric car (the Detroit Electric) was produced in 1907 by the Anderson Carriage company and was rated for a range of 80miles (130 km) with a top speed of 20 mph (32 kmph)[7].

Electric vehicles have a role to play in the future of sustainable transport in Australia. A CSIRO report titled, *Inquiry into the Impact of Higher Petroleum, Diesel and Gas Prices and Several Related Matters* reports projected that electricity is expected to steadily expand its role as a transport fuel. Increasing from a current energy level of 8 PJ (Petra Joules) which is consumed entirely by electric rail to 149PJ (equivalent to 41TWh) as road transport becomes the dominant consumer of electricity from the grid[8].

"By 2050 plug-in hybrid electric and full electric vehicles will account for around a third of the road vehicle fleet.... Leaving internal combustion vehicles responsible for just one sixth of vehicle kilometres"[8]

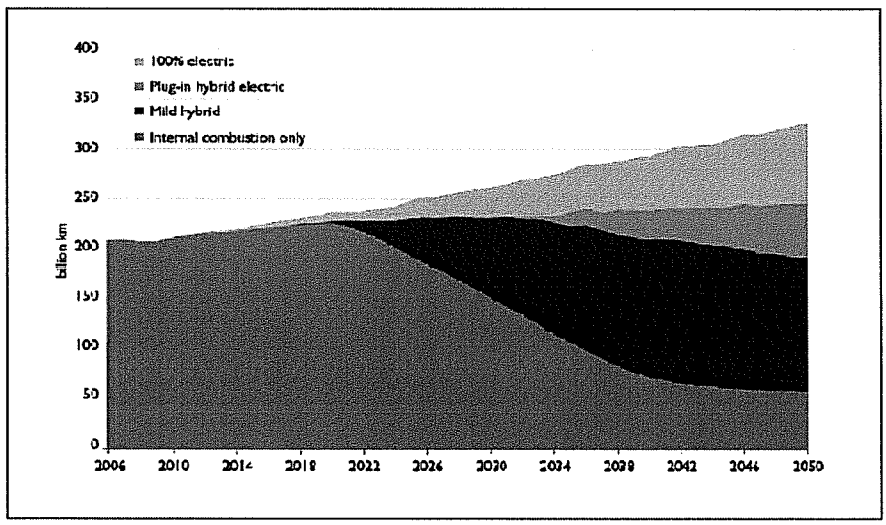

Figure 7 - Projected Increasing Electrification Of Road Transport Vehicles[8]

2.1.1 Environmental Impacts

Recent times have shown increasing awareness of possible implication of green house gas emissions, in particular the global warming through the green house effect. The green house effect is the result of green house gasses allowing the transmission of visible solar radiation to pass through the upper atmosphere, while absorbing the long-wave ultraviolet radiation that has been reflected back from Earth. Naturally occurring green house gasses include water vapour, carbon dioxide, methane, nitrous oxide and ozone. The green house effect is in essence essential for the habitability of Earth, without it the surface temperature of Earth would on average be approximately 33°C cooler. However scientists are concerned that increased production and release of green house gasses will result in additional warming of the Earth's surface[9].

"Australia's per capita greenhouse gas emissions are the highest of any OECD country and are among the highest in the world"[9]

Australia's per capita emissions in 2006 were nearly twice the OECD (Organisation for Economic Co-operation and Development) average and over four times the world average (see Figure 8). Looking more specifically at domestic transport, the use of cars and motorbikes contribute to 53% (see Figure 9) of domestic transport emissions of $CO_{2\text{-}e}$ (equivalent CO_2 emissions) in 2006 (excluding electric rail). Hence reducing vehicular emissions may assist in mitigating the possible effects of global warming through the reduction of green house gases emissions. [9]

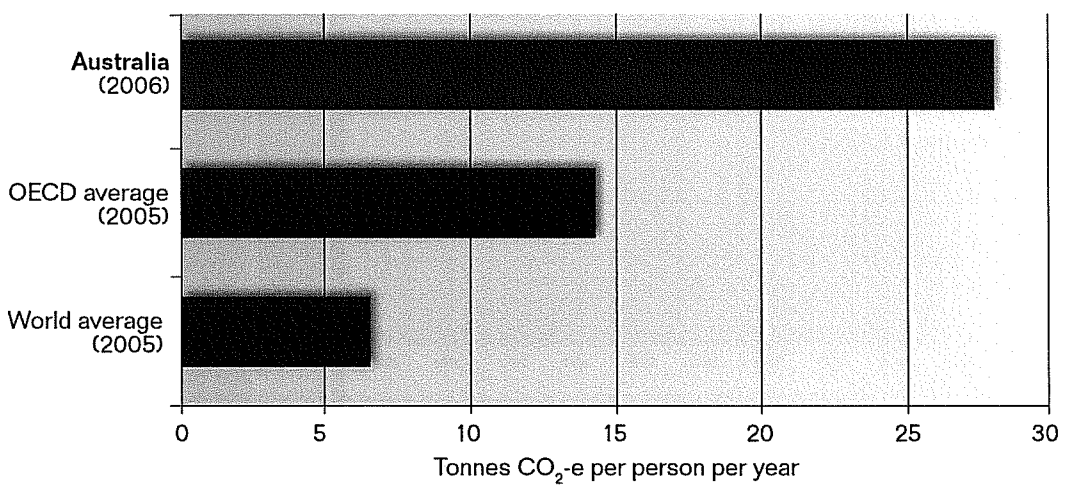

Figure 8 - Australia's Per Capita Emissions Of CO_2 Equivalent[9]

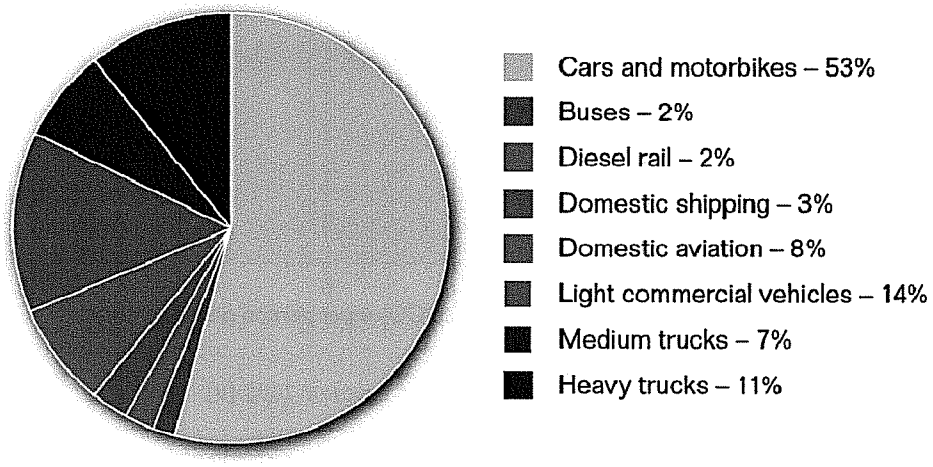

Note: Excludes electric rail and trams.

FIGURE 9 - AUSTRALIAN DOMESTIC TRANSPORT CO_{2-E} EMISSIONS [9]

While battery electric vehicles are essentially zero emission vehicles, the source of electricity may not be [10]. While it's true that Australia's dependence on coal (greater than 40% of total fuel sources see Figure 10) for electricity generation may have economic benefits (see 2.1.2 Economic Impacts), it does generate significantly greater CO_{2-e} emissions. Australia's emissions per capita due to electricity generation are approximately three times greater than the average OECD emissions (see Figure 11). [9]

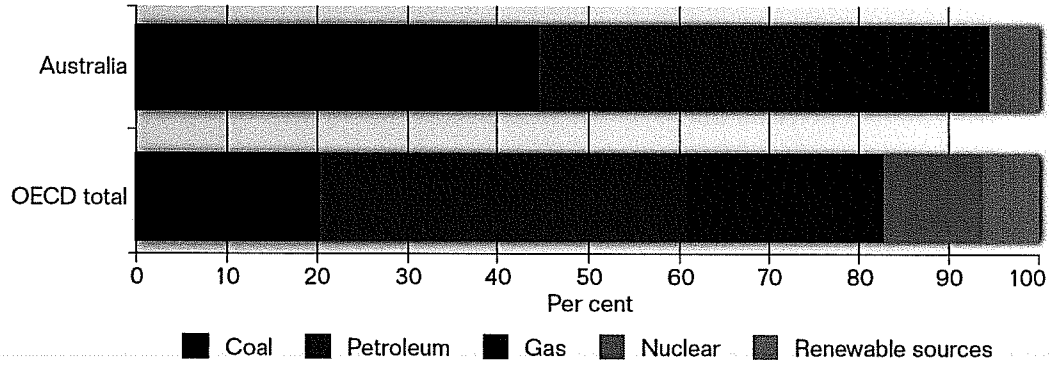

FIGURE 10 - FUEL MIX CONTRIBUTING TO PRIMARY ENERGY SUPPLY [9]

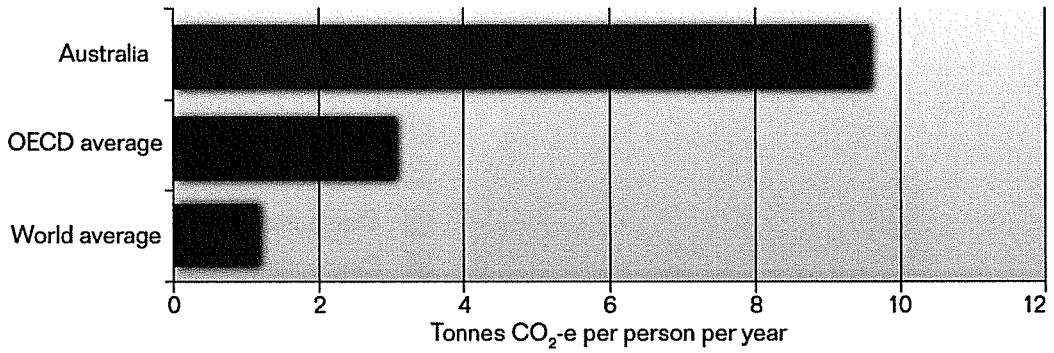

FIGURE 11 - PER CAPITA EMISSIONS DUE TO ELECTRICITY 2005 [9]

Garnaut's models show that on average an electric car would emit approximately 30% $CO_{2\text{-}e}$ emission, than the equivalent petrol vehicle if the car is powered from a typical Australian electricity grid. However this is location dependant for example in Tasmania electric cars may produce up to 85% fewer emissions than the petrol equivalent. [9] The user however does have a choice to the source of their electricity. Using renewable zero emission or low emissions electricity generation can practically remove all $CO_{2\text{-}e}$ emissions from their local domestic travel. Options include the installation of photo-voltaic panels on residential roofs that offset or replace the energy consumed by electric vehicles. Electricity suppliers such as Synergy also offer options such as Natural power allowing residential customers to select renewable electricity generation[11].

Brant argues however controlling emissions at a number of fixed and stationary power generation facilities is simpler than mobile targets such as petrol cars[10]. The CSIRO model projects that over the next decade the uptake of wind and natural gas combined cycle generation facilities will provide the majority of new energy generation facilities. With the introduction of the emissions trading scheme, the CSIRO also projects that over time, electricity generated for electric vehicles will increasing generated from low emission sources[8]. Therefore the adoption of electric vehicles powered from low emission generation facilities such as home installed photovoltaic systems or larger scale renewable generation facilities such as those offered by Synergy, can significantly reduce $CO_{2\text{-}e}$ emissions for domestic transport and play an important role in the mitigation of climate change.

2.1.2 Economic Impacts

Australia's production of crude oil reduced by approximately 40% between the years 2000 and 2004 as mature wells became depleted. More recently output production has stabilized, yet Australia which was once a country virutally self sufficient in crude oil supplies is now dependent on significant import quantities of crude oil to meet the domestic demand[8]. In the 2008-2009 financial year Australia imported a total of 14.441 billion Australian dollars of crude petroleum and an addition 12.199 billion Australian dollars of refined petroleum. The gross domestic product for the year 2008 was $1,013.1 billion US dollars ($1,214.6 billion Australian dollars) thus total petroleum imports accounted for 2.2% of Australian's GDP and 12% of total imports[12].

Petroleum oil is considered non-renewable and as such the oil supply eventually peak, after which production quantities will continually decrease as wells mature. The Energy Information Administration was formed to collect timely and accurate energy data, however it relies on 3rd parties to provide inputs or estimations of oil production and demand. OPEC, Russia and many other producers keep such information as state or corporate secrets. Data is also scarce throughout the Middle East where only a small number of 'Super Giant Middle East' fields have metering at the wells of oil production and water consumption[13].

The problem has further compounded as it is now known that many OPEC producing nations arbitrarily doubled or even tripled reported proven resources for the period of 1982 to 1988. This data then stayed stagnant for two decades creating the illusion that the quantity of resources was very conservative[13].

"Reservoir simulation models are simply educated guesses without sufficient information" [13]

The lack of good quality models has resulted in uncertainty about the future price of oil and in turn the cost of petroleum based fuels such as petrol[8, 13]. If global production of crude oil peaks in the near term and alternative fuels do not rapidly replace demand, fuel prices (petrol) may have to increase by as much as several dollars a litre to ration demand in Australia. Higher prices for petroleum based fuels will result in inflation in the Australian economy as the increased cost filters through the economy; increasing the cost of all goods and services. CSIRO report

that if oil prices are sustained at as high as US$100/bbl economic growth of Australia is expected to be reduced by approximately 3%[8].

Demand for oil is expected to continue to grow as developing nations such as China and India continue to prosper and as a result more of the population purchases petroleum fuelled vehicles. China is currently purchasing between 6-8 million cars per year, while India is currently purchasing approximately 1.8 million vehicles (mostly motorbikes) per year. The EIA expects to see Chinese energy consumption grow at an average of 3.5% per annum with a large proportion of this associated with the increasing number of vehicles on the street. Global demand for oil is therefore expected to continue to develop towards 100 MMB/D (million barrels per day), demand from oil producing nations is expected to increase also as these nations propensity to spend increases due to the increasing profitability of oil production. [13]

World peak production of crude oil occurred in May 2005 (see Figure 12) at 74.3MMB/D although crude oil producers had aimed since then to increase production capacity this record has not been breached. Resulting in the depletion of usable stocks, The EIA expects long term growth in production to be negative or at best flat while long term demand continues to grow (see Figure 13).

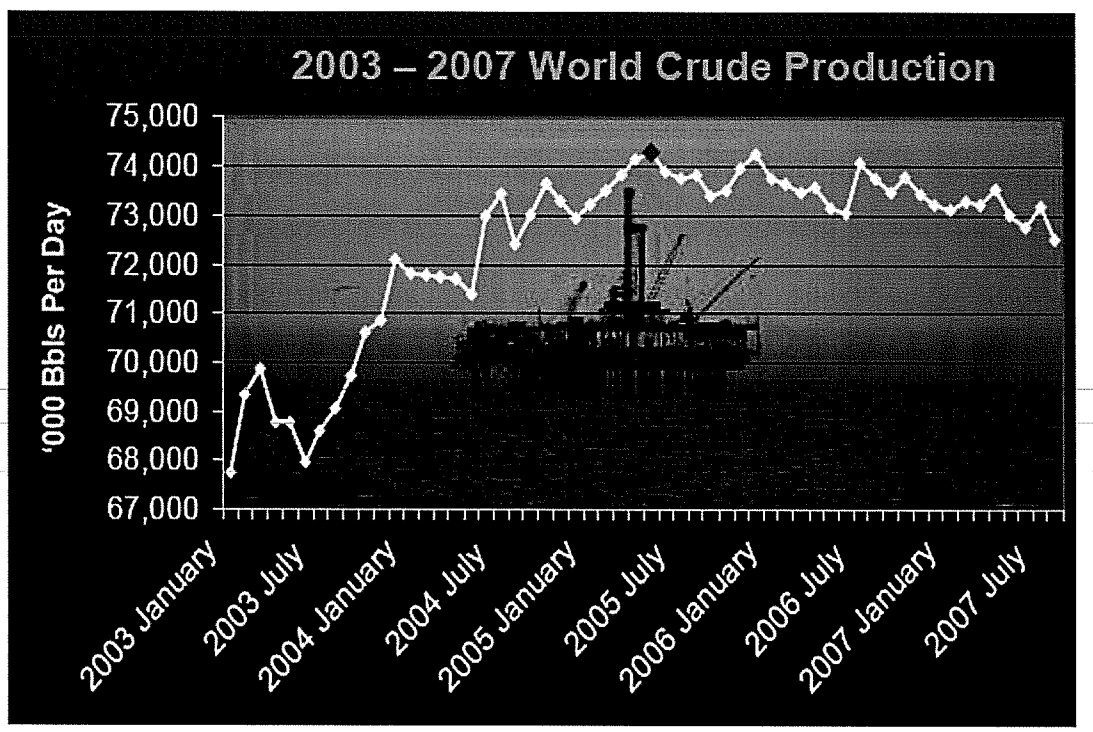

FIGURE 12 - WORLD PEAK OIL PRODUCTION [13]

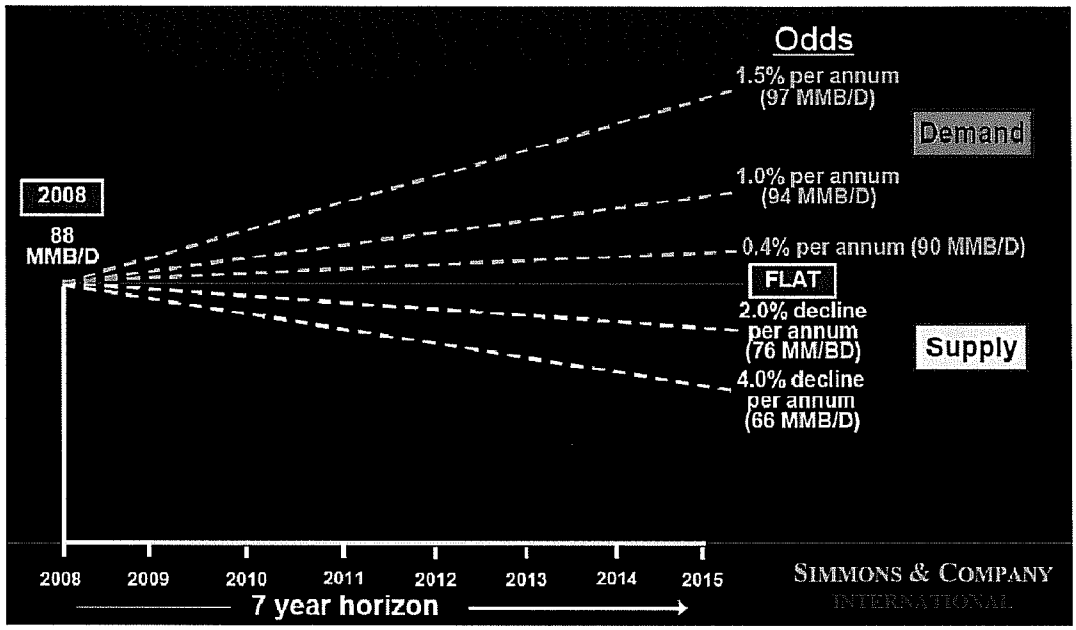

FIGURE 13 - EXPECTED DEMAND VS SUPPLY FOR CRUDE OIL[13]

Additional pressure on production costs and ultimately crude oil prices are also expected to develop as ageing infrastructure is required to be replaced. EIA expects that up to 80% of oil production infrastructure will need to be replaced in the near term as many mature wells have exceeded their original design life[13].

CSIRO have modelled future pricing of petrol, against how rapidly supply deteriorates and how fast technology is able adapt in providing alternative fuels. Figure 14 demonstrates a number of different scenarios, as one would expect a slow decline in world crude oil production with a fast technology response results in the best case scenario (smallest increase in fuel pricing). While a fast decline with a slow technology response promotes the worst case scenario with the cost of fuel peaking above $8 a litre in 2017. Technology response includes bio-fuel alternatives and alternative fuelled vehicles including plug-in hybrids and battery electric vehicles. [8]

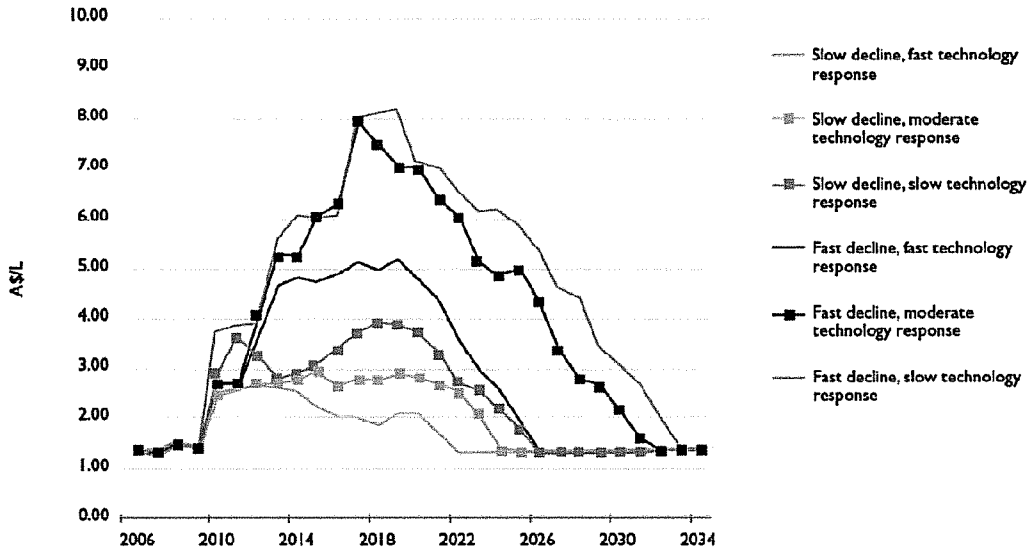

FIGURE 14 - MODELLED FUTURE PETROL PRICES[8]

Thus Battery Electric Vehicles such as those on the REV project offer two distinct advantages via transitioning the transport sector to a new more sustainable energy source. If the Australian public transitioned to electric cars that are powered from the grid, first this would result in a reduction in demand for petroleum based fuels, and hence putting negative pressure on the gap between supply and demand. If similar trends occur in other nations around the world the peak price in petroleum based fuels should also reduce from the technology response. This in turn will reduce inflationary pressures and hence reduce the impact on the nation's economic growth[8]. Secondly via converting to an energy source that is an abundant natural resource in Australia such as coal, petroleum imports will thus be reduced and henceforth reducing Australia's trade deficit.

2.2 VEHICLE BLACK BOX SYSTEMS

Vehicle black box systems are becoming almost common place is many vehicles especially those produced by General Motors. In 1994 General Motors started installing 'black box recorders' (see Figure 15) similar to the airline cousins in their cars. At the time the devices were advertised as strictly for internal to improve the safety of such vehicles. In fact this device was later used to find and subsequently correct a fault in the design of the air bag module that resulted in the air bag being inflated in-appropriately. The US National Transport Safety Bureau has recommended that black box recorders (or crash recorded) be installed in all

new car in the US. As of 2004 it was estimated that over 40 million vehicles had some form of black box crash recorder installed [14].

Although the black box recorded were originally developed for internal use GM did authorize a company called Vectronics (later purchased by Bosch) to begin developing, producing and marketing a reader to allow external third parties to access the data stored on the black box recorder. Data available to third parties included [14, 15]:

1994 Black Box Data Included:

- Vehicle speed prior to impact
- Engine speed
- Brake Status
- Throttle position
- Driver's seat belt status
- Passengers air bag status (enabled/disabled)
- Airbag Warning Lamp Status
- Time from impact to airbag deployment
- Maximum delta-velocity
- Delta V vs time
- Time from impact to maximum delta-V

Addition data available on newer vehicles:

- Low tie pressure warning system status
- Traction control status
- Anti lock brake status
- Transmission range
- Service engine lamp status
- Vehicle door open
- Outside air temperature
- Passenger seat belt switch
- Yaw rate
- Lateral acceleration
- Steering wheel angle
- Principal direction of force

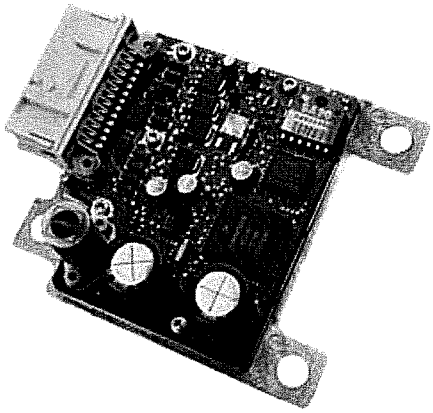

FIGURE 15 - GM AIR BAG BLACK BOX SYSTEM [15]

Notre Dame University developed a microcontroller based black box crash recorder in 2008. A number of sensors were implemented including an inductive speed sensor, conductive water sensor and various tactile switches. A PIC microcontroller programmed with PIC Basic was used, with a RS232 interface for downloading captured data. Crash data was recorded at half second intervals for a total capture time of 31.5 seconds. Data was stored on the PIC microcontroller's internal 256 byte EEPROM memory, with 4 bytes reserved for the memory counter and other status information. Windows software was also developed to playback crash data, and review analytical data [16].

Chonbuk National University, Jeonju Korea designed an embedded controller for a car black box system which was prototyped on an Altera FPGA with an 8051 processor. Stored information included photos from two onboard cameras encoded in JPEG form, driving data information (i.e. speed, brake and seat belts). Collision data (accelerometer) and positional data (GPS). A CAN bus was used to communicate with existing vehicle sensors, in addition to a number of serial busses including SPI and I^2C for board level communication. A wireless interface was also developed to allow for crash data to be received without having to remove the black box from the vehicle. [17]

Similar to the Notre Dame University design a circular buffer is used, however in this case the buffer is located in ram and only transferred to flash in the event of an accident. This design used an Secure Digital (SD) flash memory card providing a much larger dataset which aides in storing the photos from the onboard camera [17].

3. HARDWARE BLACK BOX DESIGN

3.1 BACKGROUND

The Hardware Black Box system was developed to complement existing black box systems that exist in a software form running on the car computer, both on the Eyebot controller in the Hyundai Getz and car PC in the Lotus Elise. The black box system should also be capable of running independently of an onboard computer system such that future REV vehicles which may not be fitted with an onboard computer can still have a functioning black box system.

The black box system unlike other commercial units on the market should be designed primarily for research purposes rather than post crash analysis. Hence unlike the systems discussed in the literature review, continuous data sampling will be required with a long history, instead of the few minutes around an event (crash) in the other systems.

The system should also be flexible in design, as to accommodate future data and inputs. The system should also be electrically hardened and protected against the large DC potentials that may exist between systems and inputs in an electric car, especially to maximize the chance of successful data retrieval after a fault. The system should also be designed with low power requirements such that it will be permitted to run constantly, an issue with the current software based black box systems.

The modular design of the black box system is shown in Figure 16, each module communicates to one of the two microcontrollers. The main processor is located on the Master Controller and the secondary microcontroller is located on the BMS Master Controller. Each module has its own independent serial bus, this allows for greatest flexibility, allowing several modules to be developed independently without the risk of affecting the stability of another module. Also improving the reliability of the entire system since if modules fail and prevent communication on a bus all other modules should still be able to function.

SPI (Serial Peripheral Interface bus) and UART was utilized were isolated busses are required. Since these protocols consist of unidirectional data lines, the design of the isolation circuitry is simplified, as opposed to protocols like I^2C and SMbus

whom have bidirectional data lines. SMBus was used to link the two processors since no isolation is required between the two microprocessors.

The HSPA modem is a future enhancement for vehicles unlike the Getz and Elsie that don't have an onboard computer with 3G connectivity.

The Vehicle Interface is an external module to the black box that has 32 digital IO lines and 16 analogue inputs. This module is designed to report on the vehicle status and connects to the 12V systems onboard. Possible vehicular inputs include headlights, seat belt status, warning lights, brake position, accelerator position, door switches, etc. The specific design of this board is not in the scope of this thesis, however documentation can be found on the REV project documentation server (http://www.therevproject.com/internal/).

The Car PC interface allows a UART interface emulated over USB between the car computer (Car PC or Eyebot Controller) and the black box system. This connection allows the car PC to receive the status information from all modules, removing the need for separate digital acquisition hardware. This allows informative displays to be developed on battery and vehicle status information.

The AC and DC analysis boards measures a number of power metrics of the respective power feeds. The AC analysis board is concerned with the mains power consumption during charging operations. While the DC analysis board keeps track of the traction pack power status and DC power consumption. Both of these modules use an isolated SPI busses to communicate to the main microcontroller.

Non-volatile memory storage takes the form of a microSD card installed on the Master Controller printed circuit board. The non-volatile Flash memory card is installed in a hinged card holder so that it can be removed for manual reading after an accident if the black box has been damaged, or for debugging purposes. This card communicates to the main processor through the SD SPI protocol.

The user interface consists of a graphical LCD screen for output to the user. Five buttons have been added for user navigation and input. The LCD screen is implemented by a unidirectional parallel bus. An embedded USB host was added to allow the user to download collected data easily onto a USB thumb-drive.

The BMS interface collects data from the traction pack cells individually via Battery Management System (BMS) modules. An individual BMS module is installed on every cell with a daisy chained serial interface. The charger interface predominantly is implemented to control the charging profile, and assist the BMS modules during balancing operations by reducing the charging current.

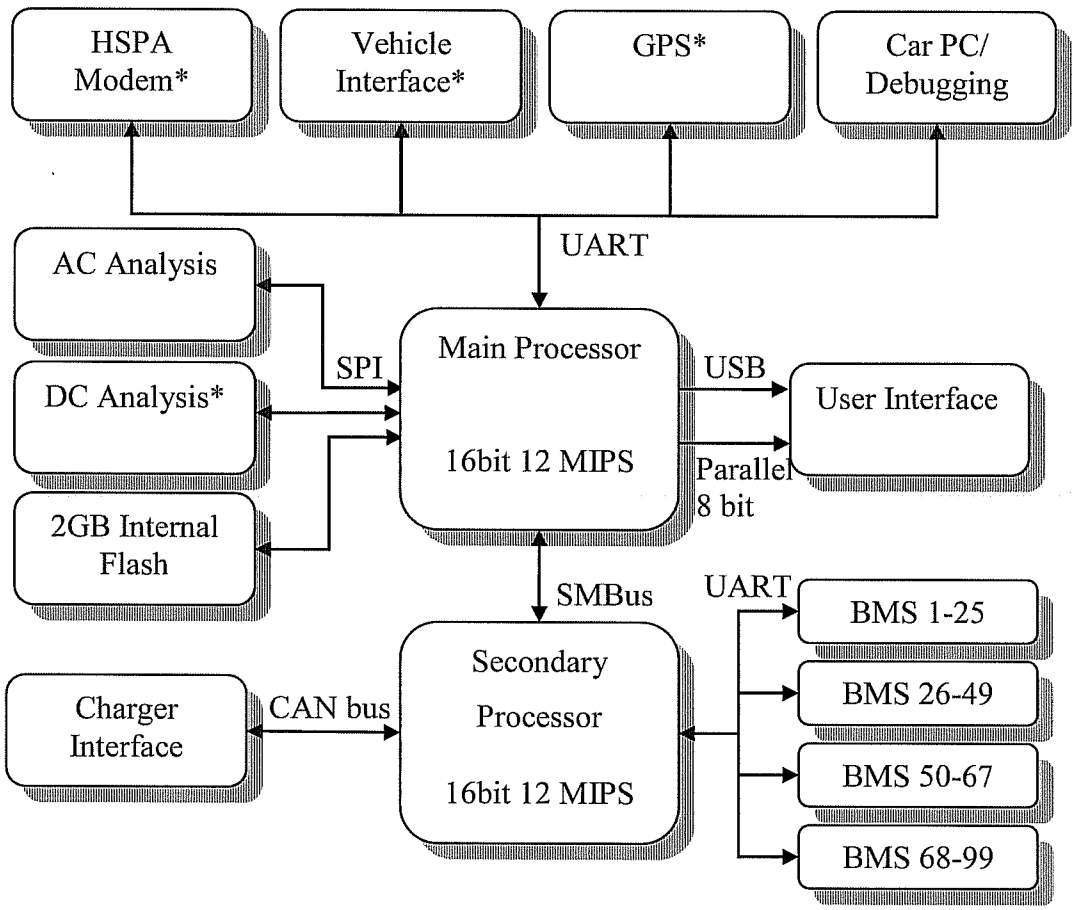

* Denotes modules not within scope of thesis

FIGURE 16 - BLACK BOX MODULES AND DATA BUSES

3.2 AC Analysis Board

3.2.1 Background

One of the central metrics of an electric car is its actual energy consumption per kilometre, as measured at the mains socket. Several methods have been used by the REV project to measure the input power in the past. Wireless sensors have been used to log total energy consumed by the vehicle, in addition to manual mechanical meters. However both of these methods require students to keep a log book of the number of kilometres travelled on a charge. Even with the best of intentions the log book often gets forgotten and is not updated. It is also difficult to ask sponsors and people external to the REV project to maintain the log book.

To solve this issue and also reduce the influence of human error, the AC Analysis board will record the power consumption during charging operations and this information is stored in the Hardware Black Box history. Since the black box also keeps a record on distance travelled through the speedometer input on the Vehicle Interface and via the GPS receiver; accurate records of power consumed per kilometre travelled can be compiled.

3.2.2 DESIGN

The final design of the AC analysis board is shown in Figure 17. The justification of design follows.

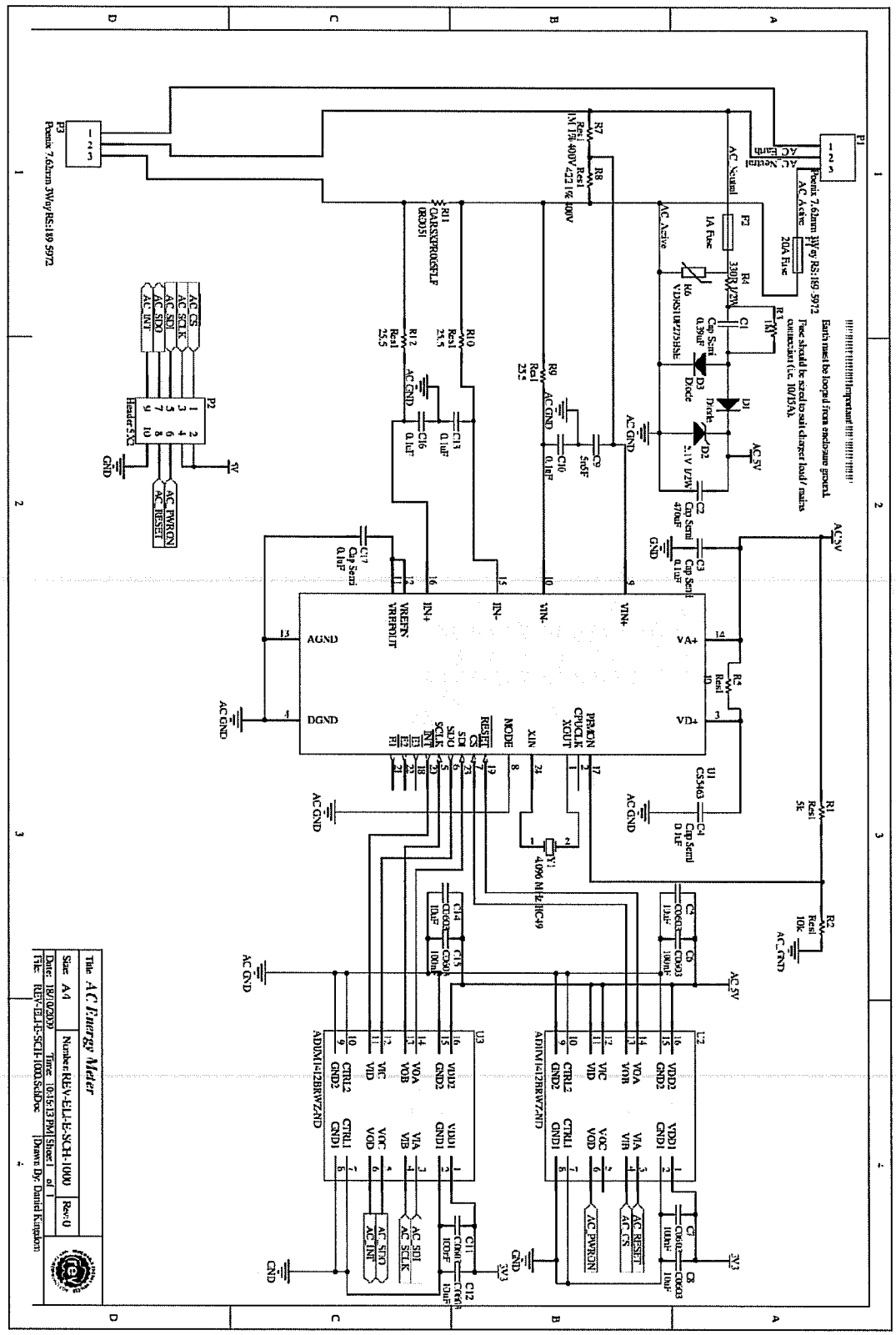

FIGURE 17 - AC ENERGY METER SCHEMATIC

The CS5463 is at the centre of this design, this devices combines two differential ΔΣ analogue to digital converters, a serial interface and a digital signal processor (DSP) core. The device is designed to accurately measure instantaneous current and voltage, Root Mean Square (RMS) voltage and current, instantaneous power, apparent power, active power and re-active power for single phase power applications[18].

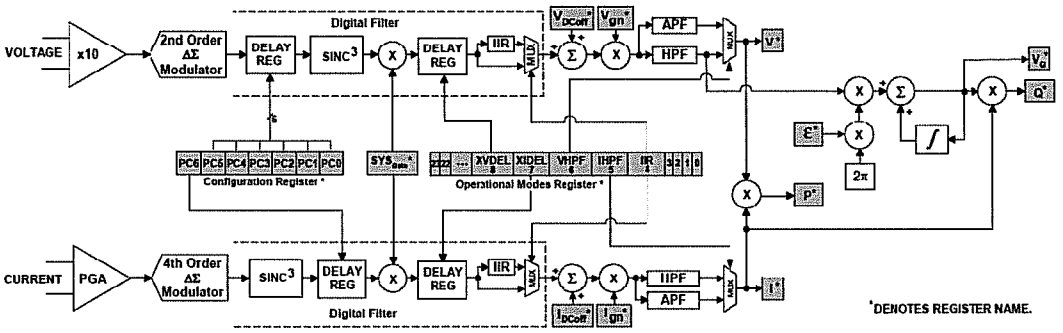

FIGURE 18 - DATA MEASUREMENT FLOW GRAPH[18]

Figure 18 shows the measurement flow, after anti-aliasing filtering is done externally, a series of digital filters are implemented in the DSP core. The $Sinc^3$ filtering is used by Cirrus Logic to reduce noise from the analogue to digital sampling process. The IIR filter is user to compensate for the magnitude roll off from the $Sinc^3$ filter and finally a high pass filter is used to remove any dc offset (or common mode) present in signal to reduce measurement error[18].

3.2.3 AC INPUT PARAMETERS

The AC analysis board is designed for a maximum AC input of 250V AC and 20A RMS. This is to allow for various charging profiles and setups, and to prevent the need for replacing components on the AC analysis board for different configurations.

The maximum input on both the voltage and current channels is 250mVp-p (176.7mV RMS)[18]. To prevent over driving the channels, a safety margin of 0.6 is used thus the maximum peak-peak voltage is:

$$V_{V_{p-p}} = 250mV_{p-p} * 0.6$$
$$= 150mV_{p-p}$$
$$= 106.07\ mV\ RMS$$

EQUATION 1 - MAXIMUM CHANNEL VOLTAGE

Knowing the RMS input voltage for both channels (with a 10x gain) the value of the current sense resistor for the current sense channel can be easily calculated using ohms law.

$$V_{RMS} = I_{RMS} * R_{shunt}$$
$$R_{shunt} = \frac{V_{RMS}}{I_{RMS}}$$
$$= \frac{106.07mV\ RMS}{20A\ RMS}$$
$$= 5.305\ m\Omega$$

EQUATION 2 - CURRENT SENSE RESISTOR

The closest available value is 5mΩ (that also meets the power requirements) to calculate total power dissipated at 20A RMS:

$$P_{RMS} = V_{RMS} * I_{RMS}$$
$$= R * I_{RMS}^2$$
$$= 5m\Omega * 20^2\ A$$
$$= 2.00W$$

EQUATION 3 - CURRENT SENSE RESISTOR POWER DISSIPATION

The IRC OARSXPR005FLF open air current sense resistor was selected, and offers 1% accuracy and a maximum power rating of 5W in addition to low inductance and a wide operating temperature range of -40°C to 125°C.

A potential divider is formed by R6 and R7. To reduce static power dissipation the series resistance formed between the active and the neutral shall be greater than 1 MΩ. Applying the 0.6 Safety factor again the AC input voltage shall be scaled to 106 mV_{RMS}. Thus setting the upper dividing resistor (R6) to 1MΩ the value of R7 can be calculated.

$$V_{scalled} = V_{in} * \left(\frac{R_7}{R_7 + R_6}\right)$$

EQUATION 4 - POTENTIAL DIVIDER

$$R_7 = \left(\frac{V_{scaled}}{V_{in}}\right) * (R_7 + R_6)$$

$$R_7 * \left(1 - \frac{V_{scaled}}{V_{in}}\right) = \frac{V_{scaled}}{V_{in}} * R_6$$

$$R_7 = \frac{\frac{V_{scaled}}{V_{in}} * R_6}{\left(1 - \frac{V_{scaled}}{V_{in}}\right)}$$

$$= \frac{\frac{106.07mV_{RMS}}{250V_{RMS}} * 1M}{1 - \frac{106.07mV_{RMS}}{250V_{RMS}}}$$

$$= 424.18\Omega$$

EQUATION 5 - REQUIRED VALUE OF R7

The nearest available lower value is 422Ω (E96) which when substituting back into the original potential divider (Equation 4) gives:

$$V_{scalled} = 250V_{RMS} * \left(\frac{422\Omega}{422\Omega + 1M\Omega}\right)$$

$$= 105.46\, mV_{RMS}(2dp)$$

EQUATION 6 - FULL SCALE RANGE OF THE VOLTAGE CHANNEL

3.2.4 ANTI-ALIASING

The sampling period of the delta sigma analogue to digital converters (ADC) on the CS5463 is a fixed ratio of the main clock input (MCLK)[19] which is derived from crystal Y1. Y1 has a frequency of 4.096MHz thus the sampling frequency is:

$$f_{samp} = \frac{MCLK}{8}$$

$$= \frac{4.096MHz}{8}$$

$$= 512kHz$$

EQUATION 7 - SAMPLING FREQUENCY

When an analogue signal is sampled at a fixed frequency aliasing of the signal can occur. This results when a component of the analogue signal has a frequency greater than $\frac{f_S}{2}$ (f_S is the sampling frequency) these frequency components are then folded back about $\frac{f_S}{2}$ such that the aliased frequency in the sampled message becomes:

$$f_{ALIASED} = |f_{IN} - Nf_S|$$

EQUATION 8 - ALIASED FREQUENCY FOLD-BACK[20]

Where N ≥ 0 and $f_{ALIASED} \leq \frac{f_S}{2}$.

Thus according to the Nqyuist-Shannon sampling theorem for a signal to be reconstructed in the digital domain the sampling frequency (f_S) must be twice the bandwidth of the analogue signal. Figure 19 shows how the analogue signal (a) which contains frequency components greater than $\frac{f_S}{2}$ is aliased once the signal is sampled at frequency f_S resulting in the components greater than $\frac{f_S}{2}$ being folded back about $\frac{f_S}{2}$ (b).

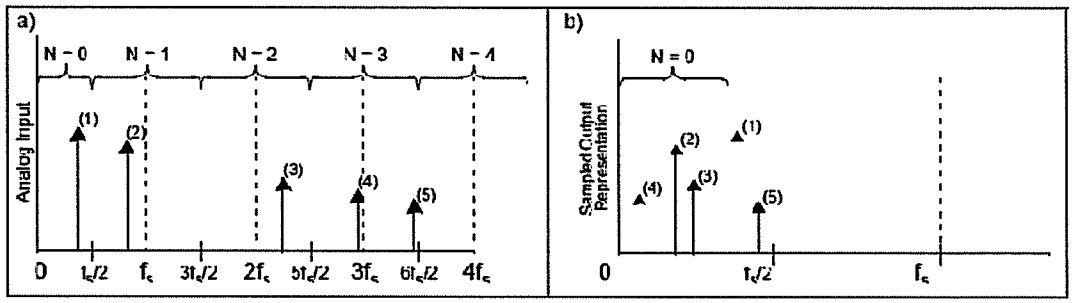

FIGURE 19 - OUTPUT FREQUENCY 'FOLDED BACK' ABOUT THE NYQUIST RATE[20]

If the analogue bandwidth of the signal was not limited, it is clear that digital representation of the signal would produce erroneous measurements. Applying a low pass filter with a 3dB corner at $\frac{f_S}{2}$ will attenuate the out of band frequencies ($>\frac{f_S}{2}$) and hence reduce measurement error due to aliasing (see Figure 20). By lowering of the corner frequency the magnitude of the frequency components will be attenuated further.

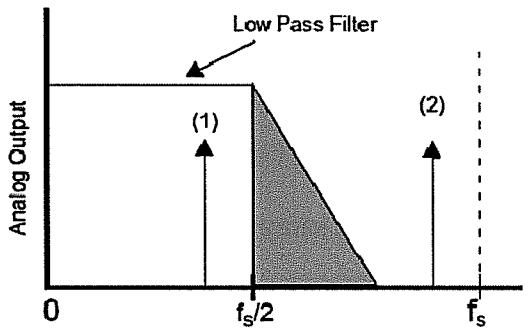

FIGURE 20 - LOW PASS FILTER[20]

The sampling frequency as previously discussed is fixed at $f_s = 512kHz$ and thus the maximum bandwidth is $B = \frac{f_s}{2} = 256kHz$. Thus the design is significantly over-sampled when compared to 50Hz AC mains, the advantage of oversampling is that it allows for the use of a simpler anti-aliasing filter with a lower order. In this case a simple passive resistor-capacitor filter of order 1 will provide sufficient attenuation (as recommended by Manufacturer [19]).

The switching frequency of the Zivan NG3 charger is nominally 30kHz[21] , the 3dB corner of the low-pass filter was set at the second harmonic of the switching frequency and thus the corner frequency (f_c) was set to 60kHz.

$$f_c = \frac{1}{2\pi RC}$$

EQUATION 9 - CORNER FREQUENCY[20]

Choosing the Capacitor to be a fixed value of 0.1μF the value for R can be simply calculated as:

$$\begin{aligned} R &= \frac{1}{2\pi C * f_c} \\ &= \frac{1}{2\pi * 0.1 * 10^{-6} * 60 * 10^3} \\ &= 26.526\Omega \end{aligned}$$

EQUATION 10 - ANTI-ALIASING SERIES IMPEDANCE

Choosing the nearest E96[22] value resistor, R = 25.5Ω and a 1% tolerance was selected to maximize filter matching between channels. The selected component was a thick film precision resistor in a 0805 package; part number RK73H2ATTD25R5F from KOA Speer. The capacitor selected was a stable

stacked metalized film chip capacitor that offers high stability in capacitance value over both frequency (see Figure 21) and temperature.

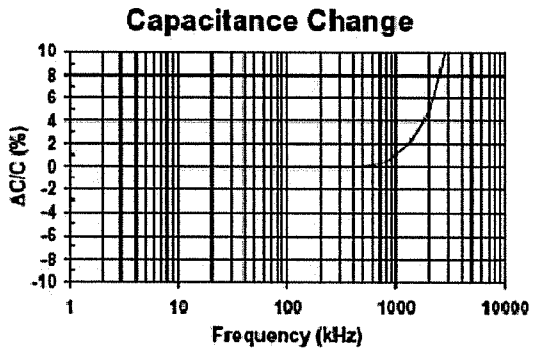

FIGURE 21 - CAPACITANCE CHANGE VS FREQUENCY[23]

The anti-aliasing filter was then modelled (see Figure 64) in OrCad Pspice with the following bode plot results. The 3dB point (corner frequency) is at 62.4KHz. Since the voltage and current channels have the same filters the phase shifting from the filter will be cancelled (within the tolerances of components) by the other channel in the power measurements.

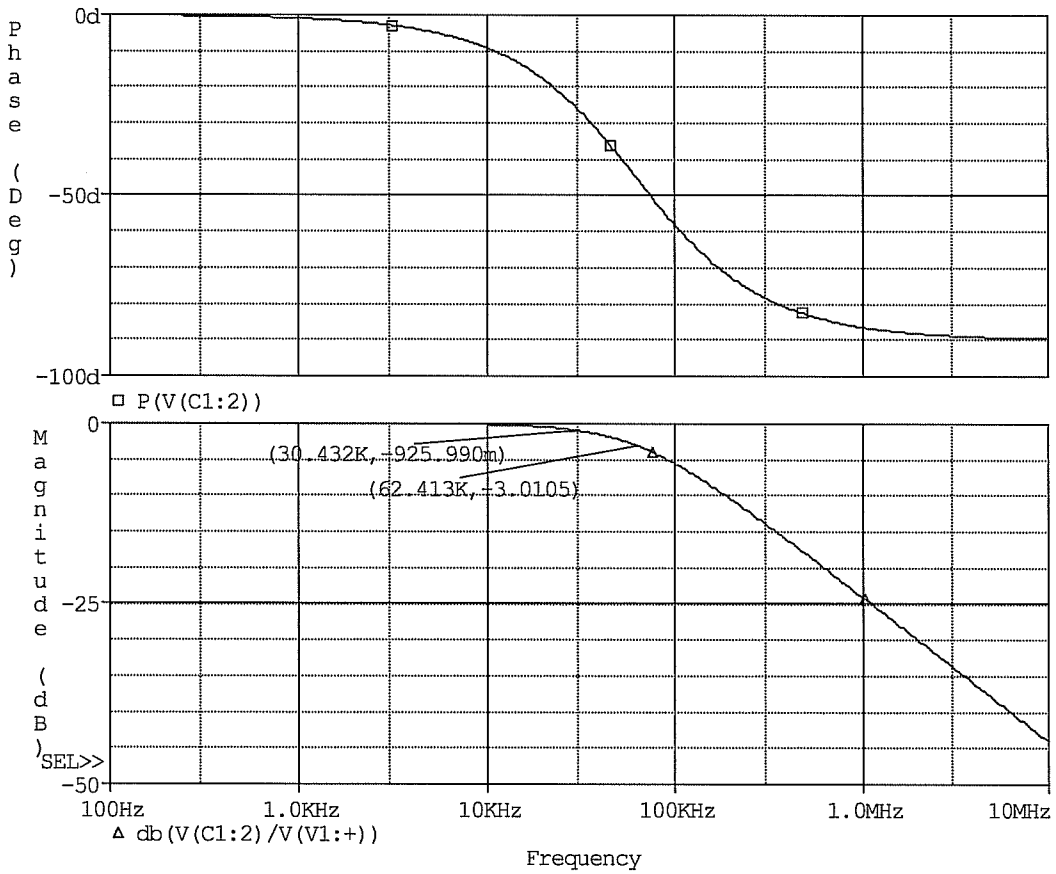

FIGURE 22 - ANTI-ALIASING FILTER BODE PLOT

3.2.5 Power Supply

The AC Analysis board is powered directly from the AC mains, the advantaged to this source of power is that the board will only be energized while the mains is present. This removes the need for the circuit to be continuously powered (via an isolated DC-DC converter) from the 5V rail, and ultimately from the traction pack. The power requirements of the AC analysis board are relatively minimal as only the Energy Meter IC (CS5463 from Cirrus Logic) and the two iCoupler Digital Isolators (ADUM1412BRWZ from Analogue Devices) need to be energized. Table 1 lists the maximum supply currents required by the two different integrated circuits.

Device	Maximum Supply Current
ADUM1412BRWZ	4.6mA (5V, < 5MHz)[24]
CS5463	2.9mA (VA+ = VD+ = 5V)[19]

Table 1 - Maximum Supply Currents Required

The Power Failure monitor (PFMON on the CS5463) also requires a resistive path from AC_5V to ground with a total impedance of 15kΩ (R1 & R2). Thus requires an additional static supply of:

$$I_{static} = \frac{4.9V}{15k\Omega} = 0.327mA$$

Equation 11 - Static Power Consumption Of PFMON

Thus the total supply current is:

$$I_{OUT_{MAX}} = I_{static} + 2I_{ADUM} + I_{CS5463} = 0.327 + 9.2 + 2.9 = 12.43\ mA$$

Equation 12 - Total Supply Current

There are a number of options for power supply designs including the traditional transformer and rectifier designs and various switch mode designs. However since the circuit only requires 12.43mA (62mW) and consumes its energy from the mains, both weight and component count take priority over the power supplies efficiency. Thus two additional transformer-less design options include resistive and capacitive. A capacitive power supply was chosen as it offers the following advantages[25]:

- Significantly smaller in size (and weight) than a transformer based solution.
- Lower cost than a transformer based power supply.
- More power efficient than a resistive power supply.

With the consequence being that it is slightly more expensive than a resistive supply due to a single additional component (the capacitor).

The following figure shows the circuit design for a capacitive transformer-less power supply.

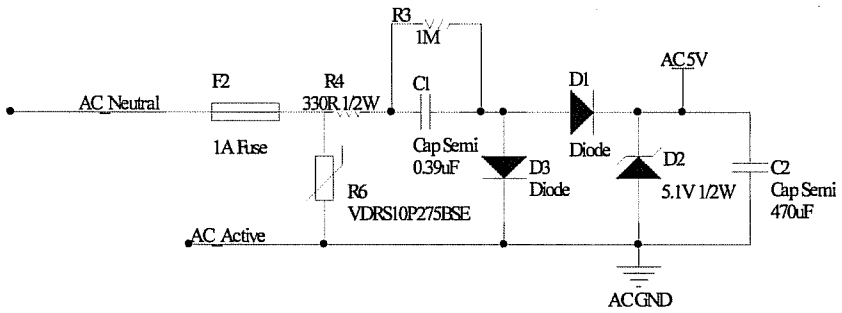

FIGURE 23 - AC ANALYSIS POWER SUPPLY[19]

It should be noted that the AC ground is at the same potential as the main active, thus extreme caution should be observed as the ground plane is at a hazardous voltage relative to earth. For this hazard two Perspex/ Acrylic panels are mounted on either side of the PCB to significantly reduce the risk of accidental contact to the mains voltage. When servicing or upgrading the black box system, all AC and DC inputs must be disconnected and sufficient time should be observed before opening the enclosure to make sure that capacitors such as C1 above have bleed to ground.

The power supply will stay in regulation as long as the half-wave RMS input current in addition with the minimum zener current is always greater than the output current. The maximum output current was calculated in Equation 12, adding a 50% safety margin the minimum input current is then:

$$I_{IN_{MIN}} = 1.5 * I_{OUT_{MAX}}$$
$$= 12.43 * 1.5$$
$$= 18.65\ mA$$

EQUATION 13 - MINIMUM I_{IN} CURRENT

From the circuit diagram the RMS input current of the circuit (for the half-wave) is:

$$I_{IN} = \frac{V_{H_{RMS}}}{X_{C1} + R_4}$$

EQUATION 14 - RMS INPUT CURRENT FOR THE HALF-WAVE [25]

Where:
$V_{H_{RMS}}$ is the RMS voltage across C1 and R4 for the half wave ($V_{Neutral} > V_{ACTIVE}$)

X_{C1} is the reactance of capacitor C1.

The half-wave voltage can be found from the Peak AC voltage minus the zener voltage and the forward voltage drop of D1:

$$V_{H_{RMS}} = \frac{V_{peak} - V_{D1} - V_Z}{2}$$

EQUATION 15 - RMS VOLTAGE OF THE HALF-WAVE [25]

The CS5463 has the most stringent supply requirements for supply voltage and requires a V_{DD} between 4.75 and 5.25V. A zener voltage of 5.1V with a 2% voltage tolerance was chosen (4.98V – 5.202V) based upon availability. The rectifying diode D1 has a voltage drop of approximately 0.9V, Thus the RMS half-wave voltage is (at mains 240V RMS):

$$V_{H_{RMS}} = \frac{\sqrt{2} * 240 - 0.9 - 5.1}{2}$$
$$= 166.7\ V_{RMS}$$

The maximum impedance formed by C1 and R4 is therefore (from Equation 14)

$$|Z| = |X_{C1} + R_4| = \frac{V_{H_{RMS}}}{I_{IN}}$$
$$= \left|\frac{166.7}{0.018565}\right|$$
$$= 8.979k\Omega$$

EQUATION 16 - INPUT IMPEDANCE

The function of R4 is to limit in rush current, the value however must also be limited such that excessive power is not dissipated through the resistor. It should also be noted that R4 and C1 has the full-wave RMS voltage across them as they are prior to the half-bride rectifier (D1 and D3). As an upper bound approximation the forward voltages of D1and D2 and the reverse voltage of D3 is ignored. Good design practice stipulates as a rule of thumb that the maximum power dissipation should not exceed half of the resistor's manufacturers rating[25]. To limit heat output the rating of R1 will be limited to half a watt and thus limiting theoretical heat production to a quarter of a Watt:

$$P_{R_4} = I^2R$$
$$= \left(\frac{V_{RMS}}{|Z|}\right)^2 * R$$
$$R_4 = \frac{P_{R_4}}{\left(\frac{V_{RMS}}{|Z|}\right)^2}$$
$$= \frac{0.25}{\left(\frac{240}{8979}\right)^2}$$
$$= 349.9\Omega$$

EQUATION 17 - AC SERIES IMPEDANCE

The nearest E24 value (5% tolerance) value for R4 is then 330Ω (maximum 346Ω at 5%).

Thus the required reactance of C1 can now be calculated using the mains frequency ($f = 50Hz$).

$$|X_{C1}| = \left|\frac{1}{2\pi f C_1}\right| = |Z| - R_4$$
$$= 8979 - 330$$
$$= 8.649k\Omega$$
$$C_1 = \frac{1}{8649 * 2\pi f}$$
$$= \frac{1}{8649 * 2\pi * 50}$$
$$= 0.368\,\mu F$$

EQUATION 18 - AC SERIES CAPACITANCE

The nearest appropriate E12 value (10% tolerance) value for C1 is 0.390µF. The voltage rating of the capacitor should be at least double the RMS voltage, and thus must be at least 500VAC. The maximum half-wave input current can be calculated by considering component values and worst-case tolerances.

$$I_{IN_{MAX}} = \frac{V_{H_{RMS}}}{X_{C1} + R_4}$$
$$= \frac{\left(\frac{V_{peak} - V_{D1} - V_Z}{2}\right)}{\frac{1}{2\pi f C_1} + R_4}$$
$$= \frac{\left(\frac{\sqrt{2} * 250 - 0.9 - 5.1}{2}\right)}{\left(\frac{1}{2\pi 50.5 * 0.390 * 10^{-6} * 1.1}\right) + (330 * 1.05)}$$
$$= \frac{173.78}{7346.3 + 346.5}$$
$$= 22.59\,mA$$

EQUATION 19 - MAXIMUM INPUT RMS CURRENT

Calculating the maximum power dissipation through the zener diode D2 is calculated using the maximum input current and the worst-case voltage tolerance of the zener(2%).

$$P_{D2_{max}} = I_{IN_{max}} * V_{D2}$$
$$= 22.59 * 5.1 * 1.02$$
$$= 118\,mW$$

EQUATION 20 - MAXIMUM ZENER POWER DISSIPATION

Good design practice[25] states that the rated power dissipation should be at least double the maximum calculated value. Thus a 5.1V 2% 1/2W zener was used based partially on availability. The sizing of D1 and D3 are selected based upon the maximum reverse voltage which should greater than the peak AC voltage (Approximately 350V). The RMS current through these rectifiers is equal to the half-wave RMS current calculated by Equation 13. Thus with a 0.9V forward voltage the power dissipated by these devices is:

$$\begin{aligned} P_{D1} = P_{D3} &= V_f * I_{IN_{max}} \\ &= 0.9 * 22.59mA \\ &= 20.33mW \end{aligned}$$

EQUATION 21 - MAXIMUM RECTIFIER POWER DISSIPATION

Thus a 1A, 400V rectifying diodes are sufficient for reliable operation.

To help suppress EMI (Electro-Magnetic Interference) a 1MΩ resistor (R3) was added in parallel with C1 to form a simple suppression filter. For circuit protection an additional 1A fuse (F2) was added, to protect the circuit from over current, as the main 20A fuse would be insufficient to protect this part of the circuit.

To protect the circuit from transient spikes that may occasional occur with a peak voltage between 1-5kV[26] a transient voltage suppression device (TVS) was added. The rated standoff voltage (V_{WM}) is the highest peak voltage that is expected under normal operation (i.e. when the TVS is at maximum impedance)[27]. Thus the rated stand-off voltage is the peak voltage of the maximum expected input voltage ($250V_{RMS}$), thus:

$$\begin{aligned} V_{WM} &= \sqrt{2} * V_{RMS} \\ &= 354\, V_{peak} \end{aligned}$$

The TVS breakdown voltage (V_{BR}) is 10-15% above $V_{WM}$and stipulates the voltage at which the TVS enters avalanche[27]. The clamping voltage (V_C) is the maximum clamping voltage during a specified peak impulse current and is typically 35-40% larger than V_{BR}. Microsemi recommends a power rating of between 400 and 600W for board mounted designs. Restricted by availability the VDRS10P275BSE VDR Metal Oxide Varistor from Vishay/BC Components, was

selected. This unit has a rated standoff voltage of $V_{WM} = 388\ V_{peak}\ (275V_{RMS})$ and a breakdown voltage of $V_{BR} = 430V_{peak}$ and a final clamping voltage of $V_C = 710V_{peak}$ [28].

3.2.6 Communication and Isolation

The CS5463 communicates to the host processor on the Master Controller via a SPI bus (3 wire bi-direction synchronous serial bus); with two additional digital signals (reset and interrupt) (refer to Table 2). The reset line is used to initialize the CS5463 once the AC power supply has stabilized, or to reset the device if a fault occurs. Chip select is asserted low prior to start of SPI communication to signal the start of a transfer. SDI and SDO contain the bidirectional serial data inputs and outputs respectively. SCLK carries the serial clock during data transfers. The interrupt line is asserted low to represent that the CS5463 requires attention from the host processor, typically this is because new measurement data is available, or the device has powered on (AC cable was plugged in). This allows the host processor to simply monitor the interrupt line as opposed to constantly polling the serial interface.

Pin	Direction at CS5463	Function
$\overline{CS}$	Input	Active low chip select
SDI	Input	Serial Data In (SPI)
SDO	Output	Serial Data Out (SPI)
SCLK	Input	Synchronous Clock Input (SPI)
$\overline{Reset}$	Input	Active low reset CS5463
$\overline{INT}$	Output	Active low Interrupt

Table 2- CS5463 SPI Specification

Isolation for the AC analysis board uses the same family of isolators as utilised on the Master Controller and the BMS Master Controller boards. The iCoupler digital isolators from Analogue Devices were selected due to their low static and dynamic power requirements compared to the more conventional opto-couplers (the ADUM1412BRWZ requires 2.3mA per channel at 5Mbps[29]), the devices also support high bandwidth up to 10Mbps and provide a Isolation working voltage of $V_{IORM} = 560V_{peak}$ the devices also offer a significant cost benefit over

optocoupler alternative, for example costing of the HCPL-2202 (5Mbps single channel) is $3.06 [30] each compared to ADUM1412BRWZ (quad channel 10Mbps) at $6.56 [31].

The isolators are also used to perform voltage level conversion from the 5V signals on the AC side to the 3.3V signals required by the Master Controller board. Pin 6 on U2 is used to detect the presence of 5V on the AC side such that initialization can commence. This is achieved by setting the CTRL1 pin to ground, the function of this pin is to set the default of an output when the isolated side does not have a valid V_{DD} available. After isolation the AC analysis board connects to the Master Controller via a 5x2 IDC cable (PIN 2 is the Key Pin) on connector P2.

3.3 BMS Master Controller

3.3.1 Background

The BMS Master Controller communicates with the individual BMS (Battery Management System) units located on every cell (see Figure 24). This board can operate independently or can be connected to the Master Controller for additional functionality. The BMS units were developed independently by Ivan Neubronner and are designed to be bolted directly on top of the Thundersky $LiFePO_4$ cells. A two wire serial link is daisy chained along the string of BMS Modules and to the BMS Master Controller.

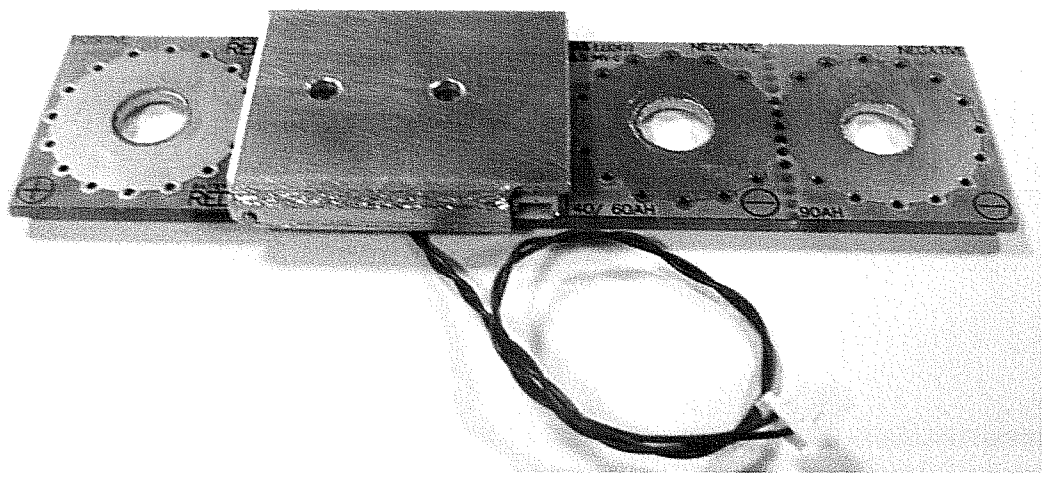

Figure 24 - Prototype BMS Unit

The Function of the BMS is firstly to improve cell life by preventing over-discharge and over-charging of the cells through the monitoring of individual cell voltages. The BMS also balance the cells during charging, that is that if a cell is approaching full charge early in the charging cycle a shunt load will be placed across the battery to 'bypass' the charging current over the cell. The bypass state will be entered into when a cell voltage reaches 3.8V, and each BMS module is capable of bypassing up to 4A for 30 seconds. The bypassing current is then limited by the MOSFET / heat sink temperature which is maintained at a maximum of 100°C. The second function of the BMS is to provide continuous measurement data of the cell status for recording in the black box system for later research use.

3.3.2 DESIGN:

The following figures show the final design of the BMS Master Controller. These documents are also available on the document control system along with the other project files.

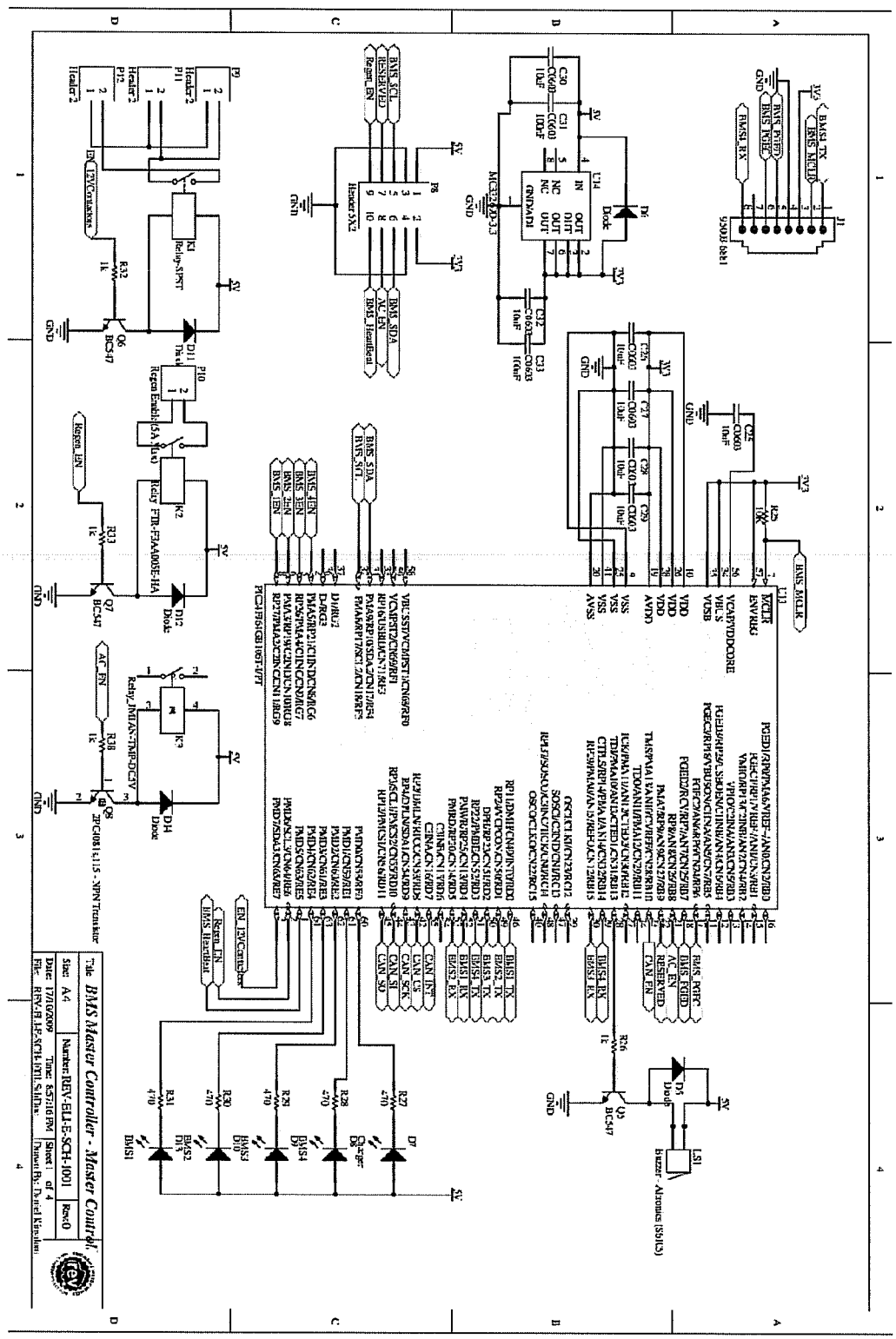

FIGURE 25 - BMS MASTER CONTROLLER SHEET 1 OF 4

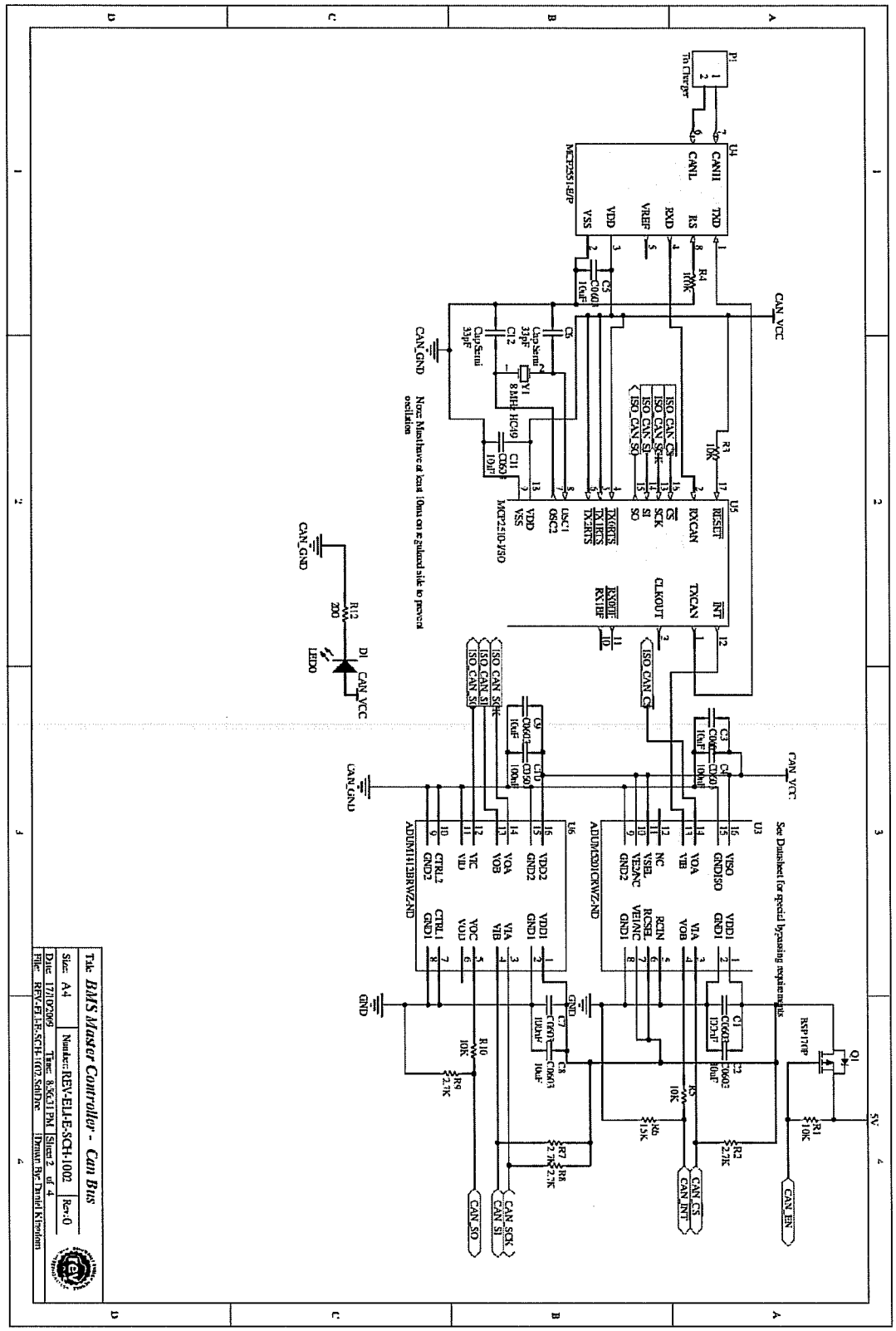

FIGURE 26 - BMS MASTER CONTROLLER SHEET 2 OF 4

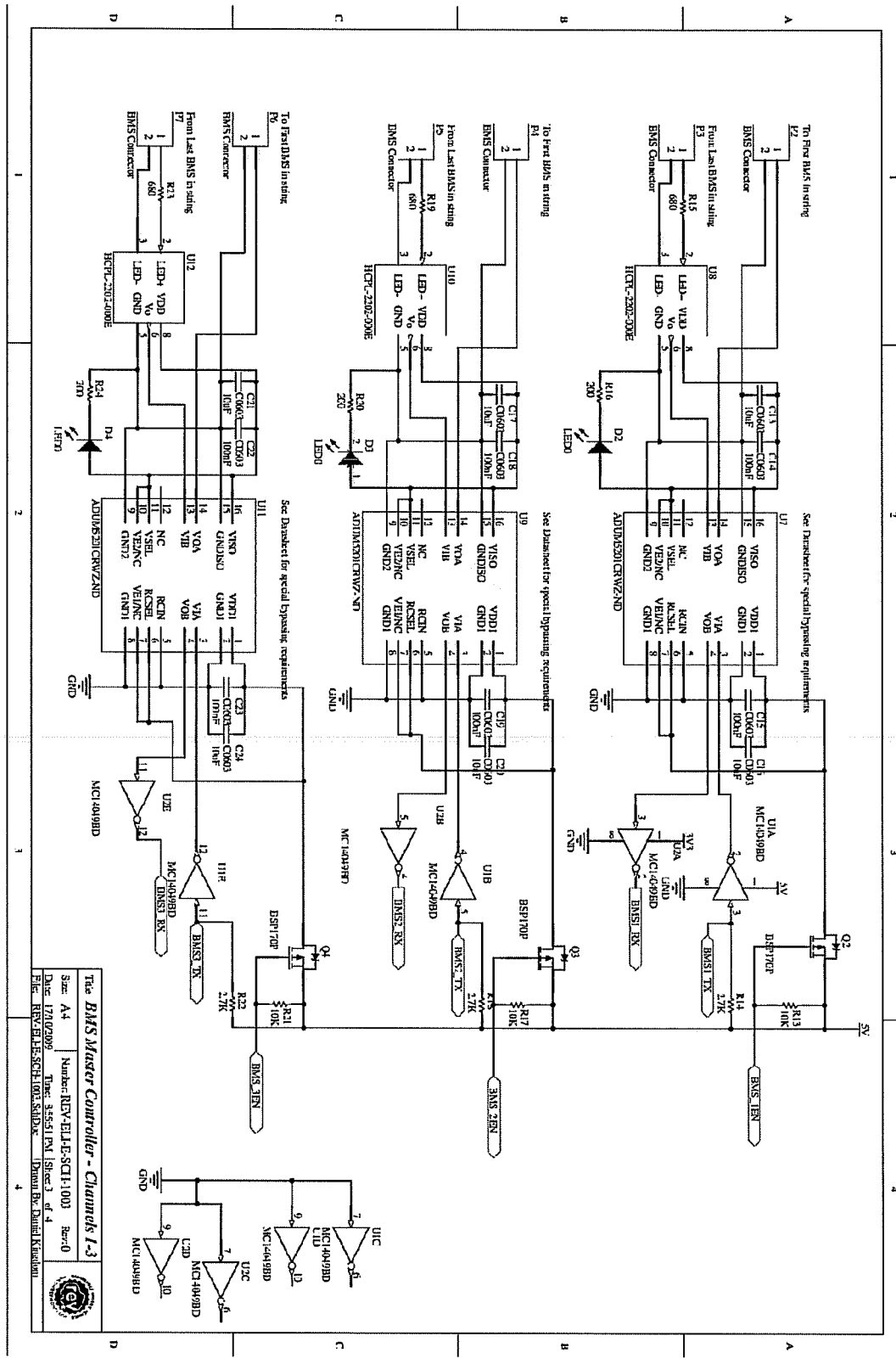

FIGURE 27 - BMS MASTER CONTROLLER SHEET 3 OF 4

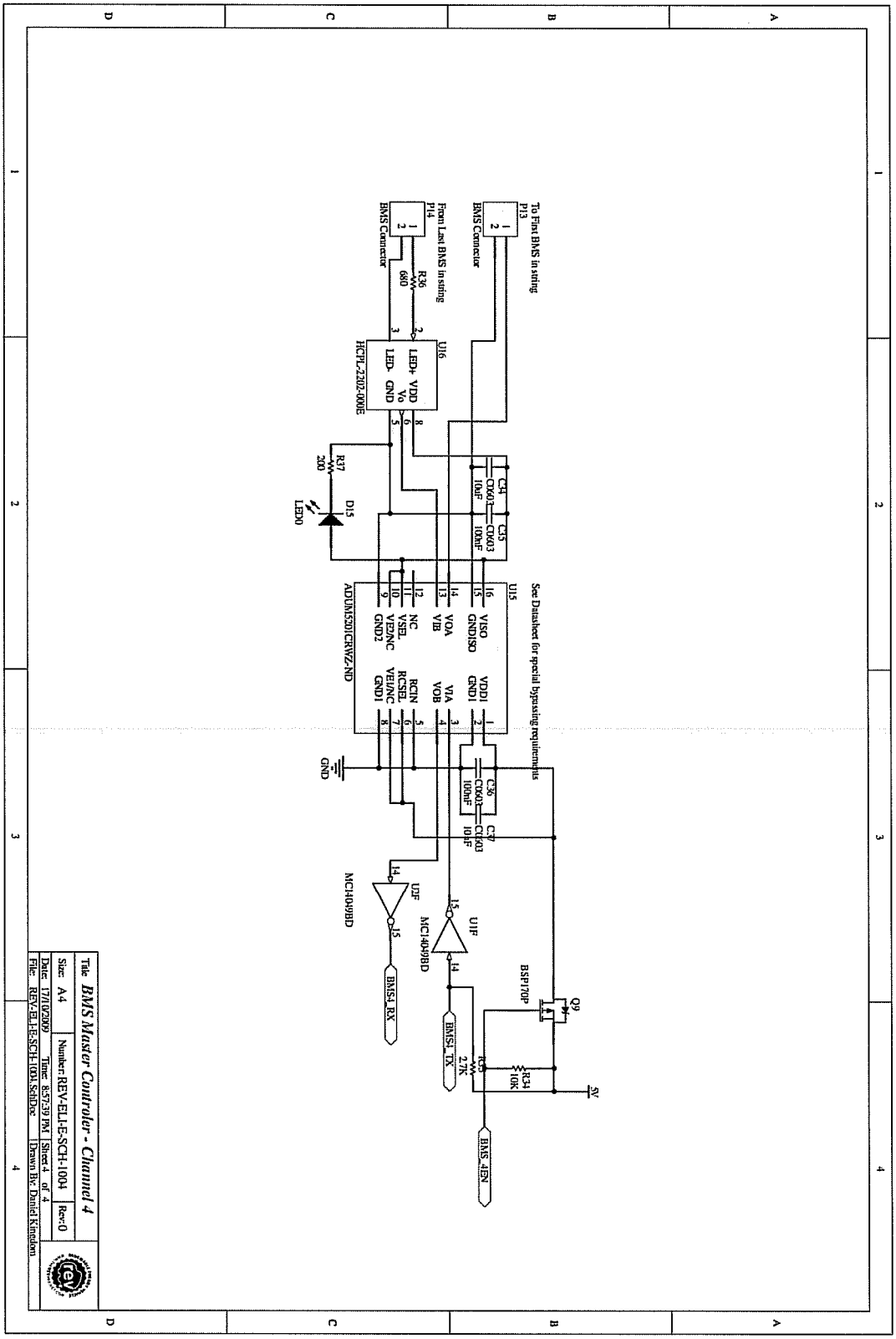

FIGURE 28 - BMS MASTER CONTROLLER SHEET 4 OF 4

The BMS modules use a modified inverted TTL UART protocol with a baud rate of 4800 bps. Each module has a single female JST connector and a fly-lead with a male JST connector, as can be seen in Figure 24. The Lotus Elise has 99 cells and as such will have 99 BMS modules. Neubronner recommends a minimum delay of 30ms between each request on the modules per metric. Under normal operation two different metrics are required (cell instantaneous voltage, and voltage range) this would lead to an update time of:

$$t_{update} = t_d * N_{cells} * N_{metrics}$$
$$= 30mS * 99 * 2$$
$$= 5.94\ seconds$$

EQUATION 22 - UPDATE TIME FOR SINGLE CHANNEL OPERATION

This impairs the research goal of the black box system as it will be difficult to determine cell behaviour as a result of vehicle events. To improve the update time the BMS modules are divided into multiple channels. Each channel operates independently, hence improving total throughput and reducing the update time. Table 3 illustrates how the BMS modules were divided among the 4 channels.

Battery Packs	Total Cells	Channel1	Channel 2	Channel 3	Channel 4
Main Pack (Upper)	49	25	24		
Fuel Tank Pack	18			18	
Rear Pack	32				32

TABLE 3 - CELLS AND CHANNEL DISTRIBUTION

Channel 4 therefore has the largest number of cells, due to installation limitations cells on the rear pack could not be added to channel 3. Hence channel 4 has the longest update latency of:

$$t_{update} = t_d * N_{cells} * N_{metrics}$$
$$= 30mS * 32 * 2$$
$$= 1.92\ seconds$$

EQUATION 23 - IMPROVED UPDATE TIME FROM 4 CHANNELS

Through the use of additional independent channels the update latency was therefore reduced from 5.94 seconds to 1.92 seconds. Figure 29 demonstrates the connection scheme used on the Lotus Elise with the 4 channel BMS Master Controller.

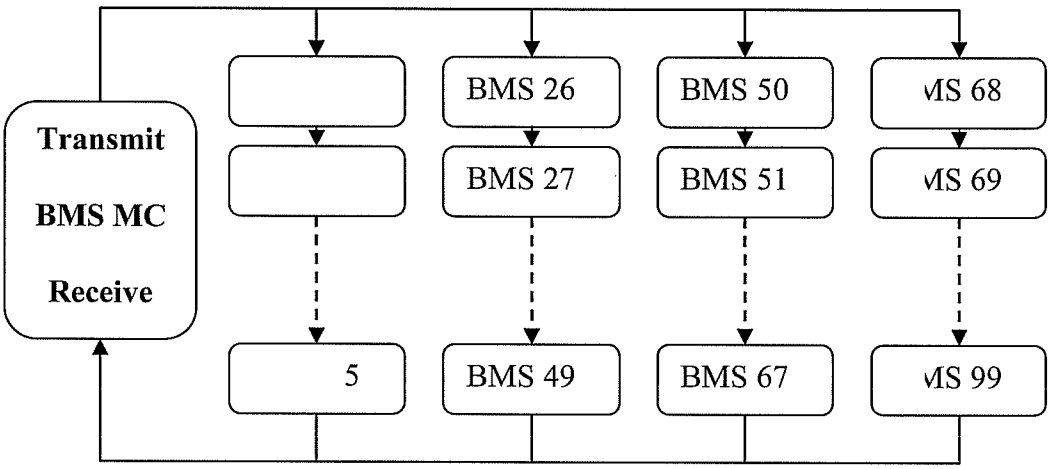

Each channel is connected to an independent UART port on the BMS Master Controller. Which in turn is isolated and connected to a hardware UART on the PIC24FJ64GB110 microcontroller. The BMS modules require a 4800 bps, 8 data bits, no parity and 1 stop bit, as an inverted UART signal (idle voltage is 0V). However as Figure 30 illustrates the communication datagram does not comply with the standard UART protocol. Once a packet has been sent, following a 1ms (minimum) delay the idle signal is inverted to 5V, and 1ms (minimum) before the next transmission, this level is switched back to the idle level of 0V.

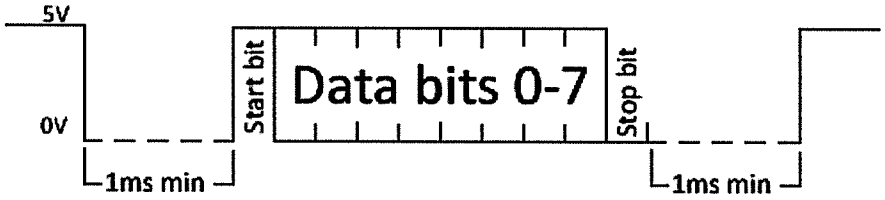

FIGURE 30 - INVERTED TTL MODIFIED UART

Each BMS module low pass filters the serial communication line, and this is then used as the enable signal for the boost regulator on the BMS module. Thus if the line is held low for an extended period of time (0.5 second) the boost regulator will shut down and the BMS module will enter low current mode (approximately 4mA). To return the BMS module to its normal operating mode the idle line voltage needs to be returned to 5V for at least half a second.

The author did recommend the BMS modules use a non-inverted TTL level UART datagram standard (see Figure 31) since the BMS modules only uses software UART. This would have the simplified the design as a standard UART datagram could be used, and the normal idle voltage would prevent the BMS module from going to sleep. Neubronner stated that such a change resulted in internal complications with the BMS module hardware and thus the original scheme is still in effect.

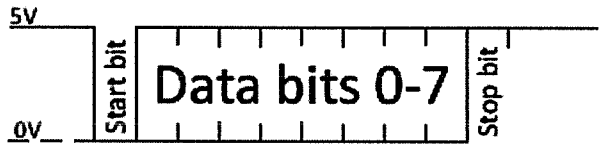

FIGURE 31 – NON-INVERTED UART BYTE

The UART functions on the 24FJ64GB106 are mapped using the Peripheral Pin Select (PPS) functionality. This allows designers to be flexible where function blocks such as the UARTs can be mapped to various pins. To software toggle the transmit pin as required by the BMS modules the digital IO pin needs to be configured for output through the TRIS registers and the required output level (low) is set in the PORT registers. The PPS unlock sequence must then be executed before the transmit pin can be mapped to null (not connected). This method allows for the receive functionality to remain active so that incoming data packets can still be processed.

To invert the UART signal transmitted from the microcontroller, two hex inverting buffers are used. These devices also perform level conversion between the 3V3 logic levels present at the microcontroller to the 5V signals required by the isolation circuitry.

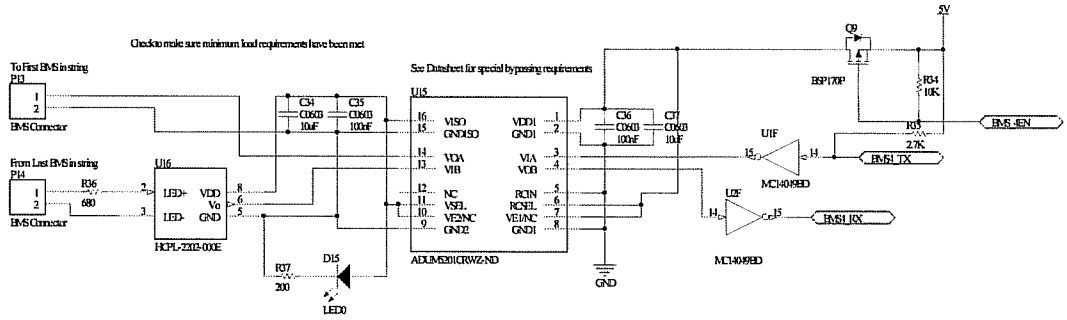

FIGURE 32 - BMS MODULE ISOLATOR CIRCUIT CHANNEL 4

U1 inverts the transmit pin and requires a 5V output to isolator, thus the buffer supply voltage is sourced from the 5V rail. U1 also requires a minimum high input voltage V_{IH} of $0.7*V_{DD} = 3.5V$[32] this is obviously greater than can be sourced from the 3.3V microcontroller. Digital only pins on the 24FJ64GB106 can be configured as open-drain outputs[33], thus with the addition of a pull up resistor such as R35 in Figure 32, 5V tolerant outputs can be achieved. On the receiver side U2 is used as an inverting buffer, unlike the transmit buffer, U2 has a V_{DD} of 3.3V and thus as well inverting the logic level also performs the task of level conversion[34].

This design uses iCoupler digital isolators with isoPower more specifically the ADUM5201CRWZ-ND. This device has the advantages of the iCoupler devices mentioned previously however it has an additional chip-scale transformer which is used to generate an isolated 5V dc supply. The isolator is able to provide up to 500mW of isolated power at 5V dc[35]. Figure 33 shows the function block diagram of the digital isolator.

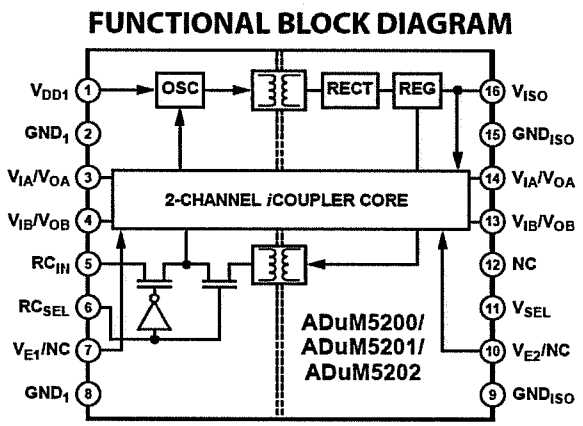

FIGURE 33 - FUNCTIONAL BLOCK DIAGRAM OF THE ASUM5201 [35]

To maintain stability Analogue Devices specifies that a minimum static load of 10mA must exist on the isolated supply. To guarantee this requirement a diagnostic LED (D15 on channel 4) was added. This LED will guarantee a minimum load of 10mA while also providing easy identification that the isolated supply is active. To reduce power consumption while the car is not active each channel has a PMOS field effect transistor with the gate pulled up to 5V, this is then connected to a digital only IO pin configured as an open-drain. When the gate is pulled low by the microcontroller the PMOS will turn on powering up the digital isolator and isolated DC-DC supply. If the microprocessor powers down

the isolator, the transmit line will also go low putting the BMS modules into a low power state.

The received signal from the last BMS module in the string should be isolated. However as an added precaution in the event that a cable accidentally contacts the pack during installation or maintenance work a HCPL-2202 optocoupler is used to isolate the receive signal from the transmit signal. The worst case scenario would be a potential of 99 cells (3.8*32 = 376.2V DC) existing between the transmit and receive lines this voltage is well within the safe working voltage ($V_{IORM} = 630V_{peak}$)[36]. Both transmit and receive pins have a SMA connector to connect to the coaxial cable for carrying the signal to the packs. A SMA to JST board was also developed (see Figure 65).

When entering the final state of charge during a recharge operation the BMS modules will enter a balancing stage once individual cells reach a preconfigured voltage (3.8 V at the time of writing). During the balancing stage the BMS places a shunt load across the cells. The BMS modules are only capable of bypassing 1A continuously, thus for the balancing stage to be successful on an out of balance pack, the charge current must be limited to less than 1A when a BMS module enters the bypass stage. To control the charge rate of the installed Brusa NLG series charger a CAN bus interface is provided on the BMS Master Controller (See Figure 26).

The CAN interface is implemented using a standalone CAN controller with a SPI interface part number MCP2510 from Microchip. The CAN controller features include: up to 8 byte message lengths, support for standard and extended data frames, up to 1Mbps baud rate with two receive buffers, three transmits buffers and acceptance filters and masks[37]. The charger requires the use of standard frames with a baud rate of 500kbps; and the charger must first be placed in to CAN mode using the PC configuration software. Upon initialization the charging profile is then controlled through the command msg 0x618 which is sent to the charger every 100ms. This message contains the target output voltage and current. If the charger fails to receive the 0x618 message from the BMS master controller for more than 300ms charging will cease with a fault code being recorded in the log tables. This fault can be cleared once CAN bus communication resumes[38].

The MCP2551 CAN transceiver was used to generate the CAN bus signals, and will not interfere with a CAN bus even when not powered[39]. While the CAN bus currently only consists of the BMS Master Controller and the Brusa charger, future enhancements will hopefully include additional devices such as the motor controller and vehicle sensors. The CAN interface is isolated using iCoupler Digital Isolators. Similar to the BMS Master Controller channels the DC-DC converter can be powered down through the use of a PMOS field effect transistor to reduce power requirements when communication to the charger is not required i.e. when the mains are not connected.

The BMS Master Controller has 3 relay outputs, the first of which is for the management of the internal traction pack isolators. In the Lotus Elise there are three traction packs, each traction pack has a contactor in series with it. Thus when the car is not being operated or charged the packs will be disconnected from each other. However for the vehicle to be charged or operated these contactors need to be energized. Thus when there is a demand for the traction pack the BMS Master Controller will close the normally open relay (K1) providing the required 12V to the traction pack contactors. The 12V is supplied to the board by a separate DC-DC converter powered from one of the individual traction packs.

Relay K2 is designed to be used as a signal to enable or disable regenerative breaking based upon cell status. Predominately this relay will be disabled when cell voltages are greater than 3.6V and the use of regenerative breaking is likely to push the cells into bypass or over charge. Cell voltages are determined from the values measured from the BMS Modules.

Relay K3 is used to switch the main AC signal to the Brusa Charger. K3 allows for the AC mains to be connected and disconnected with little load. The only static load will be that of the AC analysis board. Thus arcing at the 15A mains socket installed on the vehicle is reduced. The relay will also disengage if the CAN bus charger stops responding, or if a cell voltage reaches 4V in this case the relay will re-engage once cell return to within normal operating limits (< 3.8V). If a non-CAN bus based charger is used such as the Zivan charger in the Getz the BMS Master Controller can easily be reconfigured to control the charger by simply switching the mains input to the charger.

There is also a piezoelectric buzzer installed on the Master-Controller (LS1) this is used as a simple audible alarm if a cell voltage either exceeds 4V or is below 2V per cell when the car is operating. A second preset exists when the traction pack is at rest, in which case the alarm will be triggered at 2.5V.

3.3.3 SMBus Interface

The digital interface to the Master Controller is implemented by a SMBus. This interface allows for a bidirectional interface from the host (The Master Controller) to the slave (BMS Master Controller). Similar to the PCA9555 IO expanders discussed earlier communication takes the form of reading and writing to registers in the BMS Master Controller. The list of register is listed in Table 14 in the Appendix.

All registers are 8 bits in length, 16 bit data types are formed by reading/writing to two registers. Boolean values are written to a register as a 1 or 0, but still occupy an 8 bit register. It is important to note that the registers are virtualized and for example a Boolean register does not occupy 8 bits in ram on the microcontroller even though it is an 8-bit register.

The data refresh counter (address 0) is incremented upon each refresh of cell data. Cell data is double buffered and the cell registers are only updated once all data has been received for all channels.

Registers 1-5 set the alarm values based upon cell voltages. The maximum cell voltage is also the point at which the AC supply to the charger will be disconnected to prevent cell damage. The regenerative braking enable signal will deactivate if a cell voltage reaches the cell bypass voltage minus 0.2V.

Registers 6 enables CAN bus mode; if enabled the BMS Master Controller will control the BMS charging profile. If disabled then chargers without a CAN interface can be used such as the Zivan charger. In this case the charger is controlled by simply energizing the AC mains input on the charger and de-energizing again at the end of charge or if a cell voltage exceeds the maximum cell voltage (register 4).

Register 7-11 enable or disable the audible alarms on the BMS Master Controller from the piezoelectric buzzer. These alarms have no effect on any other operation of the BMS Master Controller. Register 12 is the event notification, when enabled

the BMS Master Controller emits a short chirp to indicate that an event has occurred, such as charging beginning /completed, AC mains connected/disconnected, etc.

Registers 50 indicates that the ignition circuit is active, this value is written to the BMS Master Controller. This input is used to enable the pack contactor relay; the origin of this signal is from the Vehicle Interface circuit. Register 51 will manually put the BMS into low power mode. In low power mode all BMS channels and CAN bus circuitry is powered down. The BMS Master Controller will stay in this state until the bit is manually cleared. The BMS Master Controller will also enter a sleep state for 10 minute periods between measurement when the car is neither operational nor charging. It should be noted that it can take up to 1 second per cell per channel for the BMS modules to enter and exit sleep. During sleep the SMbus is still active and register access is still available.

Registers greater than and including register 70 are read-only. Registers 70 contains the BMS Master Controller version number. This register is predominately exists to support new versions with different register listings. Thus it is good practice for this register to be read first upon power up. Registers 71-73 reflect if the corresponding relay outputs are active.

Registers 100-103 contain the number of BMS Modules that have been detected on each channel through the broadcast of the identity command. The identity command simply returns the number of modules on that specific chain. Each channel can support up to a maximum of 200 BMS modules, for a maximum of 300 BMS modules in total. This could be increased in the future if required as there are sufficient resources in the microcontroller remaining. However 300 BMS modules should be more than sufficient for future rev projects. Note that the Lotus Elise uses 99 BMS Modules, and the Getz has only 45.

Registers 200-1699 are an array of BMS Module data, where every BMS module will occupy 5 registers. Each channel's modules are stored concurrently, to calculate the first register number corresponding to a particular BMS module:

$$RegisterChannel1(BMS\ Module\ X) = 200 + 5X$$

$$RegisterChannel2(BMS\ Module\ X) = 200 + 5N_1 + 5X$$

$$RegisterChannel3(BMS\ Module\ X) = 200 + 5(N_1 + N_2) + 5X$$

$$RegisterChannel4(BMS\ Module\ X) = 200 + 5(N_1 + N_2 + N_3) + 5X$$

EQUATION 24 - CELL REGISTER ADDRESS

Where:

X is the desired BMS module in the specific channel

N_x is the number of modules in channel x.

Similar to I^2C bus on the PCA9555 the SMbus distinguishes between read and writes from the Host to Slave by the least significant bit of the device address that is requested.

	Read Address	Write Address
BMS MC Address	0x3B (0b00111011)	0x3A (0b00111010)

TABLE 4 - BMS MASTER CONTROLLER SMBUS ADDRESSES

A transaction will begin by the host applying a start condition on the bus, followed by the address of the slave (Table 4). The Slave (BMS Master Controller) will then respond with an ACK signal (Acknowledge Signal) and the host will transmit the register address (16 bit unsigned integer) with the BMS Master Controller acknowledging each byte unless the BMS Master Controller detects that the register address is out of range (i.e. greater than 1699) in which case the BMS Master Controller will send a NACK and the host should generate a stop condition and retry the transaction. After the address a single 8bit unsigned length byte is transferred indicating the length of the read or write, the maximum number of bytes then can be read or written in a single transaction is 32. If the length byte is less than 32 then the BMS Master Controller will send an ACK otherwise an NACK will be sent.

If the transaction was a read request then the BMS Master Controller will transmit the requested data. The host should acknowledge each byte, if the host sends a not acknowledge the slave will release the bus and the host is expected to generate a stop condition; thus this method can be used to abort a transfer. On the other hand if the transaction was a write request, the Host will continue to clock out the data to be written. The BMS Master Controller will acknowledge each byte as long as it meets the range limits of the registers (Table 14).

After the data has been transmitted from slave to host or from host to slave a final Packet Error Code byte will be sent from the host to slave this byte contains an 8 bit CRC (cyclic redundancy check) and is calculated on all bytes in the transmission (including the slave address). The BMS Master Controller will then check that the Packet Error Code (PEC) matches the data sent and received and respond with a final acknowledge. For more information on the implementation the reader is encouraged to refer to the SMBus specifications[40].

3.4 Master Controller

3.4.1 Design

The Master Controller forms the central hub to the Black Box system, and communicates to data acquisition modules and implements the serial busses in Figure 16. The following figures contain the schematics for the Master Controller.

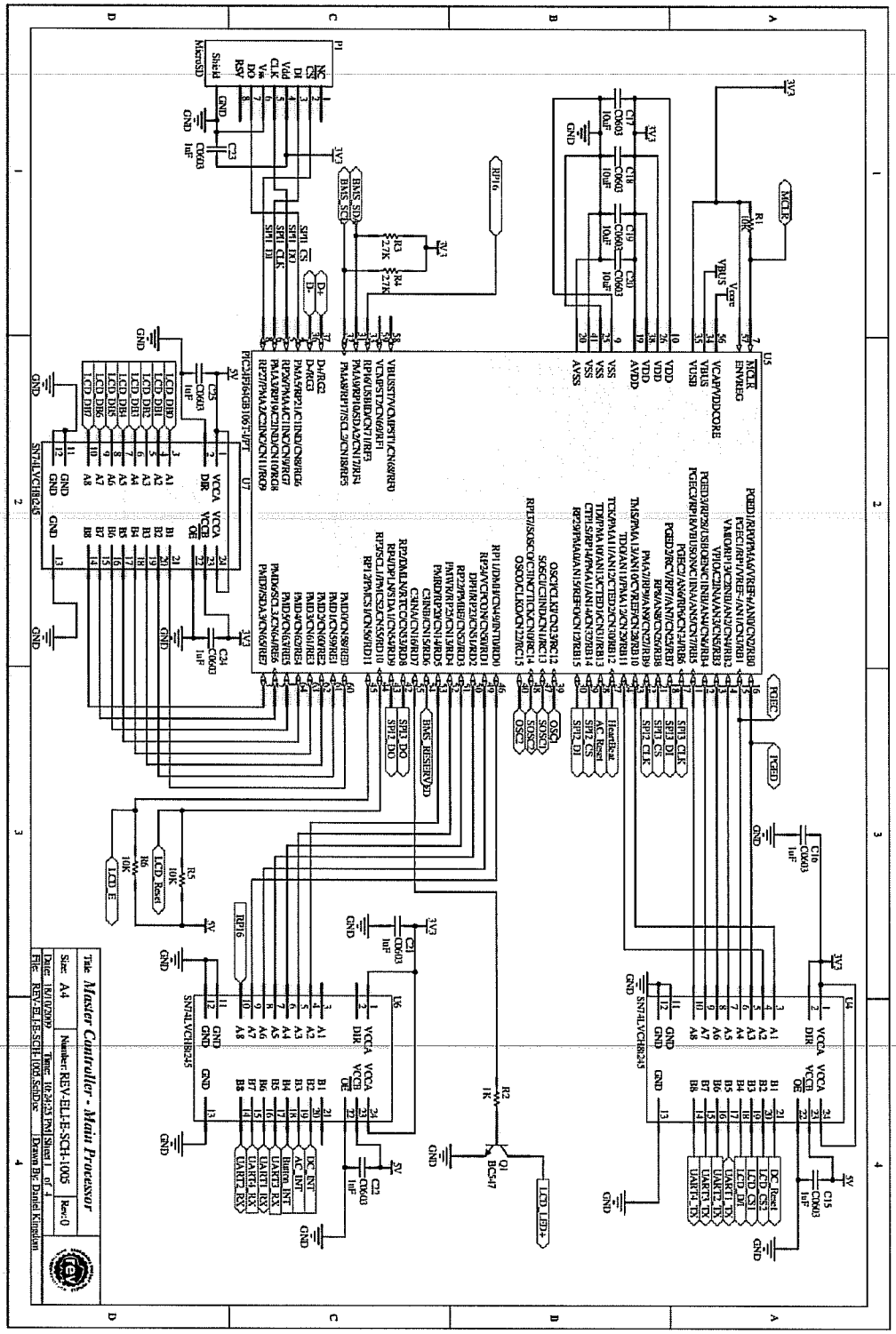

Figure 34 - Master Controller - Main Processor Sheet

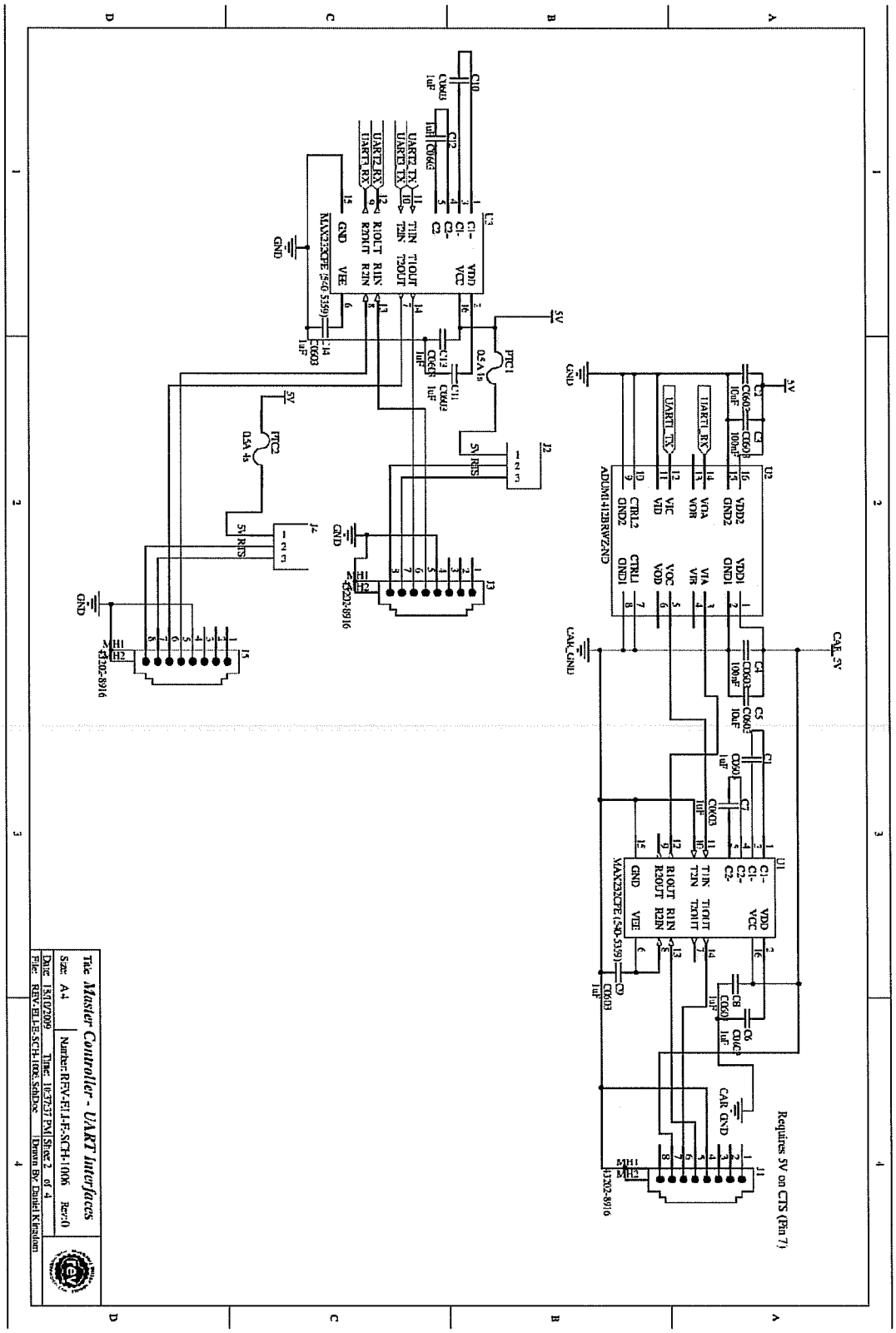

FIGURE 35 - MASTER CONTROLLER - UART INTERFACES

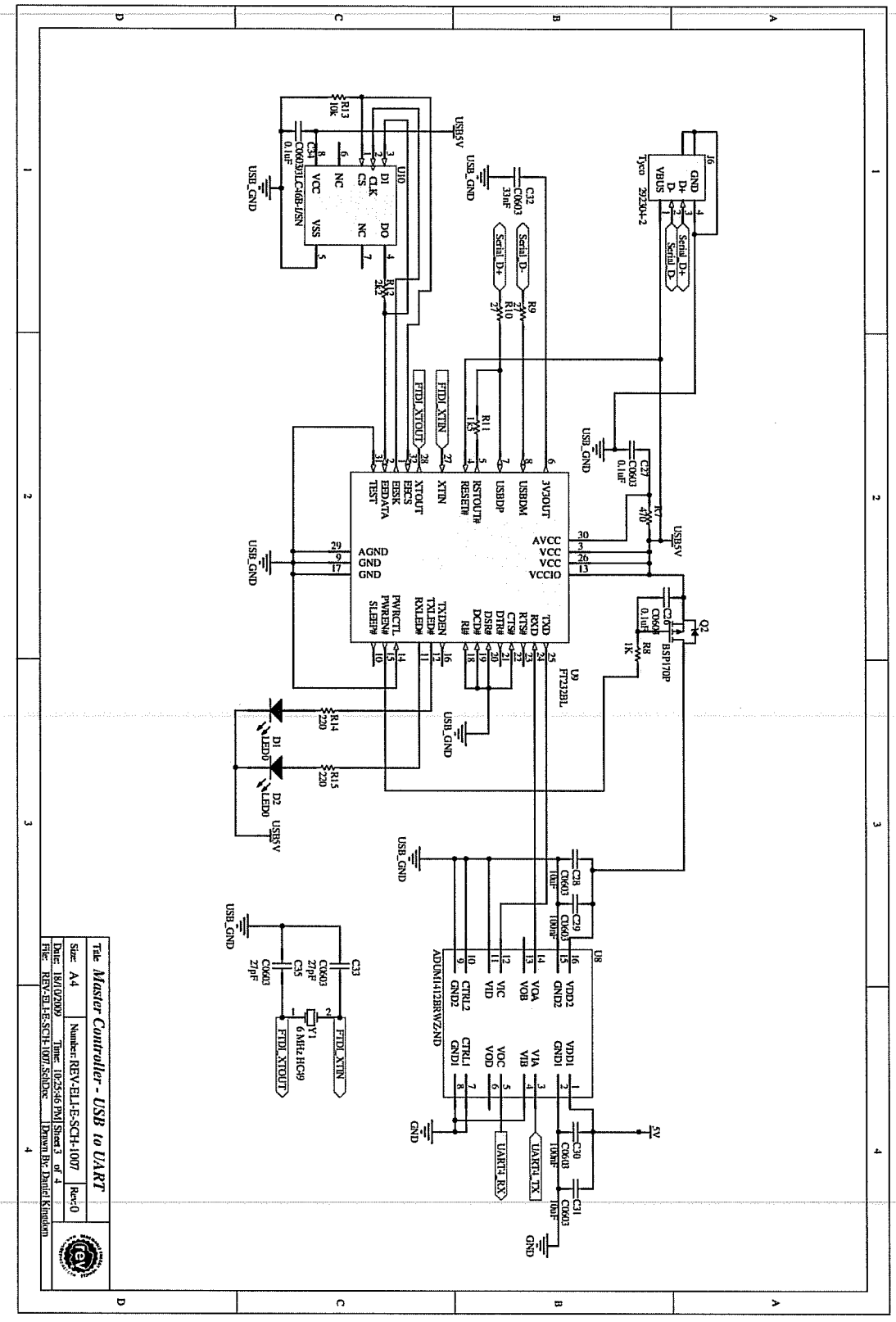

FIGURE 36 - MASTER CONTROLLER USB TO UART

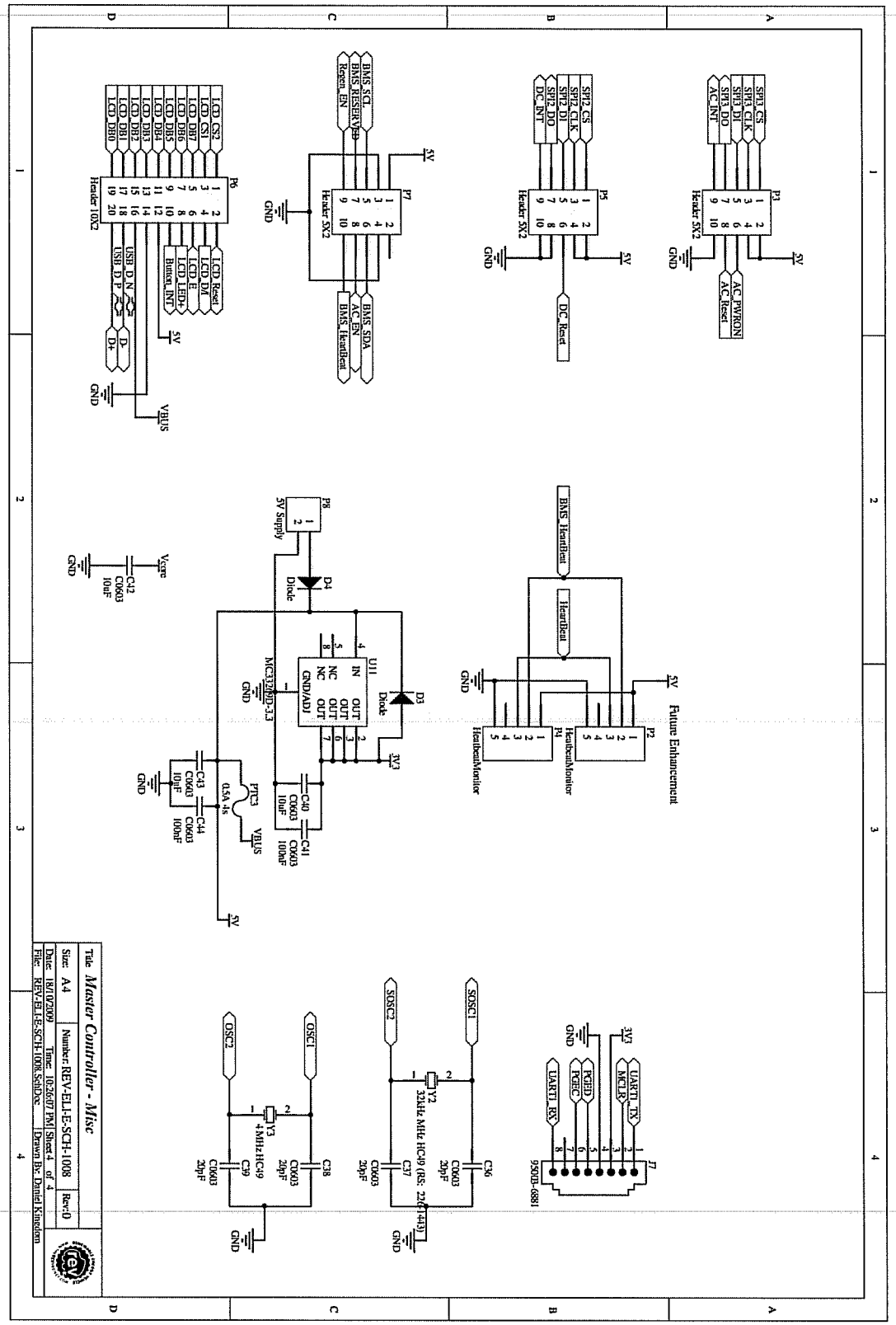

FIGURE 37 - MASTER CONTROLLER - MISC

3.4.2 HSPA AND GPS

HSPA (High Speed Packet Access) is a future enhancement along with the implementation of GPS. Two UARTs have been added so that both wireless internet access and global positioning by GPS is possible without the need for hardware modifications. All that should be required to enable this functionality is additional firmware routines to handle the AT commands and phase the incoming NEMA GPS data stream. The two RS232 ports are design to be used in conjunction with devices that are isolated, thus if this is not possible then a simple isolation circuit will be required such as an optocoupler or iCoupler design as has been used many times in this thesis.

The two rs232 ports can be accessed via J3 and J2 (see Figure 35), both of these connectors are RJ45s and are configured according to the EIA-561 standard. When connecting between two devices wired to this standard, a roll-over cable should be used such that pins 5 and 6, 7 and 8, and 1 and 2 are crossed over (similar to a null modem adapter)[41].

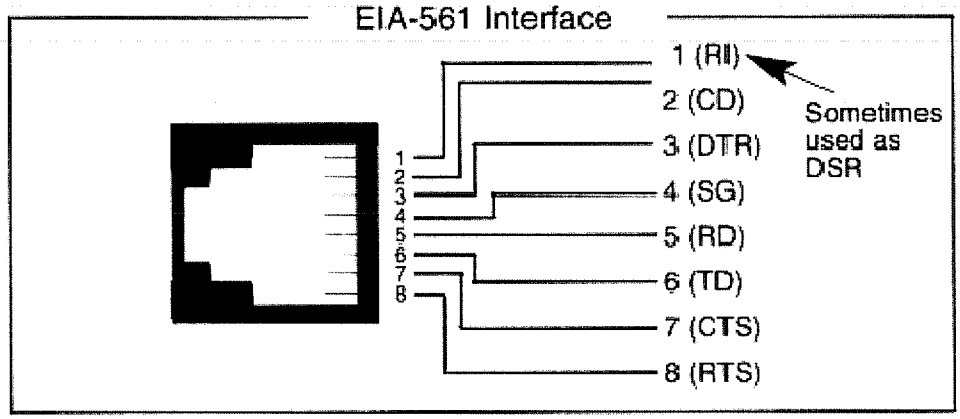

FIGURE 38 - EIA-561 RS232 STANDARD[41]

On J2 and J3 a 5V regulated supply with up to 500mA is available by setting J2 or J4 respectively such that pins 1 and 2 of J2 or J4 are shorted. To prevent damage to the Black Box system the output current is limited by two Positive Thermal Co-efficient (PTC) re-settable fuses. If a short circuit condition does occur the fuse will reset once sufficient time has passed for the fuse to cool down.

If the jumpers are placed in their alternate positions then pins 7 and 8 will be connected allowing for devices that use hardware flow control to be used (the Black Box will appear to be ready to receive whenever a request to send is issued by the other device).

3.4.3 Vehicle Interface

The vehicle interface is an external device to the Hardware Black Box system, and interfaces to the Black Box system via an isolated RS232 connection J1. The isolated RS232 port J1 is also configured as an RJ45 according to the EIA-561 standard[41]. An iCoupler device (ADUM1412BRWZ) was used to isolate the UART stream as has been used elsewhere in the design. However since the vehicle interface will have it's own supply source, namely the 12V auxiliary battery using an isoPower device would have resulted in addition power loss (due to inefficiencies). Thus the vehicle interface will be required to provide regulated 5V on the CTS line pin 7 (pin 8 on the vehicle interface if a roll-over cable is used).

3.4.4 USB PC Interface

To allow the x86/x64 ITX based computer that is installed in the Lotus to access the wealth of information that is collected by the black box from its various modules, a USB port was added. The USB port was chosen over the more readily available rs232 ports used elsewhere since there are no rs232 ports on the computer and as such would have required an external USB to rs232 adapter additional space/cabling requirements in addition to another possible point of failure.

The USB B port emulates a single UART operating at 19.2 kbps with 8 data bits, 1 stop bit and no parity. The USB port supports both USB 1.1 and USB 2.0 standards provided by the FTDI FT232BL. FTDI drives are available for a wide range of operating systems including Windows 98, 98 SE, 2000, ME, Server 2003, XP, XP 64bit, XP Embedded, CE 4.2 and MAC OS-8 and 9 and MAC OS-X and Linux 2.40 and greater[42].

The optional EEPROM (U10) was added so that USB PID, VID and product descriptions can be added, along with other configurations. This will assist in the operating system, especially in Windows from setting the same serial port number to the devices independent to which USB port it is connected to. The setting of the

product description will also aid in debugging, since the device can easily be identified in the device manager.

The digital isolator is also powered from the USB port such that it does not unnecessarily consume power when the computer is off. The digital Isolator (U8) will also be powered down when the USB interface enters a low power state or suspend state through the use of Q8. A capacitor was also added to allow for a "soft start" to prevent a drop out to occur and the FTDI chip to reset due to the low amounts of decoupling capacitance allowed for by the USB specification[42].

3.4.5 Digital IO

The 24FJ64GB106 microprocessor operates at 3.3V, while other devices on the board operate at 5V TTL logic levels. Since the number of 5V tolerant IO lines is limited (digital only pins) level translator integrated circuits are required. The SN74VCH8T245 was used to interface the 5V logic to the microprocessor and offers a number of advantages. In particular each bus is physically located on opposite sides of package simplifying PCB layout. The device also supports bi-directional level translation, and thus the same device (in different instances) can be used for both inputs and outputs[43].

Peripheral pin select on the 24FJ64GB106 is used to assign hardware peripheral IO pins that are convenient for PCB layout. This aids in improving PCB density, Q1 is used to support LCD screens with LED backlight as a future enhancement. A Powertip PG 12864-J LCD screen was implemented on the user interface board this screen support 128x64 monochrome pixels and thus allows the Black Box to display basic graphs of BMS status as well as other statistics and status information. An 8 bit parallel bus is used to interface with the screen, with 5 buttons sharing the data lines. To simplify the level translation required for the 5V bus, the bus is set as write only, via tying the read/write line to ground[44].

3.4.6 Analysis Boards

The AC and DC analysis boards both connect via 3V3 SPI busses as previously discussed. The DC analysis board is a future enhancement; however it is expected to be implemented in a similar manner to the AC board. Similar to the black box design of the Chonbuk Nation University a microSD (or transflash) memory card is used which is effectively a smaller version of the SD card supporting the same electrical specifications. Due to licensing restrictions only the SPI interface can be

supported on the flash memory card, hence High Capacity cards are not supported since these cards exclusively operate with the SD HC protocol; thus the maximum flash capacity is 2GB[45].

3.4.7 Data logging Functions

Records are sampled on average every 1.5 seconds, and are triggered every time the BMS data is refreshed. Records are always of a fixed length of 2 sectors, where sectors on trans-flash cards are of 512 bytes in length. Aligning records to sector boundaries reduces the number of reads and writes required as a write will always write to a whole sector. Thus if a write only partially occupies a sector the sector must first be read the whole sector and write back with the new data superimposed. This will also result in additional writes as two records could overlap on to the same sector, thus increasing wear on the flash cells (flash memory has a limited rated endurance lifetime).

Each record is prefixed with a 4 byte unsigned record ID, this ID value is incremented each time a record is written to flash memory. Removing the need for a record pointer to be stored in flash memory as during the boot up process the Black Box system will scan for the largest record ID with a valid error code and hence know that this was the last record committed to memory. The problem with record pointers is that they typically must resided in a fixed point in memory which would result in that memory location receiving a large number of writes and thus reducing cell life. At a 1 second sampling rate, a 4 byte ID counter will continue to increment for 132 years before an overflow occurs, which is considered significantly longer than the lifetime of the Black Box system.

A 16 bit version identify follows the ID counter, with the MSB representing the major version number, while the LSB represents the minor version number. At the time of publication the version number is set to 0x0101 i.e. Version 1.1. This allows the Black Box to detect outdated records after an upgrade, and allow manual data extraction tools to identify the record version so that the data can be recovered.

Finally there is an error code in the final 4 bytes (32 bits) of flash memory. This field contains a 32 bit CRC code of the entire record including ID field but excluding the error code field. This is used to detect a record which may have been partially written. This may have been the consequence of loss of power or

perhaps an accident where the Black Box may have been damaged, such records will be discarded upon retrieval.

3.4.8 Real Time Clock and Calendar

A real time clock and calendar is maintained by the central processor with the aid of a watch crystal tuned to 32.768 kHz. This is used to mark the time a sample occurred accurate to the nearest second. It is envisioned that when the GPS functionality is implemented, the RTCC will be updated from GPS time to reduce time error. Due to the uncertainty of the future of daylight savings, the RTCC is set to UTC (Universal Time Coordinated) this will also simplify synchronizing with GPS time.

3.4.9 USB Embedded Host

A USB Embedded host was added to allow the user/operator to be able to easily download recorded data from the Black Box system. The Embedded Host automatically detects when the user inserts a thumb drive and request if the user wishes to download all logs or just the last 24 hours. After the user makes the selection via one of the three softkeys beneath the LCD screen the transfer will begin. The USB transfer can be cancelled at any time by pressing any of the 5 keys in which case the USB transaction will stop and the file closed on the thumb-drive allowing for safe removal. FAT16 is the supported file system, and is accessed through the Microchip's Memory Disk Drive File System Library. FAT 16 is the default file system installed on most thumb drives with a capacity of 32MB to 2GB, larger than 2GB capacities will require the use of FAT32 which could be implemented in the future. However considering that the Black Box can only be installed with at most 2GB of flash memory, it was not a high priority to implement FAT32. A separate file is created on the mass storage device for each 24 hour period that was requested (if there is sufficient space) [46-48].

Most recent files are copied first, to the limits of free space or until all entries have been erased. If the file transfer is successful the user is presented with an option to delete the data from the Black Box. If the user selects this feature, the ID field of all records that were downloaded are set to 0, which will prevent these records from being downloaded in the future.

An embedded USB Host has less stringent requirements than a full USB host (as may be found on for example a personal computer). Firstly embedded USB is only required to support specific peripherals and device classes, support only the transfer types required by such devices, supporting USB hubs is optional, and have relaxed power supply requirements. The Black Box system only supports the USB Mass Storage Class (Class 0x08, Sub Class 0x06, Protocol 0x50) and does not support the use of Hubs (There is no need in the current design for multiple USB devices). The Black Box complies with the power requirements of USB and is protected by a PTC fuse (resettable) with a hold current of 500mA and a trip current of 800mA, a USB device should not draw more than 500mA as defined in the USB specification[47].

The SCSI Command set support by most if not all flash based thumb drives and is used by the Black Box system for low level file operations. The Embedded USB Host is implemented in 5 layers (see Figure 39). At the lowest level is the USB Embedded Host Driver provided my Microchip, followed by the Mass Storage Client Drive, SCSI Command Support and File System Support. The File System Support layer interfaces with the FAT files system and provides simple file based IO functions to the Application layer. The Application layer hosts two event handlers to handle the USB Events generated by the lower layers and initiates file operations through the file system layer.

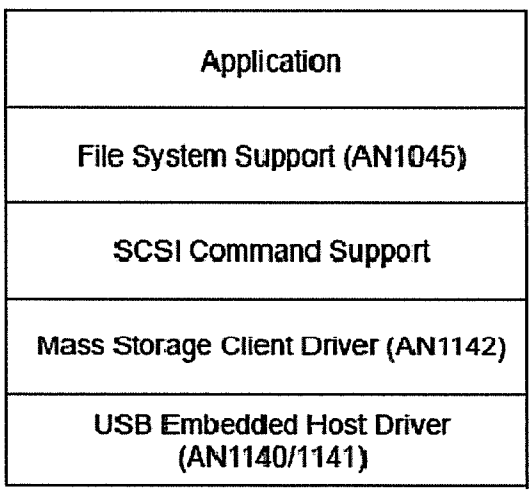

FIGURE 39 - EMBEDDED USB ARCHITECTURE[48]

3.5 User Interface

3.5.1 Design

The user interface is a simple PCB to mount the Graphic LCD screen, buttons and USB port. U1 is an inverting voltage doubler (TC682[49]) that is used to generate the -10V line (V_{EE}) for the graphical LCD Contrast Adjustment. R2 is a 10k potentiometer to allow the user to adjust the LCD screen contrast with a small Philips screwdriver. J1 is a vertical mounted USB type A connector for the user to insert a thumb drive. P2 is the LCD screen it should be noted that pins 19 and 20 are for Powertip screens with backlight, if the LCD screen does not have a backlight then these two pins are left disconnected.

There are five normally open momentary tactile switches (320.02E11.095GRY). These switches were selected primarily for their height of 15.5mm[50], so that they would be approximately level with the LCD screen and not recessed into the case. The three switches along the button (S1-S3) allow the user to select options (soft-keys) similar to that found on mobile phones or on the Eyebot controllers. Switches 4 and 5 are used for vertical scrolling of the screen, or scrolling through lists of items. Square pads were used for the switches to maximize mechanical strength since the board is only single sided without through hole plating. P1 is a 10x2 surface mount IDC header to allow for the connection of board to the Master Controller. The Final single sided PCB is shown in Figure 40.

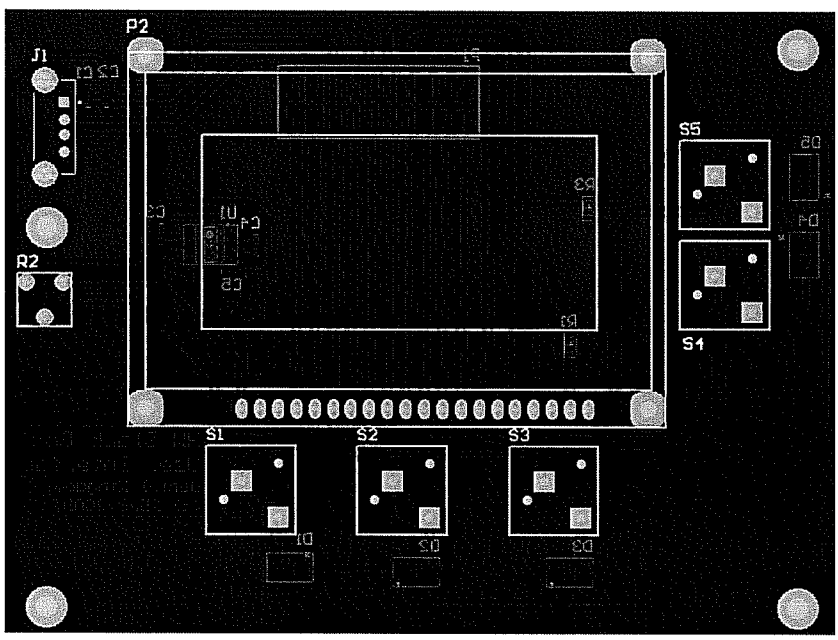

Figure 40 - User Interface PCB

4 Mobile Broadband Power Management System Design

4.1 Background

The addition of real time data publishing/reporting was seen as a very useful feature, allowing the status and history of the vehicle to be view remotely from the REV website. The EyeBot M6 controller had been previously installed into the Getz to operate as the onboard vehicle computer. A Huawei E160 HSDPA USB stick was purchased for the purpose of providing a HSDPA/UMTS connection to the internet with service plans from 3 (Vodafone Hutchison Australia). The E160 does support Windows™ and Macintosh™ operating systems however drivers for Linux operating systems was limited and implementing the device on the Eyebot M6 Operating System (Busy Box Linux) proved to be very difficult.

To overcome this limitation a Netgear MBR624GU 3G mobile broadband wireless router was installed. This unit was later replaced due to poor performance, with a Huawei D100 3G router. This new unit provided far greater performance and connected to the Eyebots M6 100BaseT Ethernet port.

Unfortunately the D100 required the user to press the momentary tactile power button on the unit each time the device's power supply was cycled. This was considered a significant inconvenience to the operator of the vehicle as the device would be regularly shutdown to conserve power in the vehicle. Firmware options to bypass the power switch were quickly exhausted, and posed a risk of damaging the device. A hardware solution was then sought which could be reliably installed inside the D100.

4.2 Design

Experimentation showed that for reliable operation the power switch should be pressed after a small delay (approx 0.25 seconds) and held down for less than one second. To allow for supply fluctuations when the device was first powered on, a one second delay was desired before the device was powered on.

While this design could have been realized using a variety of methods including resistor capacitor designs (similar to that implemented in the air conditioning compressor delay circuit) a digital design was instead implemented in this instance. The digital design focused around an 8bit microcontroller. Using a microcontroller had a number of advantages. Most importantly it offered highly repeatable results which were not affected by supply voltage fluctuations due to varying states of charge in the 12V DC battery to which the router is connected. With cost of small 8-bit processors continually decreasing (12F683 can be purchased for US$0.91 [51]) this design is competitive in small quantities. The microcontroller through reprogramming can easily be later adjusted to support various timings without the need for any changes to components in the circuit. The design also only required a small number of components which was essential to fitting the board into the existing router enclosure. The final schematic is shown in the following Figure 41.

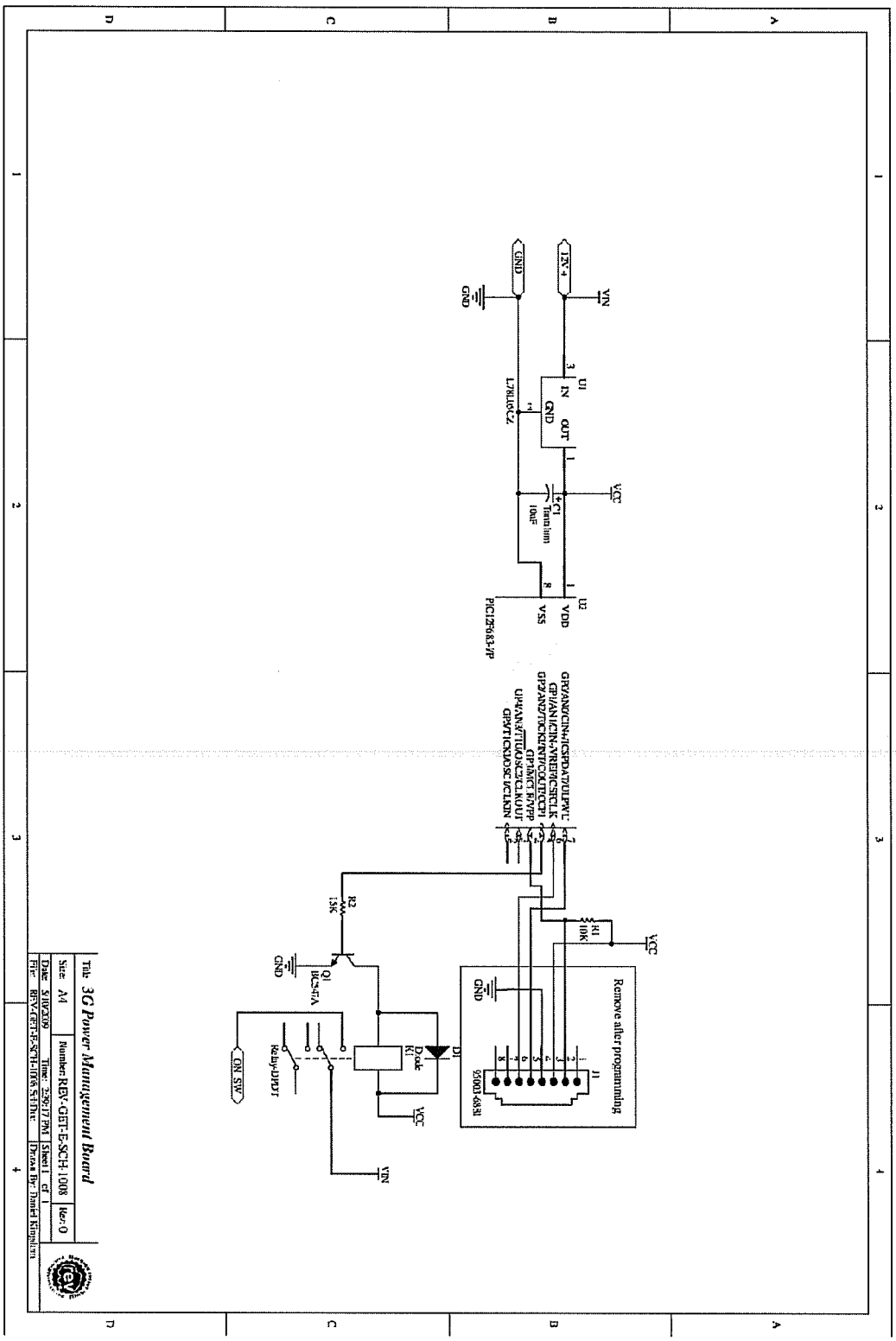

FIGURE 41 - 3G POWER MANAGEMENT BOARD SCHEMATIC

The 12V+ port was connected by flex core cable to the 12V supply side of the power switch on the reverse side of the board. GND was connected to the outer pin of the DC power socket. ON_SW was connected to the switching side of the momentary switch. The following figure shows the 3G enclosure that the board was fitting inside of, on the left of the image you can see the momentary power switch followed by the RJ45 10BaseT and DC power port.

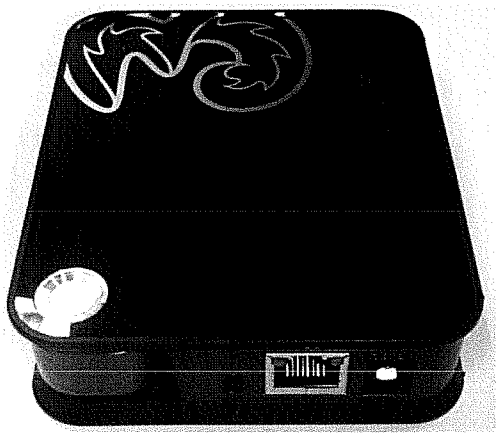

FIGURE 42 - HUAWEI D100 POWER SWITCH AND CONNECTIONS

The relay coil (K1) has an impedance of 167Ω and a maximum coil power of 200mW[52]. Maximum coil current with the coil energised to 5V DC can then be calculated:

$$I_{coil} = \frac{V_{coil}}{R} = \frac{5V}{167\Omega} = 29.9\,mA$$

EQUATION 25 – COIL CURRENT

The 12F683 microcontroller has a maximum sink or source current of 25mA[53]. Thus to prevent the microcontroller from operating outside of its' absolute maximum ratings, a buffer was required. A simple yet reliable method that satisfies the objective of maintaining a low parts count; is the use a NPN transistor in common emitter configuration (emitter connected to ground).

The BC547 was chosen as the NPN transistor due to its large minimum dc collector current gain of 110 and maximum collector current of 100mA[54]. For reliable operation the coil current through K1 should be maximized and thus the desired mode of operation for the BC547 is in the saturated region. To calculate

the required base current, the coil current is required. The saturation voltage $V_{CE\ SAT}$ of the BC547 is typically 90mV [54].

$$I_C = I_{coil} = \frac{V - V_{CESAT}}{R_{coil}}$$
$$= \frac{5V - 0.09V}{167\Omega}$$
$$= 29.9\ mA$$

EQUATION 26 – COIL/COLLECTOR CURRENT

Thus the required base current can be calculated from the minimum dc collector gain ($h_{FE} = 110$).

$$I_C = h_{FE} * I_B$$

$$I_B = \frac{I_C}{h_{FE}}$$
$$= \frac{29.9mA}{110}$$
$$= 0.27mA$$

EQUATION 27 – BASE CURRENT

The base current limiting resistor can be calculated from the base-emitter junction forward voltage and the microcontroller's high level output of V_{DD} (5V).

$$R_B = \frac{V_{IO} - V_{BE}}{I_B}$$
$$= \frac{5V - 0.7V}{0.27mA}$$
$$= 15.9k\Omega$$

EQUATION 28 – CURRENT LIMITING RESISTOR

The nearest appropriate E24 value[22] (5% tolerance resistors) is 15kΩ.

To protect the circuit from the back EMF generated when the relay coil de-energizes, diode D1 was added. R1 acts as a pull-up resistor to prevent the device from entering the reset state. The RJ45 connector J1 is placed on the board for In Circuit Serial Programming and was later removed to reduce the foot print size for installing into the router enclosure.

The firmware for the microcontroller was written in assembly and was assembled with MPLAB and then programmed with an ICD2 programmer. Total resources consumed by the firmware, consisted of a total for 56 words of program memory (4% utilization) and 3 bytes of ram (2% utilization). The program flow is illustrated in the flow chart below.

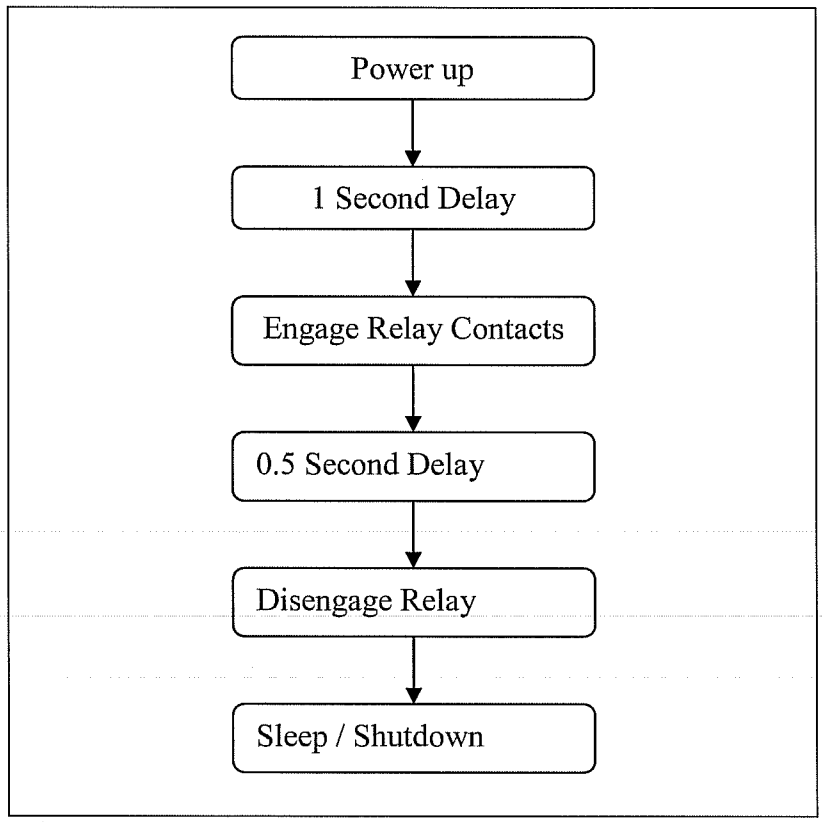

FIGURE 43 - 3G ROUTER PROGRAM FLOW

The microcontroller is put into the sleep state to both save power, and reduce the risk of abnormal behaviour once the 2.4 GHz internal WiFi radios became active in the router.

4.3 RESULTS

The key design criteria was to make sure the design will fit into the original enclosure. Figure 44 shows the final assembly after removing the programming RJ45 socket and highlights the major components.

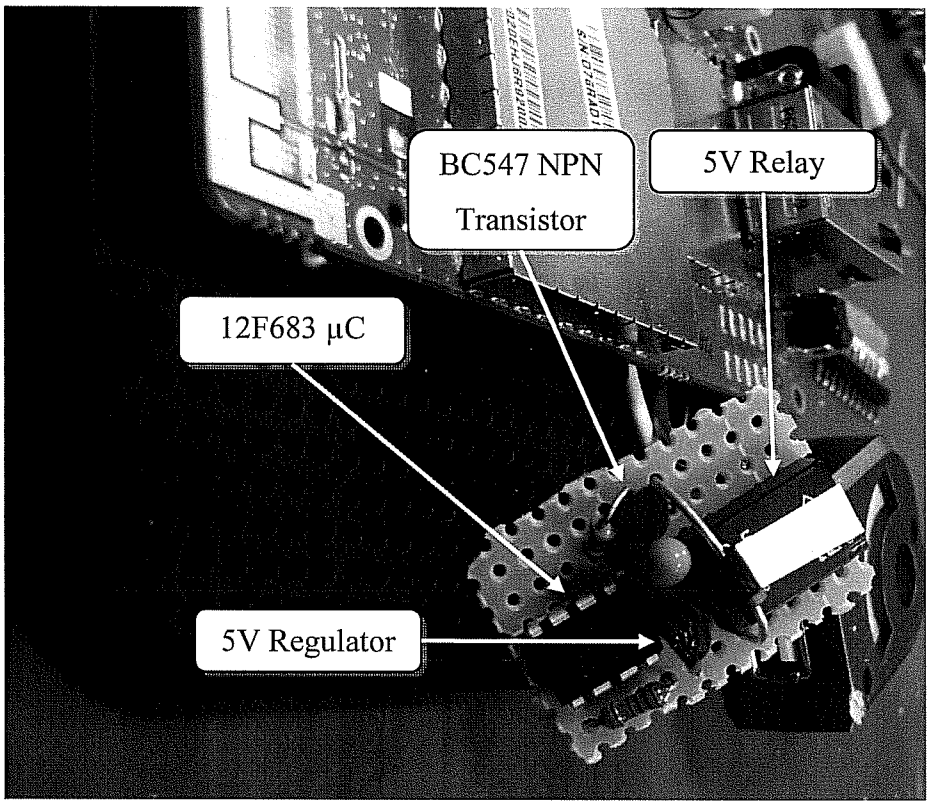

FIGURE 44 - 3G POWER MANAGEMENT BOARD ASSEMBLED

To keep the components secure and reduce fatigue from vibration as well as prevent any electrical short-circuits to the routers main PCB (Printed Circuit Board) the board was heat shrinked. Figure 45 illustrates the circuit installed before the router was reassembled.

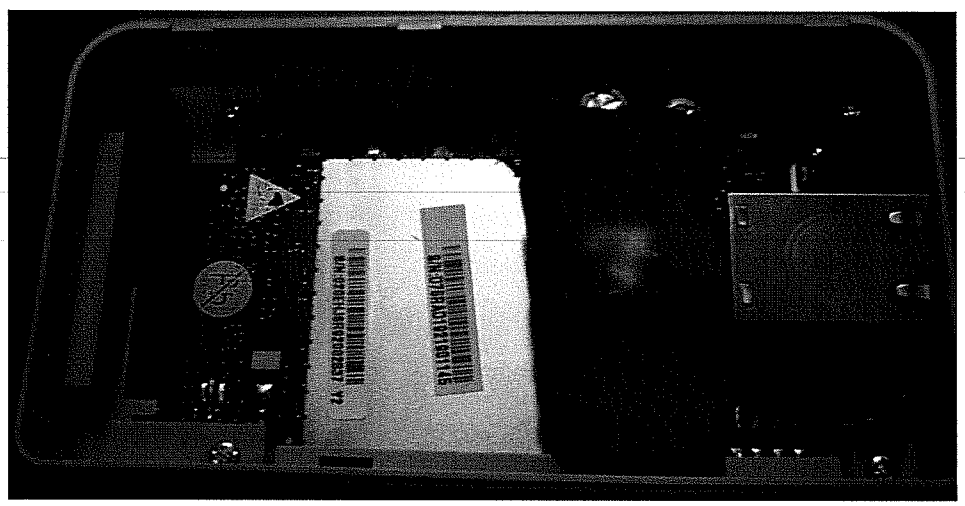

FIGURE 45 - 3G POWER MANAGEMENT BOARD INSTALLED

5 TBS Gateway Design

5.1 Background

The Hyundai Getz traction pack capacity and monitoring is handled by the E-xpert Pro developed by TBS Electronics. The TBS unit calculates a number of critical variables including:

- Instantaneous battery voltage
- Instantaneous battery current
- Battery amp hours consumed
- Remaining battery capacity
- Remaining operational time based on capacity[55]

The unit is installed in one of the cup holders in the centre of the cabin for easy viewing by the driver and or passenger. However it has been found that the driver will instinctively look at the original fuel gauge in the vehicles instrument cluster, thus the TBS gateway will also drive the original fuel gauge displaying the state of charge. Additionally it would be useful for the purpose of research and continual development to be able to log the data collected from the traction pack, so the TBS Gateway makes this information available to the Eyebot Controller.

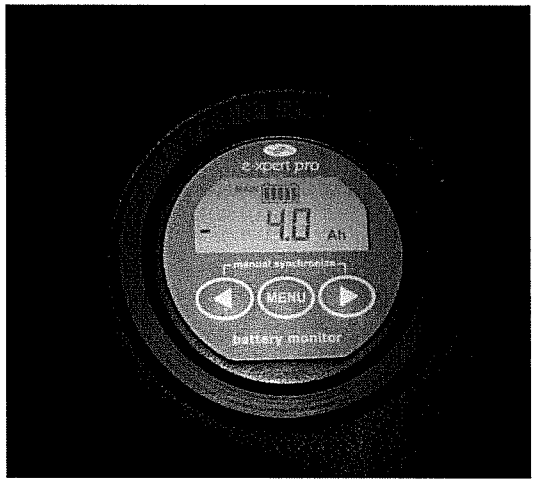

Figure 46 - TBS E-xpert Pro Battery Monitor

Previously, monitoring of the traction pack was attempted by measuring the analogue values feed into the E-xpert Pro from the voltage prescaler (traction pack voltages are called down from 144V nominal to 14.4V nominal) and the shunt resistor (±50mV/±500A) installed off the negative terminal of the traction pack. This method has a number of complications; the least of these was the

requirement to scale the voltages to the required 0-7V signals. Additionally the 12V system which the Eyebot controller is operating from is isolated from the 144V traction pack. A direct connection would be in breach of the isolation requirements demanded by the *Vehicle Standards Bulletin 14 National Code of Practice (NCOP) for light vehicle construction and modification (National Guidelines for the installation of electric drives in motor vehicles).*

"Any HV traction battery system must be isolated from the chassis of the vehicle, and also from any auxiliary SELV components and wiring. Isolation must be designed such that there is a leakage current of less than 20 mA between any part of the HV system and either the chassis or SELV components in the vehicle, measured when the vehicle is at rest." [56]

These issues could be overcome by implementing an analogue isolation circuit to interface the Eyebot to the signals originating from the traction pack. However even with the voltage and current information from the pack; the current battery state and capacity would not be able to be determined directly. This is due to relatively constant cell voltage versus remaining capacity (see Figure 47), additionally due to the internal resistance of each cell for every C (rated capacity) increase in instantaneous current there is an additional 0.2V (typical) drop in cell voltage[4].

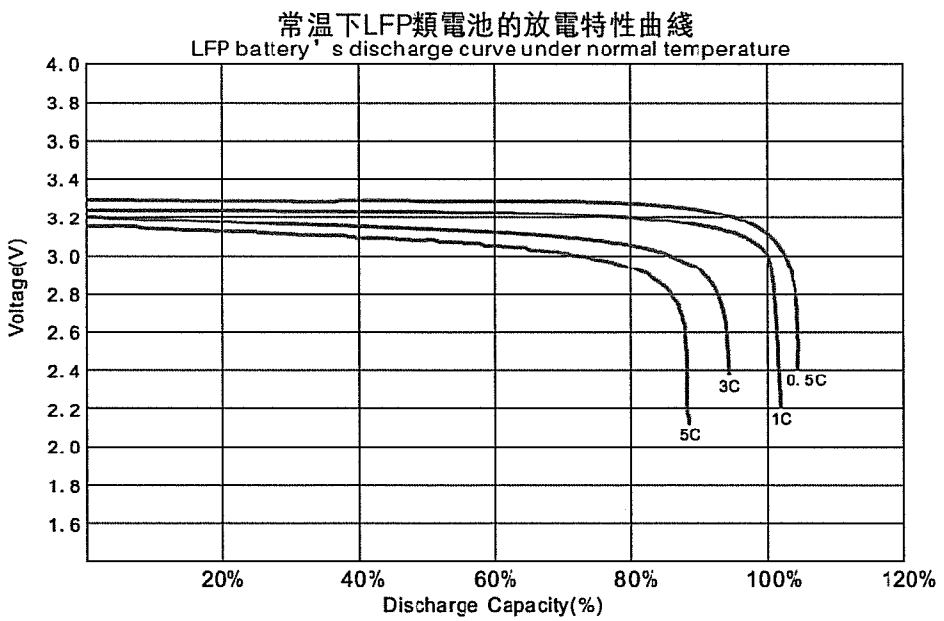

FIGURE 47 - $LiFePO_4$ CELL VOLTAGE VS DISCHARGE CAPACITY [4]

To overcome this issue, remaining capacity of the traction pack is determined by calculating the number of consumed Amp-hours and subtracting from the cells rated capacity. The downside to this method is that it requires the measuring device to be constantly active whenever there is a load on the traction pack. Since there is a constant load on the traction pack from the Battery Management System and when the 12V DC-DC converter is active this would inherently require the Eyebot M6 to be online permanently. The Eyebot M6 controller consumes approximately 0.4A from the vehicles 12V battery while active and thus would deplete the 12V battery within a couple of days (based on a 45 Ah Pb battery), and thus is not a viable solution.

The TBS gateway allows the Eyebot to connect serially to TBS E-xpert Pro providing access to all of the internal metrics calculated by the unit. In turn the Eyebot can then display user prompts and log traction pack information in the Black Box Software (independent to the Hardware Black Box).

The instrumentation team also encountered repeated issues with the discrete digital IOs on the Eyebot M6 in addition to finding themselves limited by the number of IO lines available. To assist in these connectivity issues the TBS Gateway also provides 32 discrete digital IOs that can be individually set as an input or an output as well as 3 additional analogue inputs. The TBS Gateway also offers the synthesizing of the original fuel level sender signal to drive the fuel gauge on the instrument cluster, and a variable frequency signal to drive the tachometer based upon the instantaneous traction pack current.

5.2 Design

The TBS Gateway consists of a number of modules assembled onto a single printed circuit board. The major components include the isolated serial interface to the TBS E-xpert Pro, discrete digital IO, PWM outputs and the Hall Effect sensor input (RPM - optional) and analogue inputs. The following three schematics show the design of the TBS Gateway.

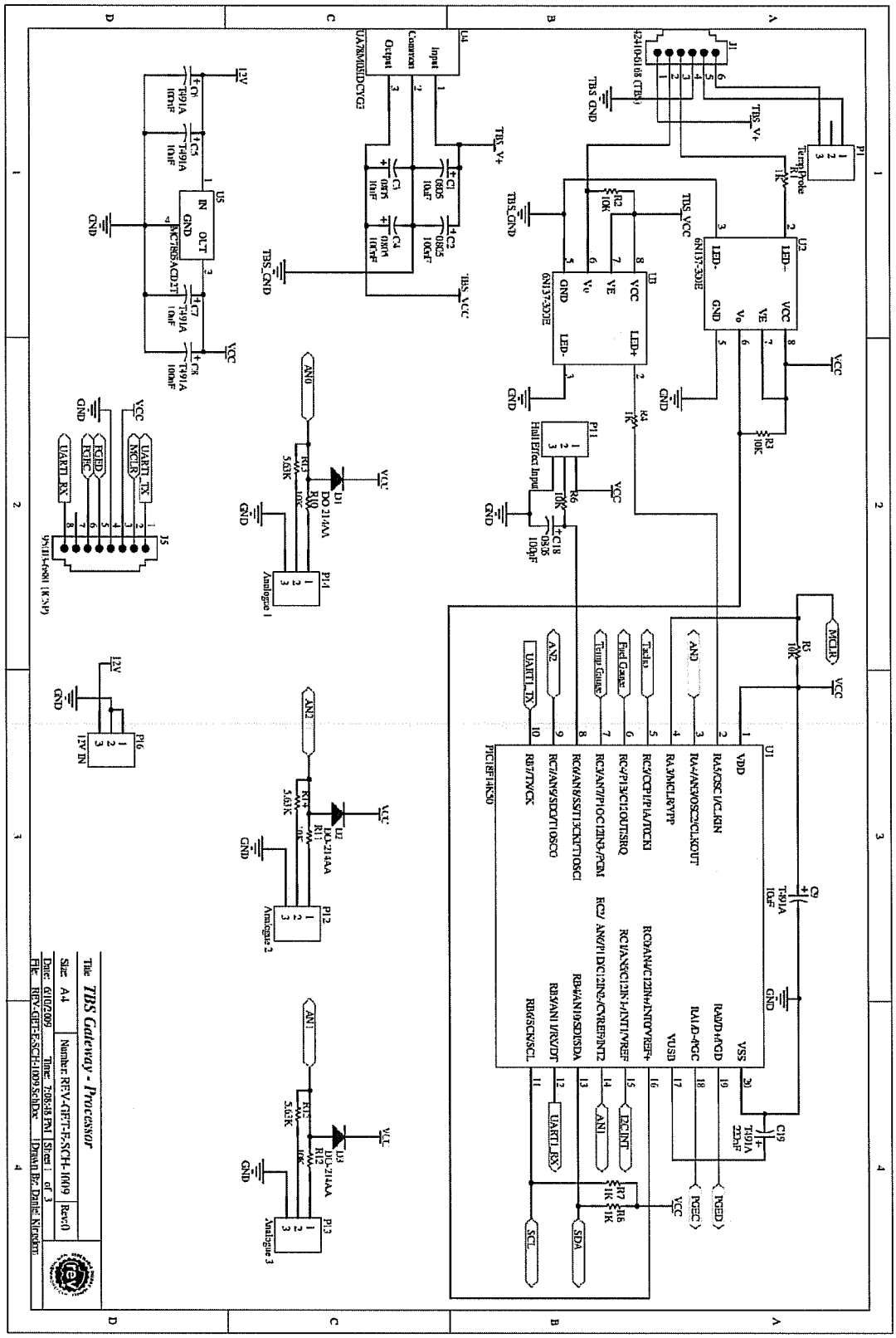

FIGURE 48 - TBS GATEWAY SCHEMATIC SHEET 1/3

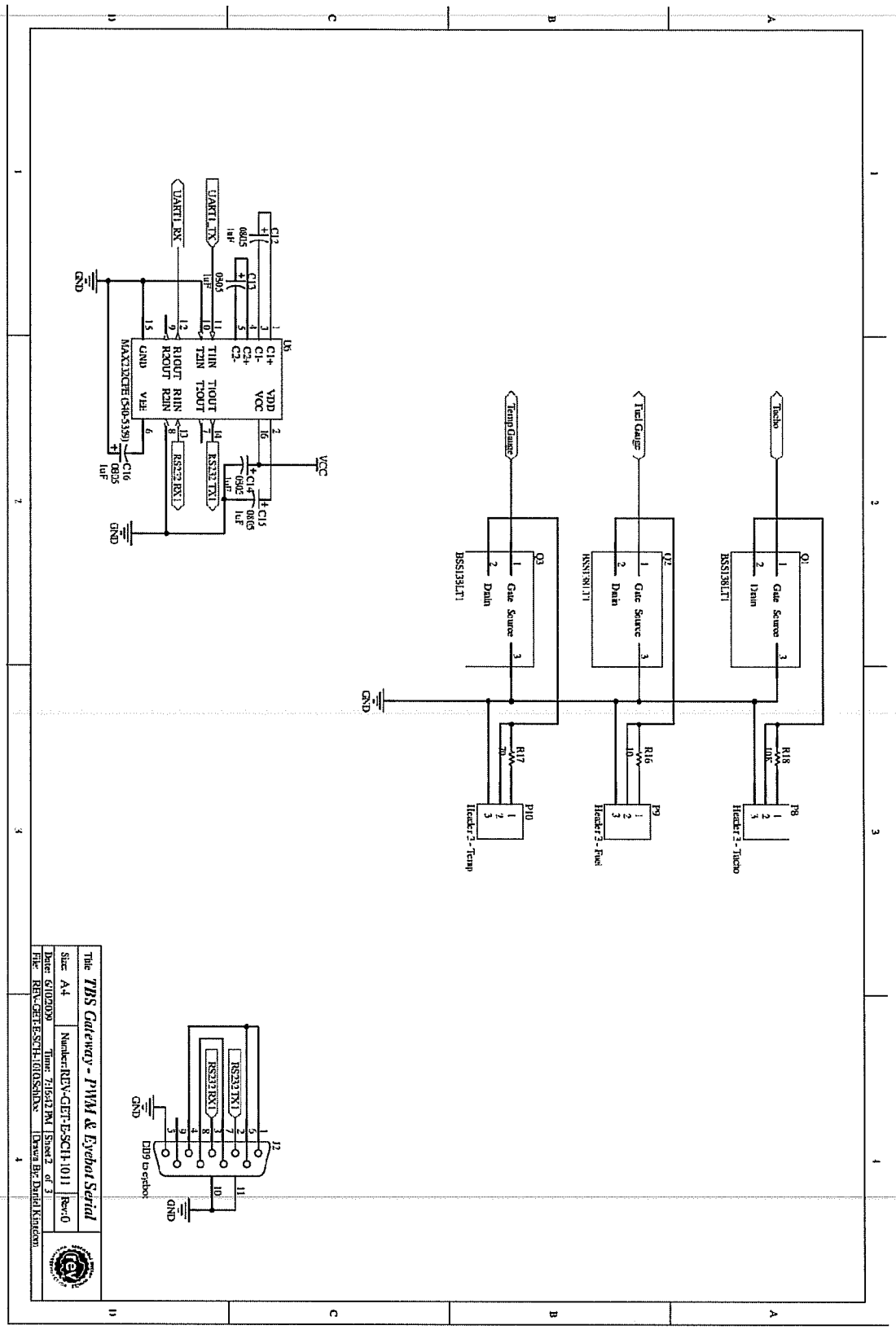

FIGURE 49 - TBS GATEWAY SCHEMATIC SHEET 2/3

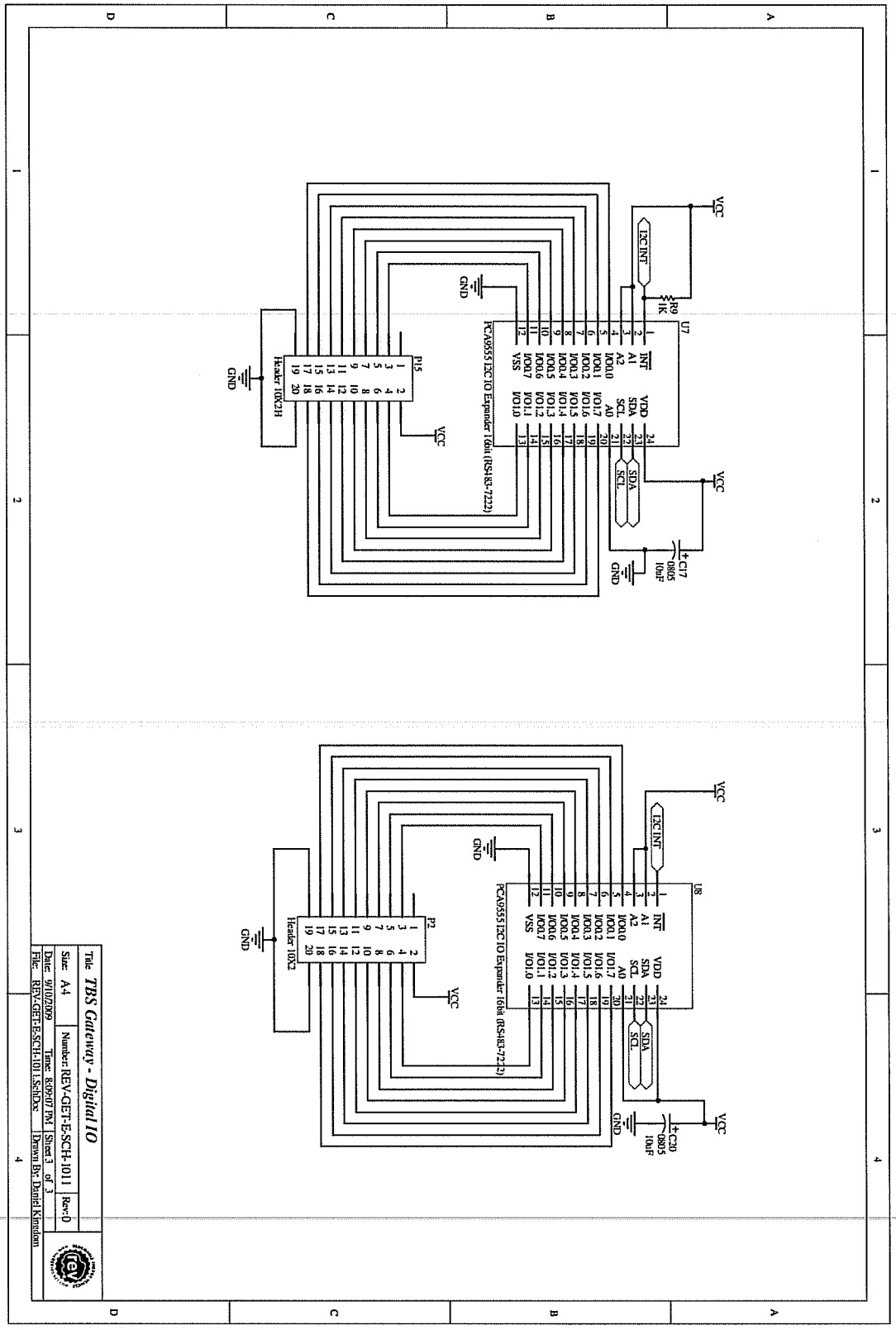

FIGURE 50 - TBS GATEWAY SCHEMATIC SHEET 3/3

The E-xpert Pro provides a TTL level UART (Universal Asynchronous Receiver/Transmitter) that is accessible from a RJ12 connector located underneath the unit (Figure 51). The UART is not isolated from the unit's 15V supply, while the Meanwell DC-DC converter (installed in the EV Power 10:1 prescaler) does offer some isolation. The supply input is common with the analogue ground for the shunt and potential divider (which is formed by a simple resistor based divider). Thus the TBS E-xpert Pro is not isolated from the traction pack.

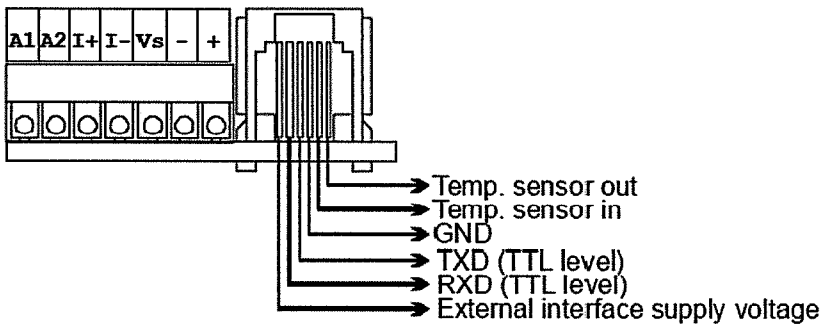

FIGURE 51 - PIN OUT OF THE RJ12 CONNECTOR OF THE E-XPERT PRO [57]

For serial communications to the TBS E-xpert Pro pins 1-4 of the RJ12 connector are required. For the purpose of future proofing, the temperature sensor pins are also broken out onto screw terminal P1. This will enable the REV team in the future to install the optional thermistor temperature probe kit if so desired.

The external interface supply voltage output is unregulated and has a nominal potential of 13V. To achieve isolation, two single channels optically coupled gates (Model number 6N137) were used. The 6N137 boasts a low required LED forward current of 6.3 mA, and also allowed the use of a weaker pull-up resistor (up to 4kΩ) thus assisting to conserve power. Which is important since the Gateway may be operating for extended periods of time from the Vehicles 12V battery. The optically coupled gate, also provides a rise and fall time of 300ns (4kΩ pull-up resistor) thus allowing a serial bandwidth in excess of 1 Mbps ($\frac{1}{2*300ns} > 1.5MHz$) readily exceeding the bandwidth requirements of the TBS E-xpert Pro, which has a relatively small bandwidth of just 2400 bps[57]. The working voltage (V_{IORM}) of the 6N137 is 630V[58] greater than the Hyundai Getz traction pack voltage of just 144V and thus does meet the required isolation requirements.

The supply voltage of the 6N137 (4.5V – 5.5V) requires the external interface voltage from the E-xpert Pro to be regulated to within allowable limits. The implemented regulator for this task is U4 (UA78M05IDCYG3) which is a low-dropout 800mA 5V regulator. The TXD and RXD operate at 5V TTL levels and are capable of sinking/sourcing at least 10mA and have a source impedance of 100Ω[59]. The forward voltage of the 6N137 is a maximum of 1.75V (1.5V Typical). Thus the required current limiting resistor value can be found through the following equation:

$$V_{TTL} = I_f * (R_{source} + R_{limiting}) + V_f$$

$$R_{limiting} = \frac{V_{TTL} - V_f}{I_f} - R_{source}$$

$$= \frac{5 - 1.75}{0.0063A} - 100$$

$$= 415\ \Omega$$

EQUATION 29 - CURRENT LIMITING RESISTOR

Selecting the nearest E24[22] value results in a value of 390Ω for the two current limiting resistors R1 and R4. The 18F14K50 PIC microcontroller includes one hardware UART (Universal Asynchronous Receiver/Transmitter), since the baud rate of the E-xpert Pro is only 2400 bps without flow control, the UART is implemented in software. While the hardware UART is reserved for the Eyebot such that a faster baud rate may be implemented.

The RXD pin (received on the TBS side) is then connected to the general purpose IO pin RA5 (set as an input) of the PIC 18F14K50. The TXD pin on the other hand is routed to RC0 and is used as the input to the external interrupt (INT0).

The 6N137 optocoupler inverts the input and thus the asynchronous serial present at the software UART is at inverted TTL level thus a logic '0' is 0V, while a logic '1' is at 5V while the idle state is 0V. The E-xpert Pro requires a 2400bps asynchronous stream with 8 data bits, 1 stop bit and even parity, software or hardware flow control is not implemented. The following figure shows a typical single byte transmission.

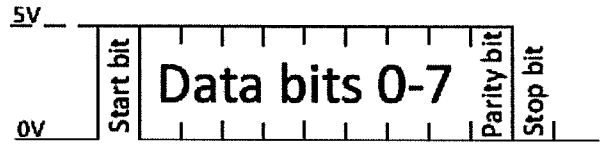

FIGURE 52 - INVERTED ASYNCHRONOUS TRANSMISSION

Figure 66 and Figure 67 (in the Appendix) demonstrate by means of software flow chart how the Software UART has been implemented. The delays are generated through the use of Timers 0 and 3 (16 bit timers[60]) on the 18F14K50 via pre-padding the timer, and using the timer overflow interrupt to signify the end of the delay. Thus other tasks can still be preformed while transfers are in progress and thus the software UART is also full-duplex (i.e. can receive and transmit at the same time).

5.2.1 TBS E-XPERT PRO COMMUNICATION PROTOCOL

The E-xpert Pro sends small packets of data through the UART every packet is a minimum of 5 bytes. The first two bytes are the destination and source addresses of the communication. The most significant bit of every byte sent over the serial link is the IDHT (Identify Header / Trailer) this bit is logic '1' for the destination address byte and the end of transfer byte and '0' for all other fields[57]. Both the Source and Destination addresses are reserved fields and for direct connection are always set to 0.

The next byte is the device ID which for the E-xpert Pro is always 0x22. Then there is the Message type byte which is Handshake, Commands, or Data. On the TBS Gateway only data packets are required. The following table contains the Message Types interpreted by the TBS Gateway:

Message Type	Data Length	Function
0x60	16 bits in 3 bytes	Main Pack Voltage
0x61	21 bits in 3 bytes	Main Pack Current
0x62	21 bits in 3 bytes	Amp hours
0x64	16 bits in 3 bytes	State of charge (%)
0x65	21 bits in 3 bytes	Time Remaining
0x66	16 bits in 3 bytes	Temperature (External Probe)
0x67	18 bits in 3 bytes	Monitor Status
0x68	16 bits in 3 bytes	Auxiliary battery voltage

TABLE 5 - TBS E-XPERT PRO MESSAGE TYPES[57]

The final byte after the data has been transmitted is the trailing byte, this byte is always 0xFF. Each of the above message types are transmitted by the TBS E-xpert Pro every second in succession. This data is then processed and stored internally before being sent to the Eyebot through the Hardware UART (see 5.2.3 EYEBOT Interface – Hardware UART).

Dest	Src	Data	Type	Value	Tail	Function
0x80	0x00	0x22	0x60	0x00 0x75 0x2C	0xFF	T Pack V
0x80	0x00	0x22	0x61	0x40 0x00 0x07	0xFF	T Pack I
0x80	0x00	0x22	0x62	0x40 0x00 0x07	0xFF	Amp hours
0x80	0x00	0x22	0x64	0x00 0x06 0x5E	0xFF	Charge (%)
0x80	0x00	0x22	0x65	0x00 0x35 0x7F	0xFF	Time Remain
0x80	0x00	0x22	0x66	0x00 0x01 0x48	0xFF	Temp Probe
0x80	0x00	0x22	0x67	0x00 0x00 0x00	0xFF	Status
0x80	0x00	0x22	0x68	0x00 0x00 0x00	0xFF	Aux Bat V

TABLE 6 - SAMPLE DATA TRANSMITTED FROM E-XPERT PRO

5.2.2 PWM OUTPUTS

There are three PWM outputs on the TBS Gateway; each one has a specific predefined role. The first of these is the fuel level sender output. The original Fuel level sender that was removed from the Hyundai Getz is pictured below. The fuel level sender consists of a float and a potentiometer. As the level of fuel in the tank changes, the resistance across the potentiometer changes also and this is used to drive the gauge in the instrument cluster.

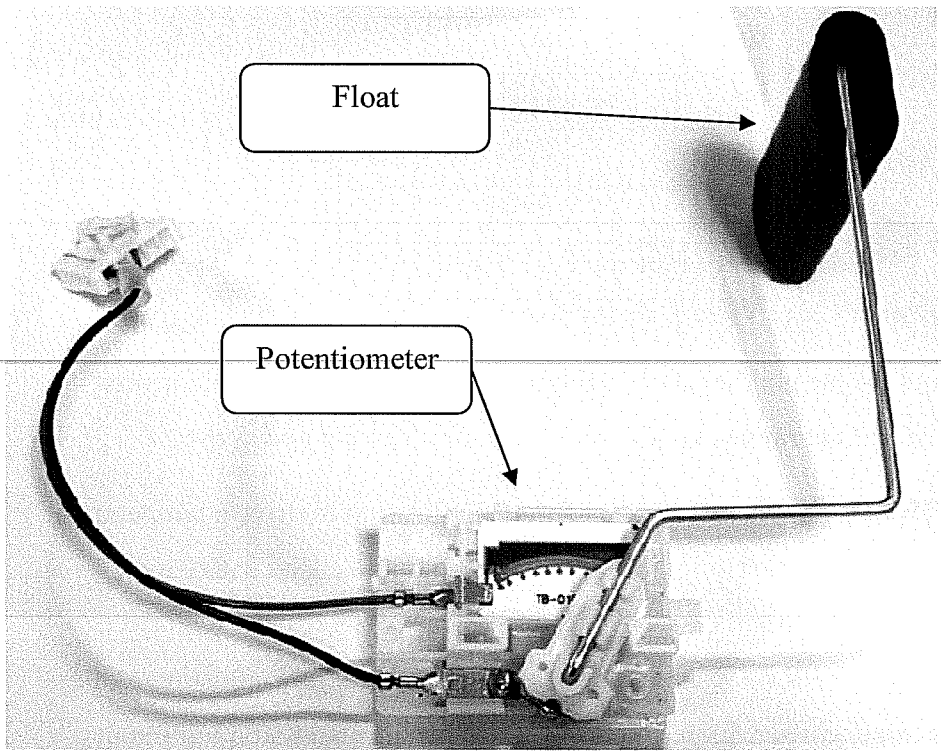

FIGURE 53 - ORIGINAL FUEL LEVEL SENDER

Table 7 below details the resistance values of the level sender in accordance with fuel tank level displayed on the instrument cluster.

Float Level	Resistance
Full	4.0Ω
Half	32.5Ω
Empty	110 Ω

TABLE 7 - FUEL SENDER RESISTANCE VS FLOAT LEVEL[61]

To drive the fuel gauge sender, an NMOS with the source connected to ground is used. A 10 Ω resistor is connected in series with the drain connected to the instrument cluster, as this was found to still be sufficient to get full range of the gauge. The NMOS is then PWM (Pulse Width Modulated) at 5kHz with a varying duty cycle to adjust the effective impedance seen after the internal low pass filter in the instrument cluster.

Experimentally lower PWM frequencies were found to cause slow oscillations in the fuel gauge display. Table 8 contains the duty cycles required at 5kHz for various fuel gauge positions.

Position	Duty Cycle
Empty	39%
1/4	52%
1/2	68%
3/4	80%
Full	89%
Fuel Light	42.5%

TABLE 8 - PWM DUTY CYCLE VS FUEL GAUGE POSITION

To compensate for the non linearity, a 50 row look up table was implemented using a piecewise linear relationship from the values determined above.

The second PWM output is reserved for future application to drive a temperature gauge (Non-existent in the Getz). The final PWM output is used to drive the tachometer in the instrument cluster. Once again an NMOS is used with the source to ground. A pull up resistor is used to allow for flexible adjustment of the input voltage to the cluster. Experimentally it has been found that a minimum

voltage of 7V is required to drive the tachometer with a maximum of 12V. A 50% duty cycle signal is used with a varying frequency range from 0 to 266Hz for the full range scale of 0-8000 rpm. The table shows the relationship between frequency and revolutions per minute, found via experimentation.

PWM Frequency (Hz)	RPM (Displayed on Cluster)
0	0
32	1000
65	2000
102	3000
134	4000
167	5000
200	6000
232	7000
268	8000

TABLE 9 - FREQUENCY VS TACHOMETER VALUE

The linear relationship can be expressed as:

$$f = \frac{f_{RPM}}{60} * 2$$

Thus for every revolution two pulses are generated. On the TBS Gateway the RPM signal is generated either by the RPM input from a Hall Effect sensor placed on the motor shaft, or from traction pack instantaneous current information from the TBS E-xpert Pro. By providing the driver with the current information directly on the instrument cluster, driving habits can be adjusted to maximize efficiency and reduce driver activities that consume high currents.

5.2.3 EYEBOT INTERFACE – HARDWARE UART

The Eyebot interface is implemented using the hardware UART on the PIC 18F14K50, using a hardware UART reduces the processing load and thus allows the use of a faster baud rate. The port settings are set to 8 data bits, 1 stop bit, no parity and 19200 bps. Instead of using the parity, error detection is instead handled in the communication protocol though the use of a checksum.

The Eyebot interface is accessible via a DB 9 port (J2) and is configured as a DCE (Data Communication Equipment) device, allowing for DTE (Data Terminal Equipment) devices such as a PC or the Eyebot controller to be connected directly without the use of a null-modem cable/adapter. The interface serves two roles, one to be used to configure the Gateway directly via a PC and the other to allow the Eyebot controller to send and receive data from the board.

5.2.4 Configuration Interface

To enter the configuration menu, simply connect a PC to the TBS gateway with the serial settings above, and type "config" (without the quotes) and press enter within 20 seconds. The 20 second limit exists to reduce the likelihood of the configuration menu from being entered into accidentally while under Eyebot control. The gateway will acknowledge that the configuration mode has been entered into with the transmission of the main menu (see Figure 54).

The user can then enter into any of the following menus typing the corresponding menu number (1-6 , 9). The configuration menus will also timeout after five minutes if no valid input is received (i.e. correct selection from a menu). This feature has been added in case the user either forgets to exit configuration mode or if the mode is accidentally entered into through software error on the Eyebot.

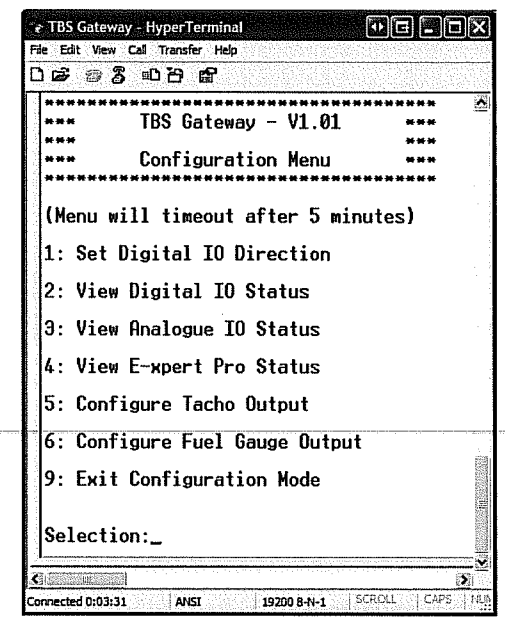

Figure 54 - Configuration Main Menu

Set 'Digital IO Direction' can be used by the user to manually set each of the 32 digital IO lines as either an input or an output. This is particularly useful for

diagnostic testing of circuits in the car attached to the TBS Gateway without the need for any additional software to be developed on the host controller (Eyebot). Caution should be followed such that an IO pin is not set to an output if the line has a low impedance path to Ground or V_{DD} or being driven from an external circuit. Care should also be taken to make sure that maximum sink and source currents are observed as well as the maximum pin voltages when the IO pin is set as an input (see 5.2.8 Digital IO).

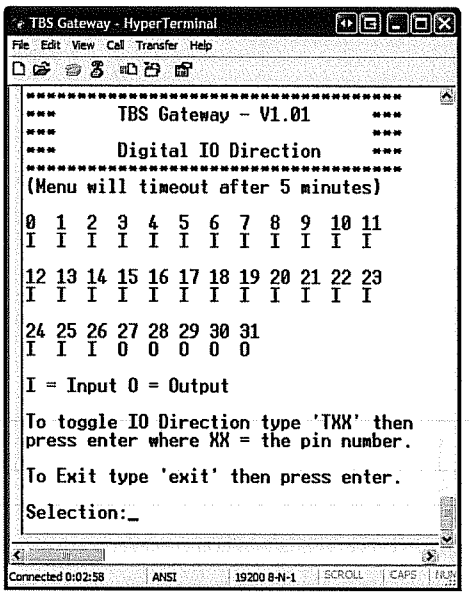

FIGURE 55 - DIGITAL IO DIRECTION MENU

The Digital IO Direction menu displays the state of all 32 digital IO pins; individual pins can then be toggled by typing 'TXX' and then pressing enter where 'XX' is the IO pin number. An 'I' or 'O' under the pin number represents the status of the pin is set to an input or an output respectively, to exit the user simply needs to type 'exit'. The output value of each pin can be assigned in the Digital IO Status Menu shown in the following figure.

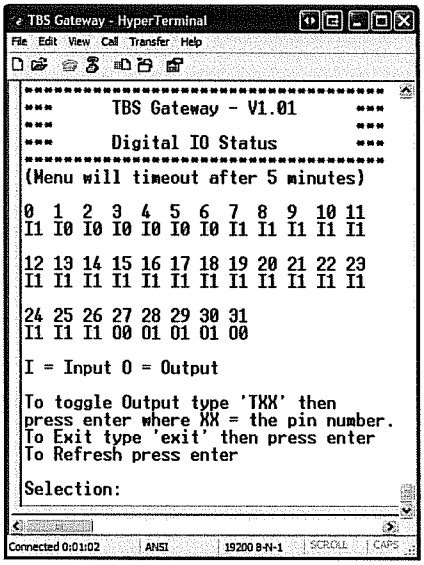

FIGURE 56 - DIGITAL IO STATUS

Digital IO Status menu displays the state and direction of each of the 32 IO lines. Following from the Digital IO Direction menu an 'I' or 'O' represents an input or output respectively while a '1' or '0' represents the value present at the pin (High or Low respectively). Only the value of output pins can be toggled, by typing 'TXX' as in the previous menu. If an input pin is attempted to be toggled the command will be ignored. The user can also opt to refresh the display by pressing the enter key which will result in the menu being re-transmitted.

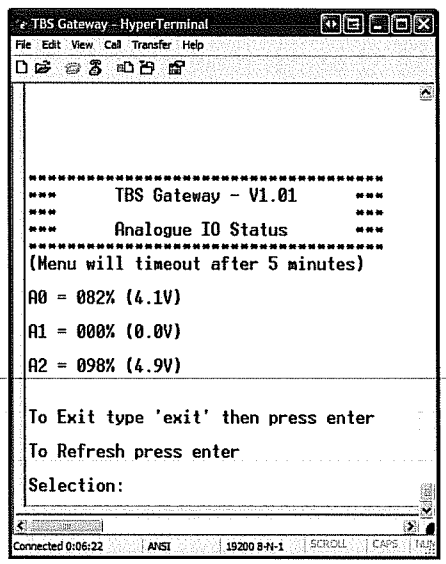

FIGURE 57 - ANALOGUE IO MENU

The Analogue IO Status menu has no options to change any parameters and displays the current values of the three analogue inputs. The value is displayed as a percentage of full scale, and the input voltage (assuming a 5V input). Similarly

to the previous menu the value can be refreshed by pressing enter or the can be exited via typing 'exit'. Like all of the menus the configuration mode will timeout after five minutes without valid input.

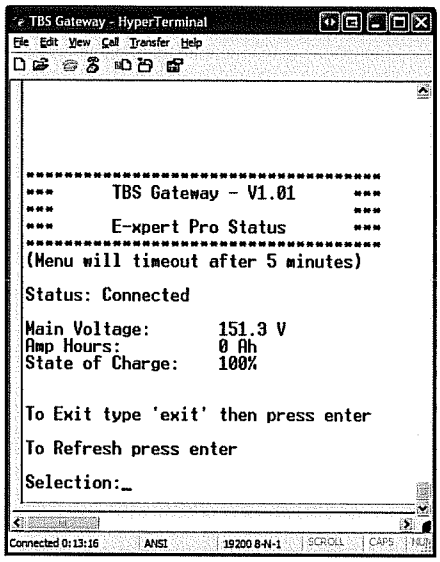

FIGURE 58 - E-XPERT PRO MENU

The E-xpert Pro Status menu shows the connection state of the TBS E-xpert Pro which is based on whether any parameters have been received in the last 2 seconds (all critical parameters should be received once per second). Main traction pack Voltage, Amp Hours consumed and present charge state are displayed as basic metrics such that the user can validate that the connection is functioning correctly.

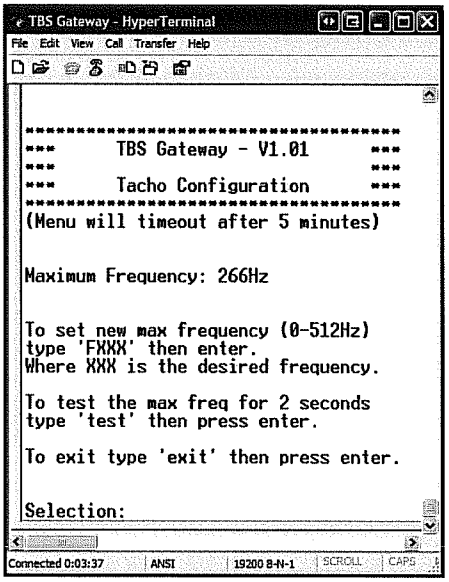

FIGURE 59 - TACHO CONFIGURATION

The Tachometer Configuration menu allows the user to set the maximum frequency that corresponds to the maximum deflection on the instrument cluster. This can be calculated from the Hall Effect sensor assembly originally used on the vehicle, or found experimentally by gradually increasing the max frequency by typing the command 'FXXX' where XXX is the desired frequency. The frequency can then be tested by typing 'test' and pressing enter, which will result in the TBS Gateway generating the maximum frequency for two seconds or until the enter key is pressed.

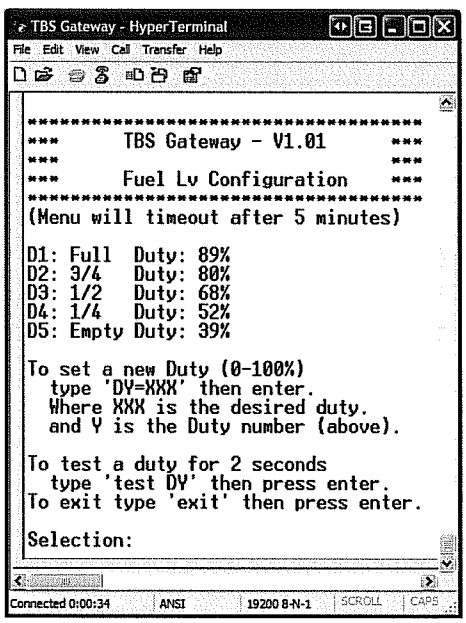

FIGURE 60 - FUEL LEVEL CONFIGURATION

The Fuel Level Configuration menu allows the user to set the duty cycles for various positions of the fuel level gauge. This is then used to generate a piecewise linear approach to the non-linear output required for the fuel level gauge. Similar to the tachometer configuration mentioned earlier the user can update each duty cycle via typing 'DY=XXX' where Y is the number of the Duty Cycle to be edited and XXX is the duty percentage (0-100%) as an integer. Each duty can be individually tested by using the 'test DY' statement (Y is the duty number) this will trigger the Gateway to output the specified duty cycle at 5kHz for 2 seconds or until the enter key is pressed.

5.2.5 Eyebot Interface

While the previous interface makes manual adjustments and testing of the TBS Gateway trivial, it adds unnecessary complexity to the UART processing threads on the Eyebot. Hence the Eyebot Interface is designed to be a machine readable protocol. The protocol is limited to printable characters to aid in debugging and simplifier the development of the serial routines implemented on the host controller. It should be noted that byte and bit ordering is as per the little endian format that is MSB/MSb (Most Significant Byte/bit) will be transmitted first and LSB/LSb (Least Significant Byte/bit) will be transmitted last. The serial protocol implemented is listed in Appendix TBS Gateway Eyebot Serial Protocol.

5.2.6 Power-On State

After a power-on reset the TBS gateway will load its configuration from the EEprom memory on the 18F14K50 microcontroller. Thus it is not necessary to resend the tachometer and fuel level parameters after power up. However the exception to this is the digital IO lines, to reduce the risk of damage to the TBS gateway from wiring changes the gateway will always power on with all IO lines set as an input. The host controller will then have to use the digital IO Direction commend to set the desired IO lines to outputs. This reduces the risk of harm from setting an IO line to an output when its load has a low impedance path to V_{DD} or ground such as you may find on an a switch which is connected to be an input.

5.2.7 In Circuit Serial Programming

The TBS gateway 18F14K50 microcontroller does not have code protection features enabled, and thus it is possible for future enhancements and features to be

implemented on the gateway. To remove the need for the processor to be de-soldered (the 18F14K50 is a SMD part) for the purposes of reprogramming, the board has a RJ45 socket installed. Microchip ICD2/3 in-circuit programmer/debuggers are recommended for the purpose of programming the TBS Gateway, these programmers come with an RJ12 interface which is compatible with the RJ45 on the board.

The RJ45 socket was chosen as it allows direct compatibility with the afore mentioned programmers (the centre 6 pins of the RJ45 mate with the RJ12 interface) while allowing an extra two pins (1&8) to be used for a connection to UART1 on the PIC microprocessor. This is convenient for debugging purposes especially for devices where the UART is not directly accessible, so that data can be monitored (with a suitable cable), if the interface is used for monitoring UART data the computers transmit pin should not be connected.

The other significant advantage to providing convenient access to the UART is to enable the use of a serial boot loader. This is not implemented on the TBS gateway, but could easily be added if so desired. Using a serial boot loader would remove the need to use either the ICD 2 or 3. Instead all that is required for programming is serial connection to a PC, reducing the inventory of tools required.

If the TBS Gateway is to be reprogrammed with an ICD 2 programmer care must be taken to prevent damage to the 18F14K50. The programming voltage (V_{PP}) must be limited to less than 9.0V and a minimum limited voltage during programming of 6.5V[60]. The ICD2 uses a V_{PP} Voltage of 12V[62] which will damage the processor. This restriction applies to all PIC microcontrollers manufactured after 2008. The 18F14K50 has another limitation which is relevant to only this family of processes and is due to the fact that the programming data and clock pins are shared with the USB D+ and D- pins. This results in a restriction of the maximum voltage present on these pin to be 3.6V. On the ICD 2 programmers the data and clock pins always operate at V_{DD}. This limitation can be overcome by carefully adjusting the input voltage of the TBS Gateway to approximately 4.3V and then using the self test feature of the ICD2 to verify that the V_{DD} voltage is 3.3V. The V_{PP} restriction requires that a V_{PP} limiter be used, the limiter is built into the programming board (see Figure 61 and Figure 63).

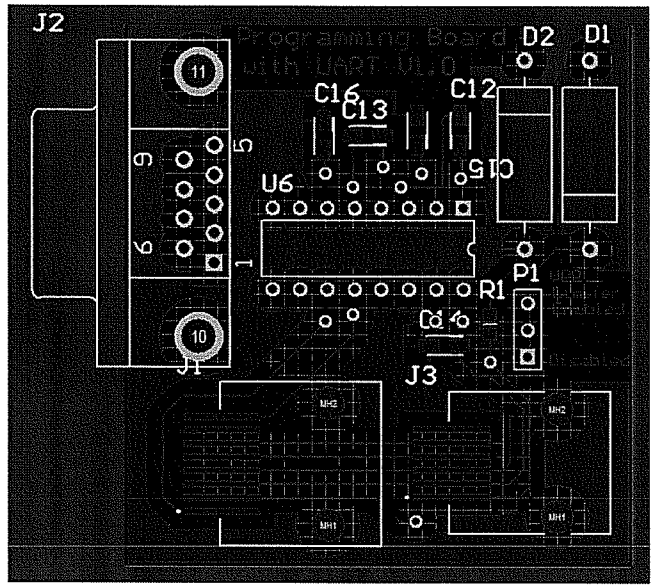

FIGURE 61 - PROGRAMMING BREAKOUT BOARD PCB

On the programming board an ICD 2/3 can be connected to the RJ12 port J3, and the target (TBS Gateway) can be connected via the RJ45 port J1. Access to UART1 is provided by the DB9 serial connection J2. The V_{PP} limiter can be selectively enabled or disabled by setting a jumper on P1. V_{PP} limiter will be disabled when the jumper is across pins 1&2, and enabled when pins 2 & 3 are connected together. The Vpp is limited by placing a 5.1V and 3.3V zener diode between R1 and ground (for more information, see the schematic in Figure 63).

If an ICD3 programmer/debugger is used, neither of these two restrictions apply. The TBS Gateway does not support in circuit debugging as the PIC 18F14k50 does not have an onboard debugging engine.

5.2.8 DIGITAL IO

The TBS Gateway offers 32 general purpose digital IO lines organized into two banks of sixteen lines. Each line is capable of a sink or source current of 50mA[63] (maximum bank limits apply) and are 5V inputs and outputs. When configured as an input each IO line has a weak pull up to V_{CC} (5V). Each block of 16 IO lines are accessible from the two 20-way (10x2) IDC headers P2 and P15, these headers also provide a 5V output (100mA Max) which can be used to power simple interface circuits.

P15 and P2 IDC headers were designed to be similar to the IO ports on the Eyebot M6 controller to allow existing interface boards developed by the instrumentation

team to be used directly without the need for any additional alterations. Since these circuits were already installed in the Getz, additional IO line protection was deemed to be un-necessary as it would duplicate the work performed by the existing circuits.

Pin	Function
1	NC
3	IO 7
5	IO 6
7	IO 5
9	IO 4
11	IO 3
13	IO 2
15	IO 1
17	IO 0
19	GND

Pin	Function
2	V_{CC} (5V)
4	IO 8
6	IO 9
8	IO 10
10	IO 11
12	IO 12
14	IO 13
16	IO 14
18	IO 15
20	GND

TABLE 10 - P15 PIN OUTS

P2 supports the same pin-outs as P15 but for the upper 16 IO lines as specified in Table 11.

Pin	Function
1	NC
3	IO 23
5	IO 22
7	IO 21
9	IO 20
11	IO 19
13	IO 18
15	IO 17
17	IO 16
19	GND

Pin	Function
2	V_{CC} (5V)
4	IO 24
6	IO 25
8	IO 26
10	IO 27
12	IO 28
14	IO 29
16	IO 30
18	IO 31
20	GND

TABLE 11 - P2 PIN OUTS

Due to the limited IO lines available on the PIC18F14K50 two 16 bit IO expanders were used, specifically PCA9555 from Philips Semiconductors. The PCA9555 interfaces to the 18F14K50 via an I^2C (two wire synchronous bus) both the U7 and U8 IO expanders are located on the same bus. The I^2C bus is clocked at 400 kHz; this is the maximum frequency supported by the PCA9555 and thus provides optimal latency between an IO line and the Eyebot Controller. The I^2C bus uses device address to communicate to individual slave devices (the two PCA9555). The I^2C bus in this design uses 8 bit addressing, the least significant bit represents whether the transfer is a read or write operation. The four most significant bits form a fixed address while the remaining three bits are determined by the logic levels on the A1, A2, A3 pins of the PCA9555 (see Figure 62).

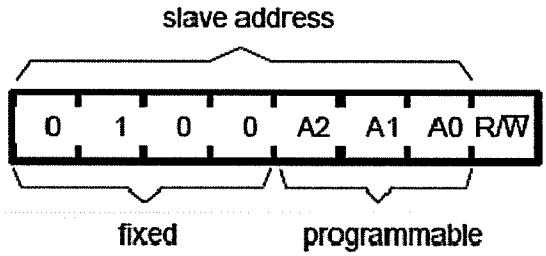

FIGURE 62 - PCA9555 ADDRESS[63]

Table 12 lists the I^2C addresses utilized on the TBS Gateway.

Bank	Read Address	Write Address
0-15 (U7 & P15)	0x4D (0b01001101)	0x4C (0b01001100)
16-31 (U8 & P2)	0x4F (0b01001111)	0x4E (0b01001110)

TABLE 12 - I^2C ADDRESSES

I^2C transactions are handled as read and writes to a number of registers in the IO expanders, all transactions are initiated by the host (18F14K50). There are eight registers on the PCA9555 each eight bits wide.

Register Address	Function
0	Input Port 0
1	Input Port 1
2	Output port 0
3	Output port 1
4	Polarity inversion port 0
5	Polarity inversion port 1
6	Configuration port 0
7	Configuration port 1

TABLE 13 - PCA9555 REGISTERS[63]

Port 0 refers to the lower 8 lines of the IO expander while port 1 represents the upper 8 lines. The input port registers (0 & 1) contain the incoming logic levels of each of the IO lines irrespective of if they are set as an input or an output. The output port registers (2 & 3) contain the outgoing logic levels; pins set as an input are not affected by this register. The polarity inversion registers sets if the input port registers values are inverted. This function of the PCA9555 is not used and thus this register is always set to '0'. The configuration registers (6 & 7) set the IO lines direction a value of '1' in these registers signify an input while a '0' signifies the IO line is set to an output[63].

The PCA9555 also feature an open-drain interrupt output, this pin connects to the interrupt output pin of both IO expanders and to the external interrupt 1 pin on the 18F14K50 the line is pulled high to V_{DD} via R9. The interrupt line is pulled low when an input line changes, the interrupt is reset if the IO line reverts back to its original state or a read occurs of the corresponding input port register. In the absence of an interrupt the input port registers are read by the processor twice a second, the output port registers are written at this time too to protect against any abnormal behaviour leaving an IO line in an unknown state. If an interrupt is detected all of the input port registers are read and the update will be sent to the Eyebot. An IO write from the Eyebot to any IO pin will result in all output ports being written too.

6 Conclusion/Future Work

The REV project continues to demonstrate that electric vehicles are not only a sustainable mode of transport (when coupled with the correct electrical supply). Through the continual development of the electric conversion projects such as the Getz and Lotus Elsie the REV project will continue to engage the public and actively demonstrate that not only are electric vehicles a sustainable means of transport, but that Electric Vehicles are possible now and not some distance into the future as the majority of the public believe. The continued collection of performance metrics for the purposes of research and development is vital to winning the battle of convincing the public of the merits of electric vehicles.

The author's Hardware Black Box was designed explicitly to assist in the collection of valuable performance data. For the first time in conjunction with new BMS Master Controller and the BMS modules it is possible to record variance in individual cell performance within the battery pack in real-time. Capturing information such as the true energy required per distance travelled, automatically with very little input from the operator. The author believes that the presence of quantitative information, will act not only as a good benchmark for future technology implemented in the car, but will be a true stimulus to advances in performance and efficiency of the future works of the REV team.

The addition of instrumentation upgrades such as the TBS Gateway, will allow drivers to be more familiar with electric cars as they can rely on instrumentation such as the fuel gauge and tachometer just as they have always done with traditional internal combustion vehicles. The availability of addition inputs and outputs for the Eyebot controller through the TBS gateway will continue to improve the effectiveness of the Eyebot controller as a user interface to the Getz and will eventually result in the development of new features in the car, including visual and audio response to vehicle events that can now be detected. The availability of traction pack metrics in the Getz allows for the development of a new suite of real time statistics that will be available to the driver and passenger alike.

The addition of a reliable HSPA connection in the car, through the inclusion of the new router and the development of the 3G power management module, will allow real time vehicle usage data to be collected externally to the vehicle. This also opens the possibilities to greater support to sponsors when using the vehicle, such as the possibility of remote diagnostics. Remote vehicle tracking has already been developed by a fellow team member through the use of this module.

The Hardware Black Box system due to its flexible nature, supports an array of future development as new requirements are discovered. Future work for this system may include adding additional support for new devices such as the motor controller through the existing CAN interface. or using one of the generic UARTs to interface to new and novel solutions such as an RFID reader to easily identify the driver and automatically customise settings to suit, and allow the collection of per user based statistics to assist in better understanding the impact driver behaviour has on vehicle performance.

The TBS Gateway also has potential to support additional features through the upgrading of the microcontroller firmware. One novel feature would be the ability for the TBS Gateway to capture and store all of the TBS parameters into the microcontrollers EEPROM. An extension of this would be the automatic detection when these settings are changed (as occurs when maintenance is carried out on the traction pack). Once a change is detected the TBS Gateway could then automatically restore all of the settings through the TBS E-xpert Pro communication protocol. Such functionality can be implemented with no hardware modification or upgrades and be done purely in firmware upgrades.

While the 3G Power Management board performs the task it was originally designed for. The design has left majority of the resources of the microcontroller un-used. Thus additional functionality could be added in the future, such as automatically power cycling the router on set periods to reduce the likely hood of the device becoming non-responsive. Another possible feature would be the automatic powering up and shutting down of the router on a fixed schedule to conserve power.

Thus while the development of the solutions presented in this report are designed to address specific functional requirements. The flexibility embedded into the design allows for the development of new functionality with minimal or no hardware requirements. The author hopes that the work that has been completed throughout 2009 will serve the REV project for many years into the future.

REFERENCES

[1] R. Mathew, "About REV - TheRevProject.com." vol. 2009 Perth, Australia: The Rev Project / UWA, 2008.

[2] U. Bossel, "Does a Hydrogen Economy Make Sense?," *Proceedings of the IEEE,* vol. 94, pp. 1826-1837, 2006.

[3] J. P. Aditya and M. Ferdowsi, "Comparison of NiMH and Li-ion batteries in automotive applications," in *Vehicle Power and Propulsion Conference, 2008. VPPC '08. IEEE*, 2008, pp. 1-6.

[4] "TS-LFP90AHA Specifications." vol. 2009 China: Thunder Sky Batteries, 2007.

[5] D. Freeman and D. Heacock, "Sophisticated battery management addresses emerging battery technologies," in *Southcon/95. Conference Record*, 1995, pp. 37-40.

[6] "User and Installation Manual For PowerPhase® 150 Traction System, PowerPhase® 125 Traction System, PowerPhase® 100 Traction System, PowerPhase® 75 Traction System, HiTor Traction System with DD45-400L Inverter/Controller, DD45-500L Inverter/Controller (With firmware version 4.05 and above)," Frederick, Colorado: UQM Technologies, INC, 2008.

[7] "Detroit Electric Car," Detroit Electric, 2008.

[8] P. Graham, "CSIRO Submission 08/308 Inquiry into the Impact of Higher Petroleum, Diesel and Gas Prices and Several Related Matters," Dickson, ACT: CSIRO, 2008, pp. 1-18.

[9] R. Garnaut, "The Garnaut Climate Change Review Final Report," Port Melbourne, VIC: Cambridge University Press, 2008, pp. 1-680.

[10] B. Brant, *Build your own electric vehicle*. New York: TAB Books, 1994.

[11] "Green Energy," Perth: Synergy, 2009.

[12] "Australia - Fact Sheet," Barton, ACT: Market Information and Research Section, Department of Foreign Affairs and Trade, 2009, p. 1.

[13] M. R. Simmons, "The Peak Oil Debate As the EIA Turns 30," in *EIA 2008 Energy Conference* Washington, DC: Energy Information Adminstration, 2008, pp. 1-31.

[14] W. D. Jones, "Black Boxes Get Green Light," in *IEEE Spectrum*. vol. 41 Los Alamitos, CA: IEEE, 2004, pp. 14-16.

[15] "General Motors air bag black box crash data retrieval ". vol. 2009 Franklin, TN: Logan Diagnostics.

[16] A. Kassem, R. Jabr, G. Salamouni, and Z. K. Maalouf, "Vehicle Black Box System," in *Systems Conference, 2008 2nd Annual IEEE*, 2008, pp. 1-6.

[17] S. M. Jung and M. S. Lim, "System on Chip design of Embedded Controller for Car Black Box," in *2007 International Symposium on Information Technology Convergence*: IEEE, 2007, pp. 217-221.

[18] "CS5463 Single Phase, Bi-directional Power/Energy IC," Austin, TX: Cirrus Logic, Inc, 2008, pp. 1-46.

[19] "Single Phase, Bi-directional Power/Energy IC," Austin, Texas: Cirrus Logic, 2008.

[20] B. C. Baker, "Anti-Aliasing, Analogue Filters for Data Acquisition Systems," in *Aplication Note AN699* Chandler, Arizona: Microchip Inc, 1999, pp. 1-13.

[21] "NG3 Installation and User Manual," Poviglio, ITALIA: Zivan S.r.I, 2003, pp. 8-9.
[22] "Standard EIA Decade Resistor Values Table," in *Analog.* vol. 2009 Reynolds Station, KY: Analog Services Inc, 2008.
[23] "Type FCP Surface Mount Film Capacitors Stable Stacked Metallized Film (PPS) Chips for Reflow Soldering," Bedford, MA: Cornell Dubilier, pp. 1-3.
[24] "Quad Channel Digital Isolators ADuM1410/ADuM1411/ADuM1412," Norwood, MA: Analogue Devices, 2007, pp. 1-24.
[25] R. Condit, "Transformerless Power Supplies: Resistive and Capacitive," in *Application note AN954* Chandler, Arizona: Microchip Technology Inc., 2004, pp. 1-14.
[26] W. H. Paul Horowitz, *The Art of Electronics*, 2nd ed. New York, USA: Cambridge University Press, 2006.
[27] K. Walters, "How to select transient voltage suppressors," Irvine, CA: MicroSemi, 1999, pp. 1-2.
[28] "VDR Metal Oxide Varistors Standard," Malvern, PA: Vishay, 2009, pp. 1-18.
[29] "Quad Channel Digital Isolators ADuM1410/ADuM1411/ADuM1412," Norwood, MA: Analogue Devices, 2007, pp. 1-24.
[30] "Mouser Price list for ADUM1412BRWZ-ND," Kwun Tong, Kowloon Hong Kong: Mouser Electronics, 2009.
[31] "Digikey Price list for ADUM1412BRWZ," Thief River Falls, MN: Digi-key Corporation, 2009.
[32] "MC14049B, MC14050B Hex Buffer," Phoenix, Arizona: ON Semiconductor, 2005, pp. 1-8.
[33] "PIC24FJ256GB110 Family Data Sheet 64/80/100-Pin, 16-Bit Flash Microcontrollers with USB On-The-Go (OTG)," Chandler, Arizona: Microchip Technology Inc, 2009.
[34] "3V Tips 'n Tricks," Chandler, Arizona: Microchip Technology Inc, 2008.
[35] "Dual Channel Isolators with Integrated DC-to-DC Converter ADuM5200/ADuM5201/ADuM5202," Norwood, MA: Analogue Devices, 2008, pp. 1-24.
[36] "Very High CMR, Wide VCC Logic Gate Optocouplers (HCPL-2202)," Santa Clara, CA: Agilent Technologies, pp. 1-16.
[37] "Stand-Alone CAN Controller with SPI Interface," Chandler, Arizona: Microchip Technology Inc, 2007.
[38] "NLG5_CAN Spec 2.01," CH - 9466 Sennwald Switzerland: BRUSA Elektronik AG, 2003, pp. 1-6.
[39] "High Speed CAN Transceiver," Chandler, Arizona: Microchip Technology Inc., 2007.
[40] "System Management Bus (SMBus) Specification Version 2.0," SBS Implementers Forum, Duracell, Inc., Energizer Power Systems, Inc., Fujitsu, Ltd., Intel Corporation, Linear Technology
Inc., Maxim Integrated Products, Mitsubishi Electric Semiconductor Company, PowerSmart, Inc.,
Toshiba Battery Co. Ltd., Unitrode Corporation, USAR Systems, Inc., 2000.
[41] "RS232 Data Interface." vol. 2009 Georgetown, TX: ARC Electronics.
[42] "FT232BL USB UART (USB - Serial) I.C," Glasgow, United Kingdom: FTDI Chip, 2005.

[43] "SN74LVCH8T245 8-bit DUAL-SUPPLY BUS TRANSCEIVER WITH CONFIGURABLE VOLTAGE TRANSLATION AND 3-STATE OUTPUTS," Dallas, TX: Texas Instruments, 2005, pp. 1-22.
[44] "PG12864-J," Powertip, pp. 1-2.
[45] "SD Specifications Part 1 Physical Layer Simplified Specification Version 2.00," San Ramon, CA: SD Card Association, Matsushita Electric Industrial Co. Ltd. (Panasonic), SanDisk Corporation (SanDisk), Toshiba Corporation (Toshiba), 2006, pp. 1-129.
[46] P. Reen and N. Mohanswamy, "AN1045 Implementing File I/O Functions Using Microchip's Memory Disk Drive File System Library," Chandler, Arizona: Microchip Technology Inc, 2008, pp. 1-20.
[47] K. Otten, "AN1140 USB Embedded Host Stack," Chandler, Arizona: Microchip Technology Inc, 2008, pp. 1-20.
[48] K. Otten, "AN1145 Using a USB Flash Drivewith an Embedded Host," Chandler, Arizona: Microchip Technology Inc, 2008, pp. 1-20.
[49] "TC682 Inverting Voltage Doubler," Chandler, Arizona: Microchip Technology Inc, 2006.
[50] "320.02 E1-1 (w/.094 GRY)," Brooklyn Park, Minnesota: E-Switch, 2000.
[51] "PIC12 MCU - Product Family - 8-bit Microcontrollers," Chandler, Arizona: Microchip Technology Inc., 2009.
[52] "Altronics & Staff Audio Visual & Electronics Engineering Catalogue," 23rd ed Sydney, Australia, 2009, p. 266.
[53] "PIC12F683 Data Sheet," Chandler, Arizona: Microchip Technology Inc, 2007.
[54] "BC546/547/548/549/550," San Jose, California: Fairchild Semiconductor Corporation, 2002, pp. 1-2.
[55] "TBS Electronics High Precision Battery Monitor e-xpert pro Owner's manual." vol. 2009 AL Zwaag, The Netherlands: TBS Electronics BV, 2008.
[56] "Vehicle Standards Bulletin 14 National Code of Practice for Light Vehicle Construction and Modification - National Guidelines for The Installation of Electric Drives in Motor Vehicles," V. S. Standards, Ed. Australia: Department of Transport 2009 (Review Stage), p. 15.
[57] "e-xpert pro communication interface specification," AL Zwaag, The Netherlands: TBS Electronics BL, 2008, p. 31.
[58] "High CMR, High Speed TTL Compatible Optocouplers - Technical Data," Hewlett Packard, (Unknown), pp. 1-146 - 1-165.
[59] D. Schouten, "TBS Electronics Contactformulier," Direct Communication to Manufacturer ed, D. Kingdom, Ed.: TBS Electronics BV, 2009, p. 10.
[60] "PIC18F13K50/14K50 Data Sheet - 20 Pin USB Flash Microcontrollers with nano-Watt XLP(TM) Technology," Chandler, Arizona: Microchip Technology Inc, 2009.
[61] "Getz 2003 Shop Manual," Korea: Hyundai, 2003.
[62] "MPLAB ICD 2 In-Circuit Debugger User Guide," Chandler, Arizona: Microchip Technology Inc, 2005.
[63] "PCA9555 16-bit I^2C and SMBus I/O port with interrupt," U.S.A: Philips Semiconductors, 2002, pp. 1-18.

APPENDICES

PROGRAMMING BOARD WITH UART SCHEMATIC

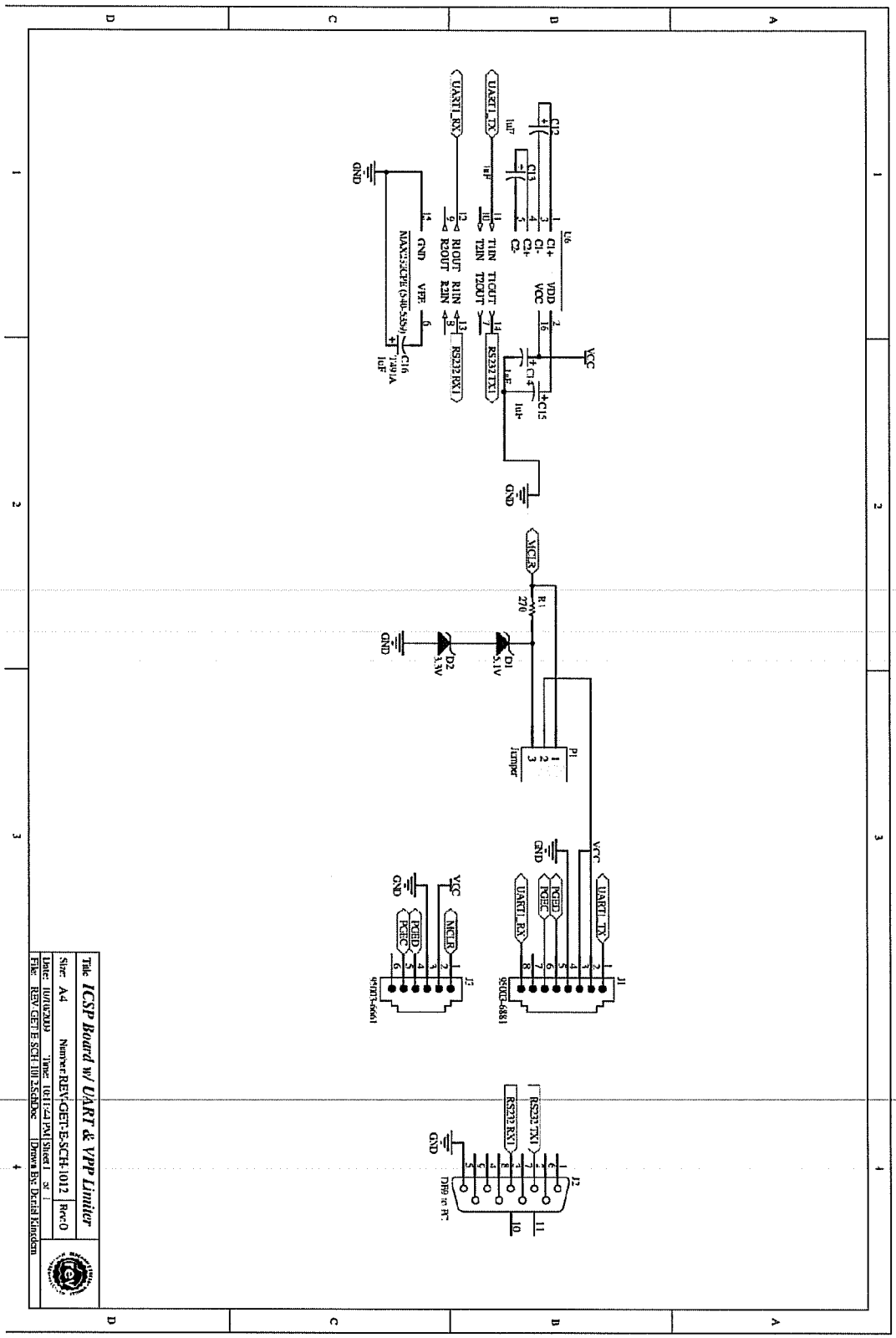

FIGURE 63 - PROGRAMMING BOARD WITH UART & VPP LIMITER

ANTI-ALIASING PSPICE MODEL

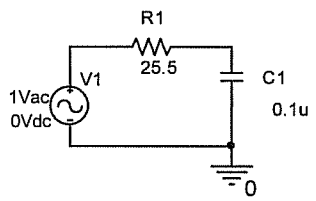

FIGURE 64 - ANTI-ALIASING FILTER SCHEMATIC FOR PSPICE SIMULATIONS

BMS MODULE COAXIAL TO JST CONNECTOR BOARD

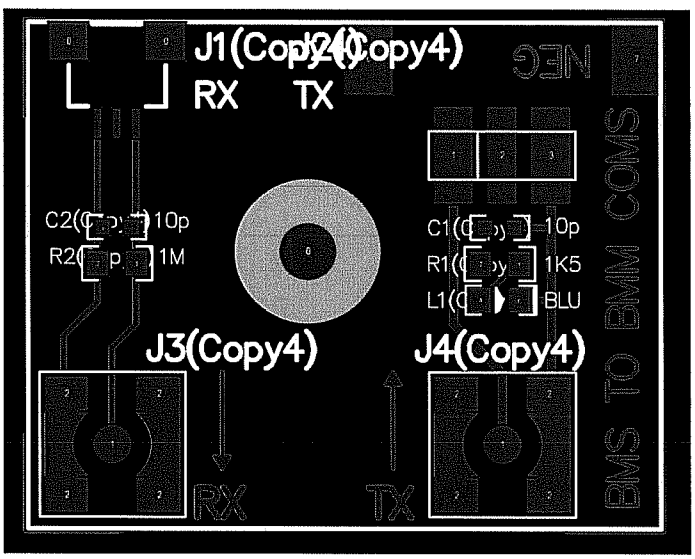

FIGURE 65 - BMS COAXIAL TO JST CONVERSION BOARD

Credit: Ivan Neubronner

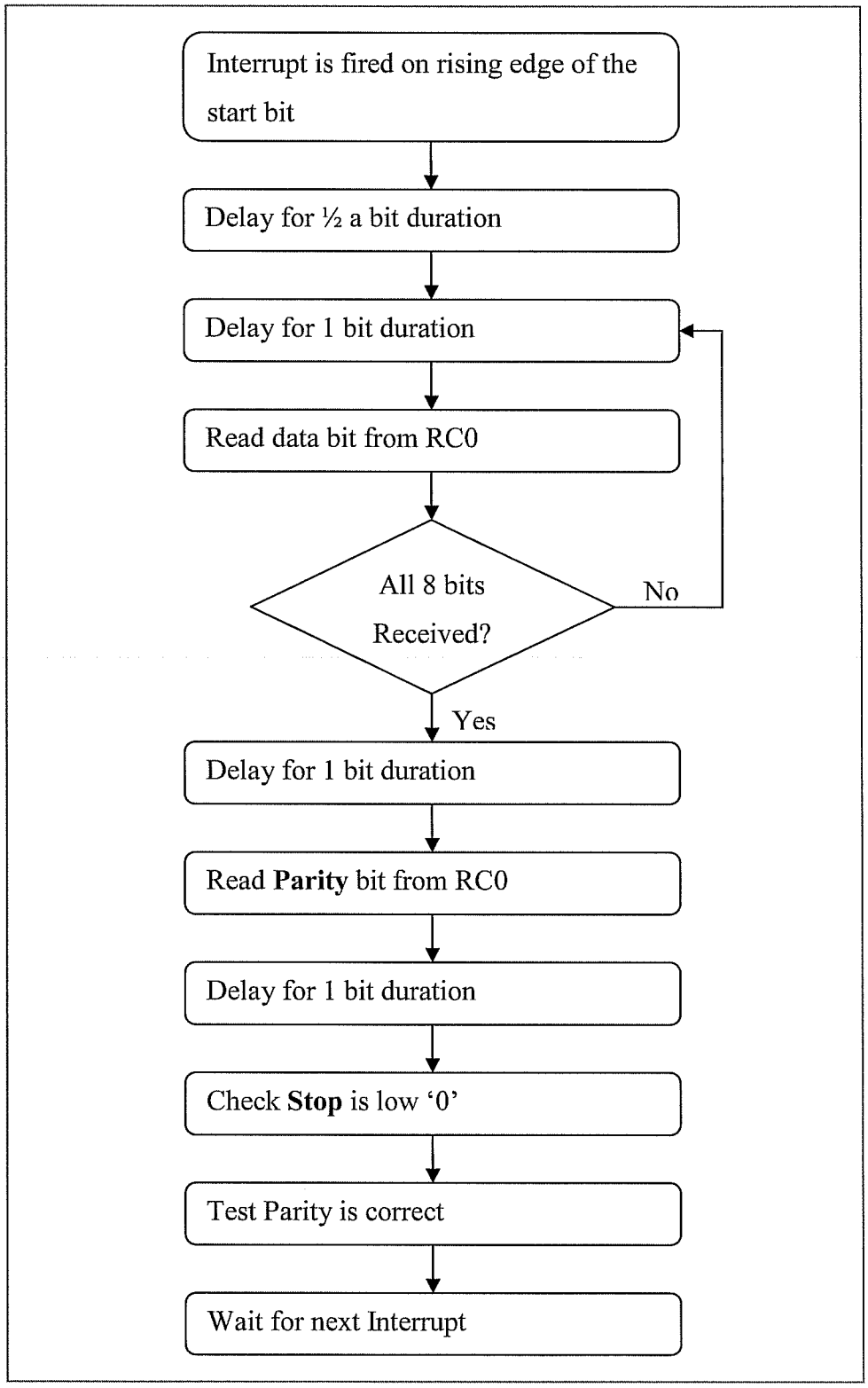

FIGURE 66 - SOFTWARE UART RECEIVE BYTE

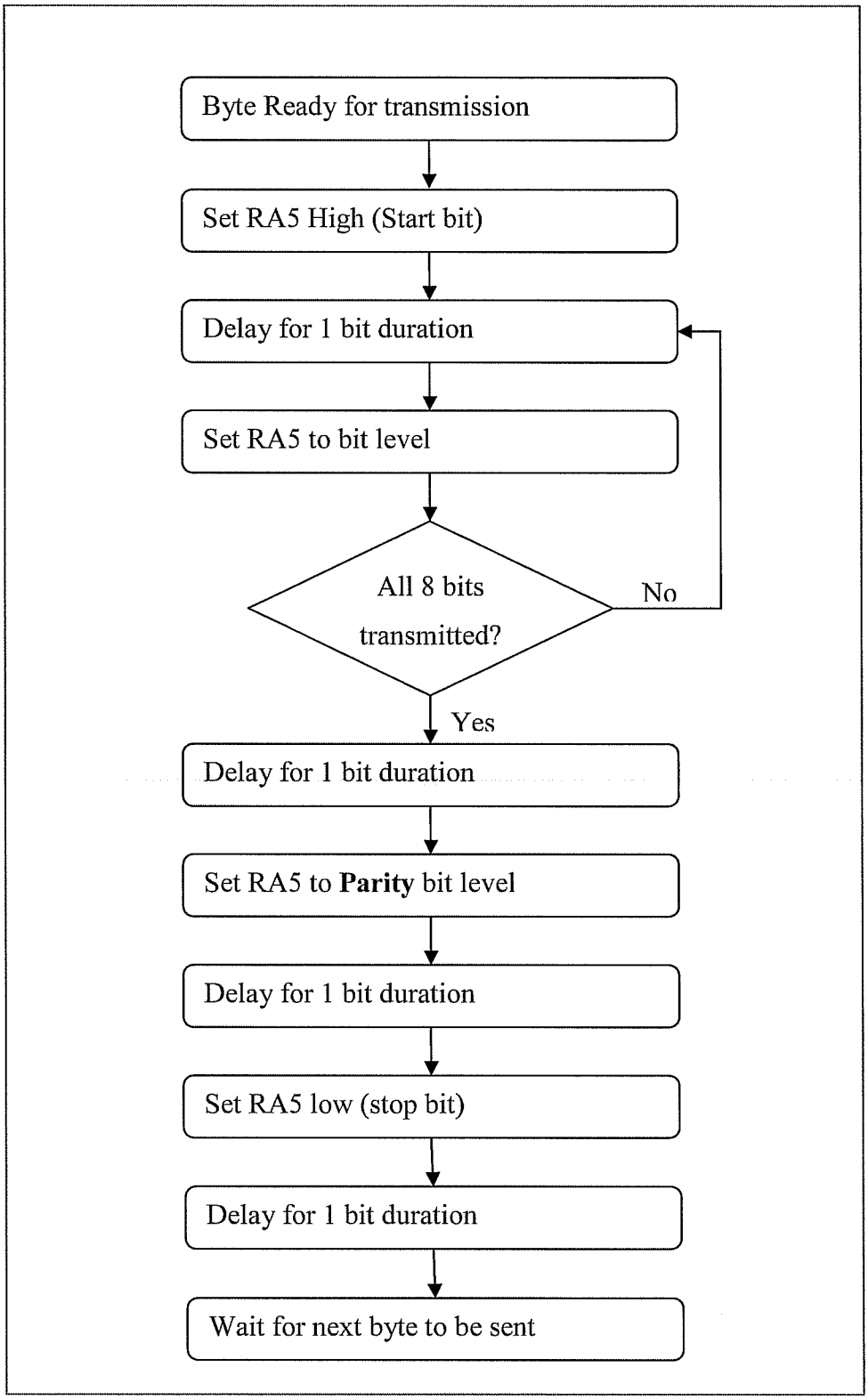

FIGURE 67 - SOFTWARE UART TRANSMIT BYTE

TBS Gateway Eyebot Serial Protocol

The protocol is split into two sub groups based upon the origin of the transmission. Transmissions from the TBS gateway are of two possible types, either a response to transmission originating from the Eyebot controller or an IO update which contains the current value of all inputs on the TBS Gateway.

!IO,$X_bX_bX_bX_bX_bX_bX_bX_b$,$X_{AN1}X_{AN1}X_{AN1}X_{AN1}$,$X_{AN2}X_{AN2}X_{AN2}X_{AN2}$,$X_{AN3}X_{AN3}X_{AN3}X_{AN3}$,$X_HX_HX_HX_H$,$X_VX_VX_VX_V$,$X_IX_IX_IX_IX_IX_I$,$X_AX_AX_AX_AX_AX_A$,$X_SX_SX_SX_S$,$X_RX_RX_RX_RX_RX_RX_RX_R$,$X_TX_TX_TX_T$,$X_SX_SX_SX_SX_SX_S$,EE<CR>

$X_bX_bX_bX_bX_bX_bX_bX_b$: 32 bits in hexadecimal (ASCII) representing the logic level on all 32 digital IO lines (irrespective if they are set to an input or an output).

$X_{ANx}X_{ANx}X_{ANx}X_{ANx}$: 16 bit unsigned integer (hexadecimal) containing the value of the 10bit Analogue to digital converter[60] (Range: 0-1023).

$X_HX_HX_HX_H$: 16 bit unsigned integer (hexadecimal) contains the value of timer 1 before being reset to 0 twice a second, this counter contains the number of rising edges of the Hall Effect sensor input with a resolution of 1 edge/ pulse (Range 0 – 65535).

$X_VX_VX_VX_V$: 16 bit unsigned integer representing the main traction pack voltage with a resolution of 0.01V (Range: 0.00 – 655.35V).

$X_IX_IX_IX_IX_IX_I$: 24 bit signed short long representing traction pack current with a resolution of 0.01A

$X_AX_AX_AX_AX_AX_A$: 24 bit signed short long representing discharge status of the traction pack in amp hours with a resolution of 0.1Ah (Range: -9999.9 – 0.0Ah).

$X_SX_SX_SX_S$: 16 bit unsigned integer representing the state of charge with a resolution of 0.1% (Range: 0.0 – 100.0%)

$X_RX_RX_RX_RX_RX_RX_RX_R$: 24 bit unsigned short long containing the time remaining with a resolution of 1 minute (Range: 0 – 14400 minutes).

$X_TX_TX_TX_T$: 16 bit signed integer representing the external probe temperature with a resolution of 0.1°C (Range -20.0°C – 50.0°C).

EE: 8 bit unsigned char in hexadecimal, which contains the sum of all bytes preceding this checksum byte including ',' and '!'.

<CR> Carriage return and new line character.

Transmissions from the host controller (Eyebot) to the gateway support a number of command types. If the command is accepted and executed correctly the TBS gateway will respond with an acknowledge command:

!ACK,1D,<CR>

'1D' is the checksum of acknowledge command.

$$EE = ('!' + 'A' + 'C' + 'K' + ',')\%255$$
$$= 29 = 0x1D$$

If the command is not accepted or if it failed the checksum comparison, a not acknowledge command will be sent.

!NACK,6B,<CR>

Where 6B is the checksum for the not acknowledge command.

$$EE = ('!' + 'N' + 'A' + 'C' + 'K' + ',')\%255$$
$$= 107 = 0x6B$$

The first command from host to the gateway is the digital IO direction command, which sets the direction of the digital IO lines as either an input or an output:

!DIOD,XXXXXXXX,EE,<CR>

XXXXXXXX: 32 bits in hexadecimal each bit sets the input/output state for the corresponding bit. A '1' represents an input while '0' represents and output.

EE: 8 bit unsigned char in hexadecimal, which contains the checksum of all bytes preceding this checksum byte including ',' and '!'.

<CR> Carriage return and or new line character.

!DIOV,XXXXXXXX,EE,<CR>

XXXXXXXX: 32 bits in hexadecimal each bit sets the value of the corresponding bit. A '1' represents a high output, '0' represents a low output. This command will only affect the IO pins which are set to an output.

EE: 8 bit unsigned char in hexadecimal, which contains the sum of all bytes preceding this checksum byte including ',' and '!'.

<CR> Carriage return and or new line character.

!TACO,XXXX,EE,<CR>

XXXX: 16 bit unsigned integer (hexadecimal) with maximum frequency for the tachometer output. Valid range is 0-512 Hz (Note: 0 will disable the tachometer output), a value outside this range will be ignored. A valid input will result in the configuration being updated in the eeprom on the 18F14K50.

EE: 8 bit unsigned char in hexadecimal, which contains the sum of all bytes preceding this checksum byte including ',' and '!'.

<CR> Carriage return and or new line character.

!FLVL,X_FX_F,$X_{3/4}X_{3/4}$,$X_{1/2}X_{1/2}$,$X_{1/4}X_{1/4}$,X_EX_E,EE,<CR>

X_FX_F: 8 bit unsigned char/byte (hexadecimal) which contains the duty cycle in 1% resolution for full level of the fuel gauge output. The valid range of this output is 0-100%, any value outside this range will result in the command being rejected (NACK).

$X_{3/4}X_{3/4}$: 8 bit unsigned char/byte (hexadecimal) which contains the duty cycle in 1% resolution for 3/4 level of the fuel gauge output. The valid range of this output is 0-100%, any value outside this range will result in the command being rejected (NACK).

$X_{1/2}X_{1/2}$: 8 bit unsigned char/byte (hexadecimal) which contains the duty cycle in 1% resolution for ½ level of the fuel gauge output. The valid range of this output is 0-100%, any value outside this range will result in the command being rejected (NACK).

$X_{1/4}X_{1/4}$: 8 bit unsigned char/byte (hexadecimal) which contains the duty cycle in 1% resolution for ¼ level of the fuel gauge output. The valid range of this output is 0-100%, any value outside this range will result in the command being rejected (NACK).

X_EX_E: 8 bit unsigned char/byte (hexadecimal) which contains the duty cycle in 1% resolution for empty level of the fuel gauge output. The valid range of this output is 0-100%, any value outside this range will result in the command being rejected (NACK).

EE: 8 bit unsigned char in hexadecimal, which contains the sum of all bytes preceding this checksum byte including ',' and '!'.

<CR> Carriage return and or new line character.

The final command is the reset command; this command will reset the TBS gateway to the state it would be in after a power-on (see 5.2.6 Power-On State).

!RST,47,<CR>

47 is the checksum for the reset command.

$$EE = ('!' + 'R' + 'S' + 'T' + ',')\%255$$
$$= 71 = 0x47$$

<CR> Carriage return and or new line character.

BMS MASTER CONTROLLER SMBUS REGISTER LIST

Address	Function	Data type	Default	Range
0	Data Refresh Count	8 bit unsigned integer	0	0-255
1	Min Steady State I (1A)	8 bit unsigned integer	10	0-255
2	Min Steady State Cell V (0.1V)	8 bit unsigned integer	25	0-255
3	Min Cell V (0.1V)	8 bit unsigned integer	20	0-255
4	Max Cell V (0.1V)	8 bit unsigned integer	40	0-255
5	Bypass V (0.1V)	8 bit unsigned integer	38	0-255
6	Enable CAN Bus	Boolean	1	0-1
7	Enable Min steady V Alarm	Boolean	1	0-1
8	Enable Min V Alarm	Boolean	1	0-1
9	Enable Max V Alarm	Boolean	1	0-1
10	Enable BMS Error Alarm	Boolean	1	0-1
11	Enable BMS Comm Error Alarm	Boolean	1	0-1
12	Enable Audible Event Notification	Boolean	1	0-1
13-49	Reserved for future use			
50	Ignition Status	Boolean	0	0-1
51	Power Save Mode	Boolean	0	0-1
51-69	Reserved for future use			
70	BMS MC Version #	8 bit unsigned integer	0	0-255
71	Contactors Enable	Boolean (read only)	0	0-1
72	AC Enable	Boolean (read only)	0	0-1
73	Regen Braking Enable	Boolean (read only)	0	0-1
74-99	Reserved for future use			

100	Channel 1 BMS Count	8 bit unsigned integer		0-200
101	Channel 2 BMS Count	8 bit unsigned integer		0-200
102	Channel 3 BMS Count	8 bit unsigned integer		0-200
103	Channel 4 BMS Count	8 bit unsigned integer		0-200
104-199	Reserved for future use			
200	Cell 1 Voltage MSB			0-255
201	Cell 1 Voltage LSB (0.01V)	16 bit unsigned integer		0-255
202	Cell 1 Bypass Current (0.1A)	8 bit unsigned integer		0-255
203	Cell 1 Maximum V (0.1V)	8 bit unsigned integer		0-255
204	Cell 1 Minimum V (0.1V)	8 bit unsigned integer		0-255
205-1699	Cells 2 – 300 data			

TABLE 14 - BMS MASTER CONTROLLER REGISTER LIST